Vol. 67 • No. 2

February 2024

Microwave Journal

horizon house®

Founded in 1958

mwjournal.com

DC TO 86 GHz

Filter Technologies

For Every Application

Selection and Solutions

- 1500+ in-stock models
- Low pass, high pass, band pass, band stop, diplexers and triplexers
- In-house design and manufacturing capability
- Fast, affordable custom capabilities

LEARN MORE

Cavity

- Passbands to 43.5 GHz
- Stopbands to 57 GHz
- Bandwidths as narrow as 1%
- 100+ dB rejection

Ceramic Resonator

- Fractional bandwidths from 0.5 to 40%
- Excellent power handling, up to 20W
- High Q in miniature SMT package

Lumped L-C

- Wide catalog selection
- Several package options including aqueous washable
- Variety of filter topologies

LTCC

- Tiny size, as small as 0202
- Industry's widest selection of mmWave LTCC filters
- Proprietary designs with stopband rejection up to 100 dB

Microstrip

- Connectorized designs with 4 to 40% fractional bandwidth
- Power handling up to 10W
- Flat group delay

MMIC Reflectionless

- Patented topology absorbs and internally terminates stopband signals
- Perfect for pairing with amplifiers, mixers, multipliers, ADC/DACs & more
- Cascadable with other filter technologies

Rectangular Waveguide

- WR-12, WR-15 and WR-28 interfaces
- Passbands up to 87 GHz
- High stopband rejection, 40 dB

Suspended Substrate

- Ultra-wide passbands up to 26 GHz
- Wide stopbands up to 40 GHz
- High Q

Thin Film on Alumina

- Passbands from DC to 40 GHz
- High rejection with wide passband
- Miniature SMT package

Mini-Circuits®


RF-LAMBDA
THE LEADER OF RF BROADBAND SOLUTIONS
BROADBAND SSPA / EMC BENCHTOP
SOLID STATE POWER AMPLIFIER
0.1-22GHZ
ULTRA BROADBAND SSPA
RFLUPA01M22GA
4W 0.1-22GHZ
RFLUPA0218GB
20W 1-19GHZ
300W 6-18GHZ SOLID STATE BROADBAND
400W 8-11GHZ
SOLID STATE BROADBAND
0.1-6GHZ VHZ,
UHF, L, S, C BAND
RFLUPA02G06GC
100W 2-6GHZ
RFLUPA0706GD
30W 0.7-6GHZ
MADE IN USA
6-18GHZ C, X, KU BAND
RFLUPA08G11GA
50W 8-11GHZ
RFLUPA0618GD
60W 6-18GHZ
RFLUPA06G12GB
25W 6-12GHZ
18-50GHZ K, KA, V BAND
RFLUPA18G47GC
2W 18-47GHZ
RFLUPA27G34GB
15W 27-34GHZ
RFLUPA47G53GA2
10W 47-53GHZ
RFLUPA27G34GB
30W 18-40GHZ
BENCHTOP RF MICROWAVE SYSTEM POWER AMPLIFIER
RAMP00G06GA- 30W 0.01-6GHZ
RAMP39G48GA- 4W 39-48GHZ
RAMP01G22GA- 8W 1-22GHZ
RAMP27G34GA- 8W 27-34GHZ
www.rflambda.com
sales@rflambda.com
1-888-976-8880
1-972-767-5998
San Diego, CA, US
Carrollton, TX, US
Ottawa, ONT, Canada
Frankfurt, Germany

Microwave Journal

CONTENTS

February 2024
Vol. 67 • No. 2
Satellite & Radio Communications
mwjournal.com

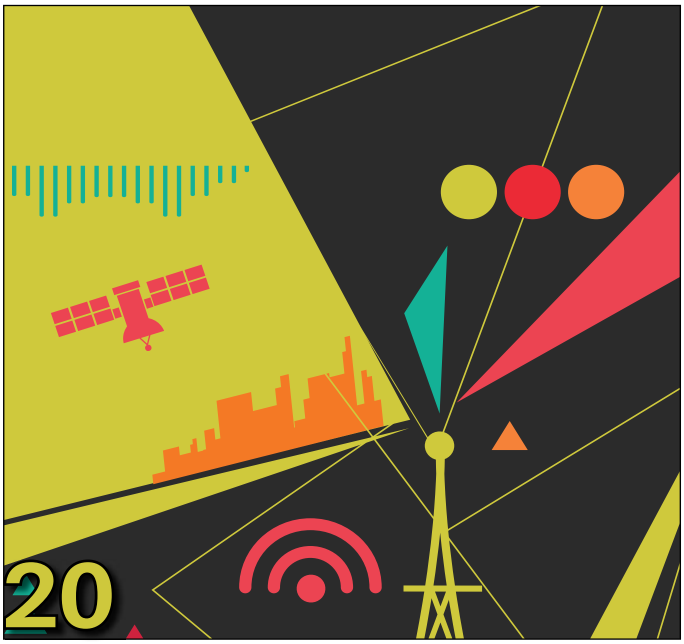

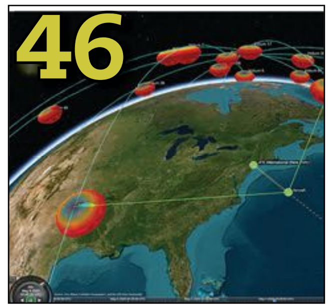

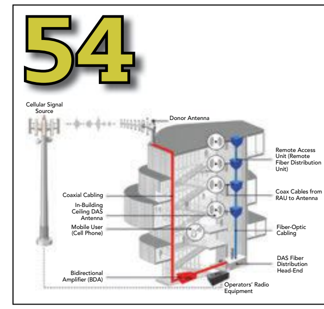

online spotlight

Look for this month's exclusive article online at mwjournal.com

An Improved Grey Wolf Optimization for Parameter Extraction of HBT Small-Signal Model

Min Liu, Deyong Wang, Panpan Zhang, Xuefeng Hou and Jincan Zhang, Henan University of Science and Technology

William Shockley: The Father of a Complicated Legacy 18
Eric Higham, Microwave Journal Technical Editor

Cover Feature

20 **A Sub-Terahertz MIMO Testbed for 6G Research**
Greg Jue, Keysight Technologies

Special Reports

46 **Addressing Low Earth Orbit Satellite Communications System Design Challenges**
Mike McLernon, MathWorks

54 **Revolutionizing Wireless Coverage With DAS Integrated Solutions**
Hamed M. Sanogo, Analog Devices

66 **6G and The Long RF Journey Ahead**
Stefan Pongratz, Dell'Oro Group

Application Notes

70 **MMIC Filter Advancements Drive New Tools**
Doug Jorgesen, Marki Microwave

86 **Unlocking the Potential: A Guide to Electronically Steered Antennas**
Eran Agmon, Pacific Grove Consulting

67 YEARS OF PUBLISHING EXCELLENCE

Has Amplifier Performance or Delivery Stalled Your Program?

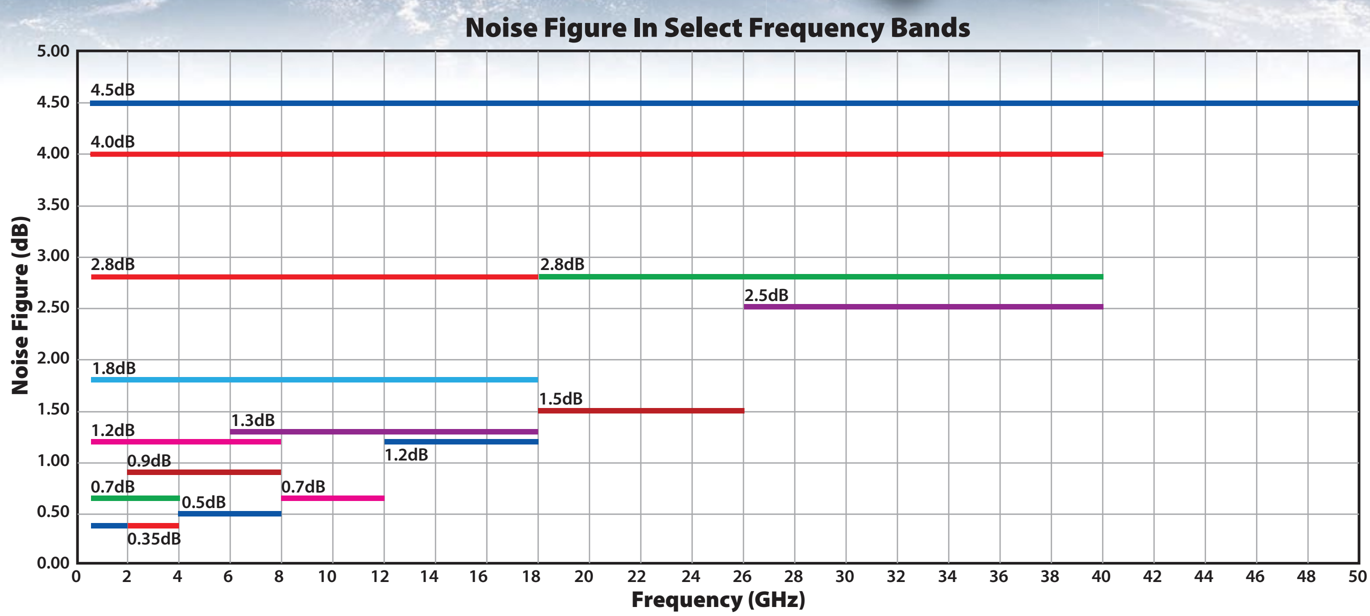

B&Z TECHNOLOGIES
Innovating to Excel

www.bnztech.com

Microwave Journal

CONTENTS

mwjournal.com

Product Feature

98 MMIC Power Amplifier for LEO Satellite Downlinks
mmTron Inc.

Tech Briefs

102 New Waveguide Power Sensor Products
LadyBug Technologies

102 Wideband mmWave Testing Solution
TMY Technology, Inc.

103 Tunable Notch YIG Filters Operate to 20 GHz
Micro Lambda Wireless, Inc.

Departments

17 Mark Your Calendar
31 Defense News
35 Commercial Market
38 Around the Circuit
104 Making Waves
106 New Products
110 Book End
112 Ad Index
112 Sales Reps
114 Fabs & Labs

Microwave Journal (USPS 396-250) (ISSN 0192-6225) is published monthly by Horizon House Publications Inc., 685 Canton St., Norwood, MA 02062. Periodicals postage paid at Norwood, MA 02062 and additional mailing offices.

POSTMASTER: Send address corrections to Microwave Journal, PO Box 1028, Lowell, MA 01853 or e-mail mwj@e-circ.net.com. Subscription information: (978) 671-0446. This journal is issued without charge upon written request to qualified persons working in the RF & microwave industry. Other subscriptions are: domestic, $130.00 per year, two-year subscriptions, $200.00; foreign, $225.00 per year, two-year subscriptions, $400.00; back issues (if available) and single copies, $20.00 domestic and $30.00 foreign. Claims for missing issues must be filed within 90 days of date of issue for complimentary replacement.

Posted under Canadian international publications mail agreement #PM40612608

STAFF

Group Director: Carl Sheffres
Associate Publisher: Michael Hallman
Media Director: Patrick Hindle
Brand & Content Director: Jennifer DiMarco
Technical Editor: Eric Higham
Associate Technical Editor: Cliff Drubin
Editorial & Media Specialist: Kelley Roche
Associate Editor: Kaitlyn Joyner
Multimedia Staff Editor: Barbara Walsh
Electronic Marketing Manager: Chris Stanfa
Senior Digital Content Specialist: Lauren Tully
Digital Content Specialist: Vincent Carrabino
Audience Development Manager: Carol Spach
Director of Production & Distribution: Edward Kiessling
Art Director: Janice Levenson
Graphic Designer: Ann Pierce

EUROPE
Office Manager: Nina Plesu

CORPORATE STAFF
CEO: William M. Bazzy
President: Ivar Bazzy
Vice President: Jared Bazzy

EXECUTIVE EDITORIAL OFFICE
685 Canton Street, Norwood, MA 02062
Tel: (781) 769-9750
FAX: (781) 769-5037
e-mail: mwj@mwjournal.com

EUROPEAN EDITORIAL OFFICE
16 Sussex Street, London SW1V 4RW, England
Tel: Editorial: +44 207 596 8730 Sales: +44 207 596 8740
FAX: +44 207 596 8749

SUBSCRIPTION SERVICES
Send subscription inquiries and address changes to:
Tel: (978) 671-0446
e-mail: mwj@e-circ.net

www.mwjournal.com

Printed in the USA

Microwave Journal ONLINE .COM

E LEARNING CENTER

Improve Wireless RFFE Design with Highly Linear RF Switch for Interference and De-sensitivity Mitigation
Sponsored by: Menlo Micro 2/14

Achieving SWaP-C Goals with Qorvo's Highly Integrated Radar Solutions
Sponsored by: RFMW and Qorvo 2/22

Catch *Frequency Matters*, the industry update from *Microwave Journal*,
microwavejournal.com/FrequencyMatters

WHITE PAPERS

ANALOG DEVICES
How Minimizing Pulse Droop in GaN Power Amplifiers Improves Radar Range

COPPER MOUNTAIN TECHNOLOGIES
Understanding Shield Effectiveness

Quantic Croven
The Application of Pressure Correction to RGA Test Results for Vacuum Sealed Quartz Resonators

Quantic MWD MICROWAVE DYNAMICS
Phase Noise Impact on Satellite Uplink and Downlink Channel Bandwidth

Look for additional content from: ROHDE & SCHWARZ Make ideas real | Wireless Telecom Group

Executive Interviews

Tim Winter, President of **iDirect Government**, talks about the company, his priorities and his vision for the future evolution of defense satcom and iDirect Government.


Mark McCabe, Managing Director, and **Ion Fortuna**, Vice President, Sales and Business Development, talk about the **CML Micro** product portfolio and future directions of the company, and how the recent acquisition of Microwave Technology fits these plans.

Join Us Online

Follow us
@Pathindle
@MWJEric
@MWJEditor

Join us at the RF and Microwave Community

Become a fan at facebook.com/microwavejournal

Visit us @ mwjournal.com

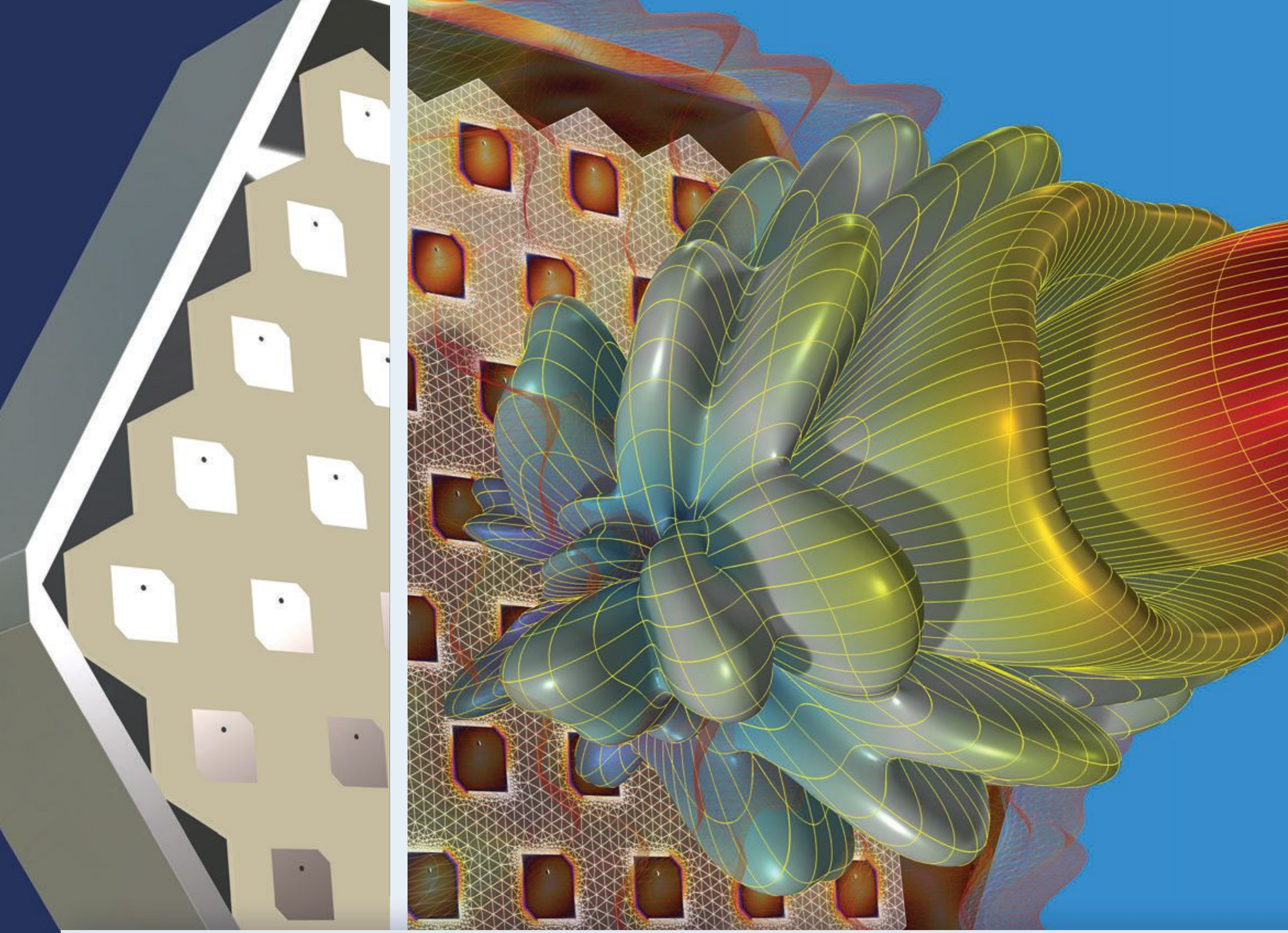

10.7 TO 31 GHz

SATCOM Filters

Proprietary LTCC Designs

- Surface-mountable 1008 package size
- 1W power handling
- Available for space upscreening
- Wide rejection band

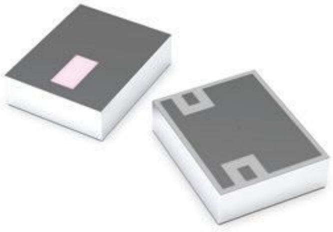

Model Number	Passband (MHz)	Stopband F3 (MHz)	Rejection @ F3 (dB)	Stopband F4 (MHz)	Rejection @ F4 (dB)
BFCQ-2702+	22000-31000	100-17100	42	35700-48000	43
BFCQ-2872+	27500-30000	100-22200	32	35300-55000	28.4
BFCQ-1932+	17700-21000	DC-14600	30	25600-40000	40
BFCQ-1982+	17700-20200	100-14500	55	24000-40000	45
BFCQ-1162+	10700-12700	100-8800	40	15100-27000	38

Mini-Circuits®

MARK YOUR CALENDAR

STAY CONNECTED TO COMING EVENTS

FEBRUARY

21-23
IMFW 2024
Cocoa Beach, Fla.
https://imfw-ieee.org

26-29
MWC Barcelona
Barcelona, Spain
www.mwcbarcelona.com

MARCH

12-14
emv 2024
Cologne, Germany
https://emv.mesago.com

17-22
EuCAP 2024
Glasgow, Scotland
www.eucap2024.org

18-21
SATELLITE
Washington, DC
www.satshow.com

APRIL

3-4
IEEE Texas Symposium
Waco, Texas
https://texassymposium.org

15-16
WAMICON 2024
Clearwater Beach, Fla.
www.ieeewamicon.org

MAY

13-15
Space Tech Expo USA
Long Beach, Calif.
www.spacetechexpo.com

20-23
CS Mantech
Tucson, Ariz.
https://csmantech.org

JUNE

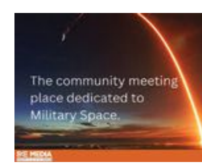

3-4
Future Military Space Technology USA
Los Angeles, Calif.
www.smgconferences.com/defence/northamerica/milspace-usa

ONLINE PANEL SERIES

3/26
Will Flat Panel Beamsteering Arrays Meet the SATCOM Challenge?

Call for Papers Deadlines

2/9	WAMICON
3/17	EuMW
5/13	IEEE Phased Array

FOR DETAILS VISIT MWJOURNAL.COM/EVENTS

TIME TRAVEL

Eric Higham
Microwave Journal

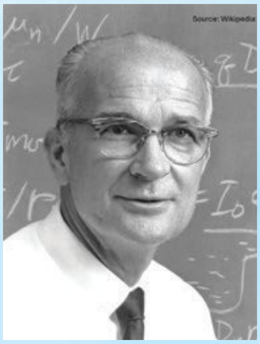

William Shockley: The Father of a Complicated Legacy

Electronics revenue is forecast to surpass $3 trillion in the next decade. Life without electronic devices is unimaginable, and these devices would not exist without the transistor. This month's Time Travel focuses on the complicated life and contributions of William Shockley, the man who co-invented the bipolar transistor and became the "Father of Silicon Valley."

Born in London in 1910, his family moved to Palo Alto, Calif., when Shockley was three. Shockley developed an interest in physics by absorbing theories from his neighbor, a physics professor, before entering high school. After receiving degrees from Caltech and MIT, Shockley became one of the first Bell Labs recruits to a group seeking to replace vacuum tubes with solid-state semiconductors.

Shockley made progress on transistor development, publishing papers and receiving a patent on electron multipliers. However, World War II interrupted his research and he left Bell Labs for radar activities. His contributions resulted in the Medal for Merit in 1946.

After the war, Shockley rejoined Bell Labs and led a group, including John Bardeen and Walter Brattain, that demonstrated a point-contact transistor design in 1947. Bell Labs patent attorneys determined Shockley's work could be inferred from earlier patents and filed the Bell Labs point-contact transistor patent without Shockley's name. This angered Shockley and he continued to develop a junction-based transistor in secret.

Shockley refined his efforts and the results came quickly. He announced the "sandwich" transistor proof of principle in 1949. He published his foundational "Electrons and Holes in Semiconductors with Applications to Transistor Electronics" in 1950 and announced the bipolar junction transistor in 1951. Shockley's singular involvement in these announcements pushed him to the forefront of transistor development at the expense of Bardeen and Brattain.

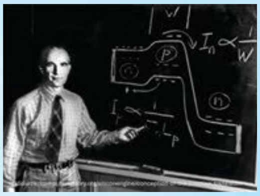

Despite Shockley, Bardeen and Brattain receiving the Nobel Prize in Physics in 1956 for their transistor development efforts, their relationship was fractured.

Shockley left Bell Labs, ultimately moving closer to his mother. In 1956, Shockley started Shockley Semiconductor Laboratory in Mountain View, Calif. Shockley's company was devoted to a silicon transistor replacement. The design proved difficult to build and Shockley ended silicon transistor research in 1957. This and Shockley's management style caused eight engineers to leave and form Fairchild Semiconductor. Among these employees, Robert Noyce and Gordon Moore went on to found Intel.

William Shockley's importance to the electronics industry is indisputable. The man is a giant in that respect. However, Shockley also adopted some reprehensible views on race, human intelligence and eugenics later in life. So, his legacy is complicated; he should be celebrated for his work on solid-state devices, but he should be denounced for the social views he came to embrace.

Cover Feature
Invited Paper

A Sub-Terahertz MIMO Testbed for 6G Research

Greg Jue
Keysight Technologies, Santa Rosa, Calif.

6G aims to be the first generation of wireless technology to improve the quality of human life by bridging the physical, digital and human worlds. Accomplishing this will mean adding artificial intelligence to networks to make them more efficient and building high-fidelity digital twins. It will also require building upon network architectures like non-terrestrial networks and highly virtualized disaggregated networks that began in 5G and expanding spectrum use.

For 6G to meet these goals, the spectrum allotted for wireless communications must be used more efficiently and new spectrum must be studied. Without expanding into new spectrum bands, it will be impossible to meet the high data throughput and volume needs of applications like immersive telepresence, virtual reality and extended reality. There are three fundamental approaches to achieving high data throughput.

One approach involves using higher-order modulation schemes such as 64-QAM to increase the number of bits transmitted for each symbol. Given a fixed and finite spectrum bandwidth, increasing the modulation order from QPSK, which transmits two bits for each symbol to 64-QAM, which transmits six bits for each symbol would increase the data throughput by a factor of three if channel conditions and radio performance allow. A 1 GHz QPSK symbol rate would result in a 2 Gbps theoretical raw calculated data throughput without forward error correction (FEC) coding rate redundancy. However, increasing the modulation order to 64-QAM would result in a 6 Gbps data throughput, while using the same spectrum-occupied bandwidth.

The second approach uses more spectrum bandwidth and increases data throughput by using a higher symbol rate. For example, with the 1 GHz symbol rate, the occupied channel bandwidth is approximately 1.22 GHz, assuming a 0.22 root-raised cosine filter alpha or excess bandwidth. Increasing the symbol rate by a factor of 10 to 10 GHz would increase the QPSK data throughput to 20 Gbps but would use a much wider swath of spectrum, approximately 12.2 GHz. However, increasing the modulation order as the symbol rates and modulation bandwidths increase becomes more challenging due to reduced signal-to-noise (SNR) ratio, greater amplitude and phase impairments and other technical challenges.

A third approach transmits multiple and independent streams of data using multiple antenna techniques such as MIMO. MIMO exploits radio channel complexity and simultaneously transmits and receives multiple and independent data streams for higher data throughput. The data throughput can be increased using 2 × 2 MIMO for the 1 GHz QPSK symbol rate by transmitting two streams of data simultaneously. The actual increase, however, would depend on the channel conditions and system overhead so this will increase the data throughput but not necessarily double it.

The second approach of using a large swath of spectrum bandwidth was previously explored and published in a *Microwave Journal* article[1] demonstrating a quasioptic over-the-air (OTA) transmission at 285 GHz with 30 GHz bandwidth. 30 GHz occupied bandwidth corresponds to a bandwidth where data throughput can exceed 100 Gbps for a single stream of data.[2] The data throughput for the quasioptic OTA transmission was calculated to be 97 Gbps without FEC coding rate redundancy using an 802.15.3d frame structure.

This article will explore and discuss the third approach of using sub-terahertz (THz) MIMO to exceed 100 Gbps. A sub-THz MIMO testbed for 6G research demonstrates simultaneous 2 × 2 MIMO at D-Band (142 GHz) and H/J-Band (285 GHz). These two sub-THz frequency bands were selected to show feasibility in two key frequency bands of interest for 6G high data throughput. The total theoretical data throughput across all four channels is calculated to be approximately 126 Gbps for cus-

tom orthogonal frequency-division multiplexing (OFDM) waveforms with a 16-QAM modulation order, transmitting OTA and using a 12.5 GHz occupied bandwidth for each signal.

SUB-THZ MIMO TESTBED FOR 6G RESEARCH

Figure 1 shows a sub-THz MIMO testbed that can be used for 6G research. An M8199A 128 GSa/s four-channel AWG generates wide bandwidth modulated IF signals. The M8199A AWG has an analog 3 dB bandwidth of 65 GHz. Channels 1 and 2 of the AWG generate wide bandwidth modulated IF signals centered at 11 GHz that are input into the Virginia Diodes Inc. (VDI) compact WR6.5 dual up-converter inputs on the top left of the four VDI converters shown in Figure 1. Channels 3 and 4 of the AWG generate wide bandwidth modulated IF signals centered at 16 GHz. These signals are input into the VDI compact WR3.4 dual up-converter inputs on the bottom left of the four VDI converters.

An M9384B VXG dual-channel microwave signal generator generates two different local oscillator (LO) signals for the VDI compact dual up-converters and dual down-converters. Channel 1 of the VXG generates a 25.5 GHz CW LO signal, which is power split with an external power splitter to provide LO signals for the WR6.5 dual up-converter on the top left and the dual down-converter on the top right of the four VDI converters. Channel 2 of the VXG generates a 22.4166 GHz CW LO signal which is power split with an external power splitter to provide the LO signals for the WR3.4 dual up-converter on the bottom left and dual down-converter on the bottom right of the four VDI converters shown in Figure 1. The LO signals are internally multiplied within the VDI WR.6.5 dual converters by a factor of six to yield a high-side LO signal of 153 GHz and a factor of 12 within the WR3.4 dual converters to yield a low-side LO signal of 269 GHz.

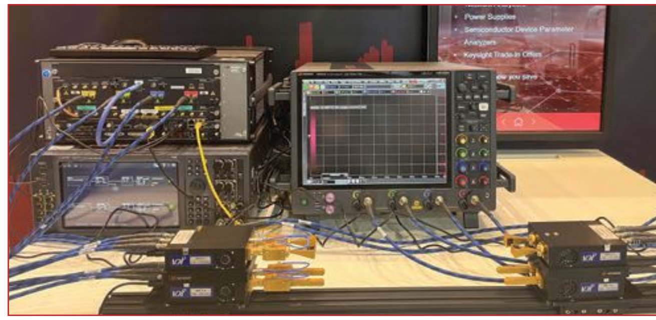

Fig. 1 Simultaneous 2 x 2 sub-THz MIMO OTA transmission at D-Band and H/J-Band.

The two 11 GHz wide bandwidth modulated IF signals are up-converted to 142 GHz by the WR6.5 dual up-converter on the top left. The two D-Band output waveguide ports have orthogonal polarization, with one output horizontally polarized and the other output vertically polarized. VDI waveguide bandpass filters are used to filter out the undesired upper sideband signals and LO feedthrough signals and pass the desired lower sideband signals of 142 GHz (153 GHz LO - 11 GHz IF = 142 GHz). The 142 GHz signals are amplified with a VDI WR6.5 waveguide amplifier and transmitted OTA with two WR6.5 rectangular horn antennas. On the receive side, the 142 GHz signals from the two receive WR6.5 rectangular horn antennas are down-converted to two 11 GHz IF signals by the WR6.5 dual down-converter shown on the top right.

The two 16 GHz wide bandwidth modulated IF signals are up-converted to 285 GHz with the WR3.4 dual up-converter shown on the bottom left of Figure 1. The two H/J-Band outputs have orthogonal polarization, with one output horizontally polarized and the other output vertically polarized. VDI waveguide highpass filters are used to filter out the undesired lower sideband signals and LO feedthrough signals and pass the desired upper sideband signals (269 GHz LO + 16

CoverFeature

GHz IF = 285 GHz). A higher IF frequency of 16 GHz is used, instead of the 11 GHz used for 142 GHz, to provide more rejection of the LO feedthrough and undesired lower sideband signal (269 GHz LO – 16 GHz IF = 253 GHz) with the highpass filter. The 285 GHz signals are amplified with a VDI WR3.4 waveguide amplifier and transmitted OTA with two WR3.4 diagonal horn antennas. On the receive side, the 285 GHz signals from the two receive WR3.4 diagonal horn antennas are downconverted to two 16 GHz IF signals with the WR3.4 dual down-converter shown in the bottom right.

The waveguide slot orientations for the WR6.5 and WR3.4 dual upconverters and dual down-converters are aligned to provide the correct horizontal or vertical polarization when the dual up-converter and down-converter waveguide ports are facing each other, as they are in Figure 1. This can be seen in the width, height and orientation of the four WR6.5 rectangular horn antennas facing each other since the width and height dimensions are different. This is more difficult to observe with the WR3.4 diagonal horn antennas since the width and height dimensions are the same.

The two 11 GHz wide bandwidth modulated IF signals from the WR6.5 dual down-converter and the two 16 GHz wide bandwidth modulated IF signals from the WR3.4 dual down-converter are input into channels 1 and 3 and channels 2 and 4 of the 33 GHz UXR four-channel real-time oscilloscope to digitize and analyze the MIMO wide bandwidth IF signals. The 33 GHz UXR has a 128 GSa/s sample rate on all four channels.

MIMO TESTBED SIGNAL GENERATION SOFTWARE

Keysight's N7068C Signal Studio Pro for Custom Modulation and N7618APPC PathWave Signal Generation Advanced Waveform Utility (PWSG AWU) are used to generate and download the custom OFDM waveforms to the M8199A AWG. The symbol index, subcarrier index, resource modulation order (QPSK, 16-QAM) and payload PN sequences can be specified for data

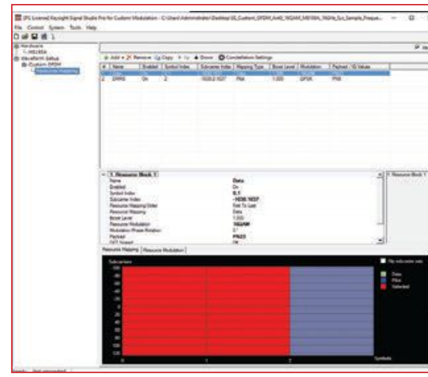

Fig. 2 N7608C custom OFDM MIMO signals.

Fig. 3 N7618APPC PathWave Signal Generation Advanced Waveform Utility display.

and DMRS resource blocks using N7068C Signal Studio Pro for Custom Modulation shown in ***Figure 2.*** The system sample frequency is set to 16 GHz and over-sampled by two to 32 GHz before exporting the .csv files.

PWSG AWU in ***Figure 3*** imports the .csv files and up-samples the waveforms to download them to the M8199A AWG using IF frequencies of 11 GHz for channels 1 and 2 and 16 GHz for channels 3 and 4.

The waveforms downloaded to the M8199A for the MIMO measurements are ideal. However, wideband channel flatness performance may not meet the test requirements when waveforms are played from real hardware. PWSG AWU provides a pre-correction wizard to automate correction filter file generation using PathWave 89600 vector signal analysis (VSA) software, which can be useful for very wide bandwidth signals at sub-THz frequencies. This pre-correction occurs by digitizing the waveforms with the UXR and then applying the reverse of the channel response from the VSA to the waveform. Users can download the waveform applied with the correction filter file to M8199A or export it to a new waveform file.

Fig. 4 **Applying precoding in N7618APPC PathWave Signal Generation Advanced Waveform Utility.**

Precoding could also have been applied in the PWSG AWU software to help maximize data throughput for non-LOS scenarios. Consider the precoding matrix shown in ***Figure 4*** for example. The two pre-coded waveforms can be generated with the phase setup shown after the two MIMO waveforms are imported as two carriers, assuming that different payload bits are used for the two waveform setups. However, the custom OFDM waveforms for this demonstration were directly mapped to the antennas and not pre-coded. Waveguide horizontal and vertical polarization were used to separate the MIMO streams of data, which was sufficient for this LOS application.

MIMO TESTBED SIGNAL ANALYSIS SOFTWARE

PathWave 89600 VSA software is used to analyze and demodulate

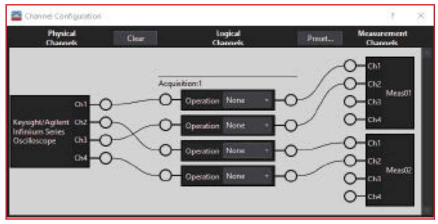

Fig. 5 **VSA channel configuration.**

the four digitized IF signals from the UXR oscilloscope. A custom channel configuration is set up in the VSA to map the UXR input channels to logical channels and VSA measurement channels shown in ***Figure 5***. UXR physical channels 1 and 3 correspond to the WR6.5 dual down-converter IF outputs. These are mapped to VSA Meas01 channels 1 and 2. UXR physical channels 2 and 4 correspond to the WR3.4 dual down-converter IF outputs. These are mapped to VSA Meas02 channels 1 and 2. Meas01 is the D-Band MIMO demodulation measurement and Meas02 is the H/J-Band MIMO demodulation measurement. The VSA measurement acquisition mode is set to acquire Meas01 and Meas02 simultaneously and not sequenced. VSA multi-measurement is set up to process and display multiple MIMO measurements (Meas01 and Meas02) concurrently.

For the VSA demodulation setup, the 89600 VSA setup files are exported from N7068C Signal Studio Pro for Custom Modulation with the OFDM setup parameters specified previously for signal generation. These parameters include, for example, symbol index, subcarrier index, resource modulation order and payload PN sequences for DMRS resource blocks. Equalizer and tracking parameters are set in the VSA software for the physical testbed measurement, for example, least squares equalizer averaging mode.

VSA demodulation of the simultaneous 2 × 2 custom OFDM MIMO signals at 142 GHz and 285 GHz is shown in ***Figure 6***. Two PSG signal generators with option UNY were used for the two LO signals, instead of the VXG dual-channel

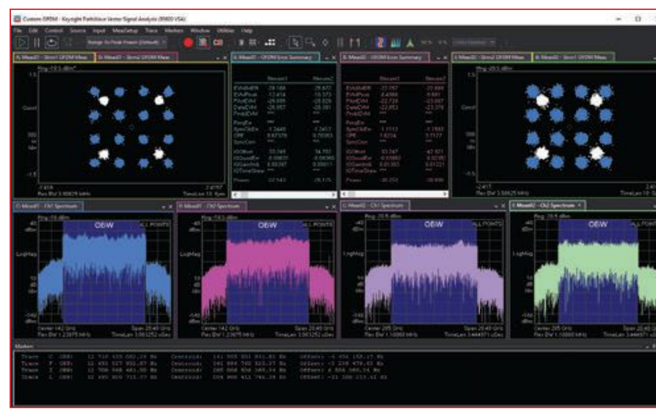

Fig. 6 **Display of VSA demodulation of custom OFDM MIMO signals.**

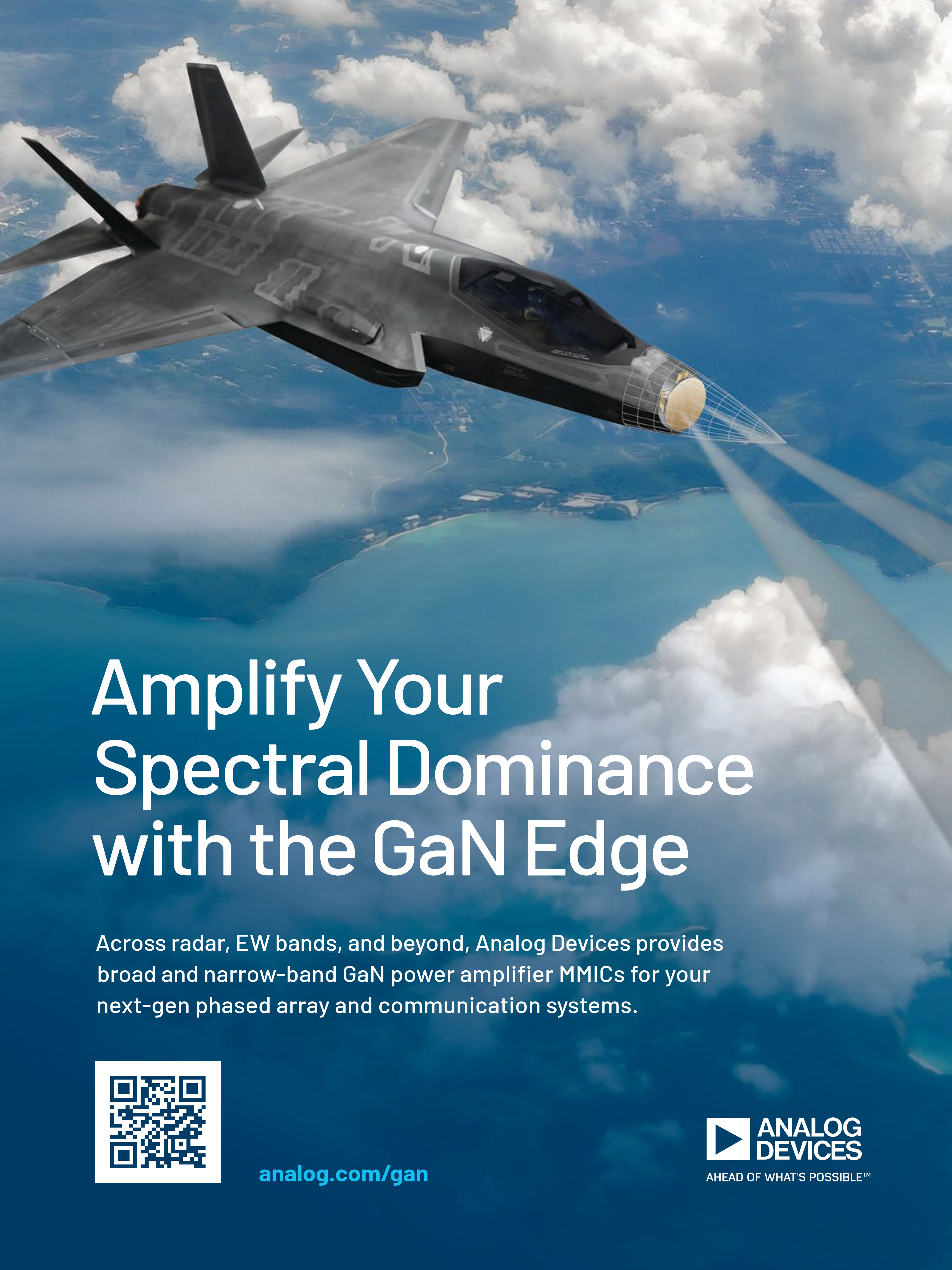
Amplify Your Spectral Dominance with the GaN Edge
Across radar, EW bands, and beyond, Analog Devices provides broad and narrow-band GaN power amplifier MMICs for your next-gen phased array and communication systems.
analog.com/gan
ANALOG DEVICES
AHEAD OF WHAT'S POSSIBLE™

signal generator shown in Figure 1. In addition, a four-channel 110 GHz UXR was used instead of the 33 GHz UXR. Pre-corrections were applied with PWSG AWU for the waveguide-to-waveguide connected signal path including the AWG, VDI dual up-converters, VDI filters, VDI dual down-converters and UXR. The VDI amplifiers and horn antennas were not included in the pre-corrections.

The 142 GHz MIMO demodulation results are shown on the left of Figure 6 and the 285 GHz MIMO demodulation results are shown on the right of Figure 6. The 16-QAM constellation and OFDM error summary tables are shown on the top row of the display in Figure 6 for 142 GHz (left) and 285 GHz (right). The four spectrum measurements are shown in the middle row for 142 GHz channels 1 and 2 (left two spectrums) and 285 GHz channels 1 and 2 (right two spectrums). The measured occupied bandwidths of each of the four spectrum measurements are shown at the bottom of the VSA display in Figure 6. The occupied bandwidths are measured to be approximately 12.5 GHz for each of the four sub-THz signals.

For simultaneous 2 × 2 custom OFDM MIMO signals at 142 GHz and 285 GHz, the total theoretical data throughput across all four channels is calculated to be approximately 126 Gbps for a 16-QAM modulation order. Although a specific MIMO configuration is shown in this example for demonstration purposes, the testbed is flexible for emerging sub-THz MIMO research. The flexibility of software combined with flexible multichannel instruments in this testbed can be used to research and explore candidate 6G MIMO waveforms and to evaluate their performance for various MIMO configurations at different frequencies and bandwidths.

SUMMARY

Using sub-THz MIMO to transmit multiple independent streams of data using multiple antenna techniques is one approach for achieving 100 Gbps data throughput for 6G. Alternatively, or additionally, using extreme SISO transmission bandwidths, such as 30 GHz bandwidth at 285 GHz, is another approach for achieving 100 Gbps. The sub-THz MIMO testbed for 6G research discussed in this article demonstrates an example of using sub-THz MIMO to exceed 100 Gbps.

Simultaneous 2 × 2 MIMO at D-Band (142 GHz) and H/J-Band (285 GHz) is demonstrated using VDI compact WR6.5 and WR3.4 dual up-converters and dual down-converters with horizontal and vertical polarization. The total theoretical data throughput across all four channels is calculated to be approximately 126 Gbps for a 16-QAM modulation order. These data rates were obtained while transmitting OTA and using a 12.5 GHz occupied bandwidth for each signal.

Custom OFDM MIMO waveforms were generated and analyzed using flexible signal generation and analysis software for candidate 6G waveform research. Precoding could have also been applied using signal generation software. Combining flexible signal generation and analysis software with flexible multichannel high performance AWGs, multichannel microwave sources, multichannel high performance oscilloscopes and VDI compact dual up-converters and down-converters provides a high performance and flexible testbed for emerging sub-THz 6G MIMO research. ■

References

1. "A Quasioptic OTA Transmission at 285 GHz with 30 GHz Bandwidth," *Keysight*, 2022, Web: https://www.microwavejournal.com/articles/39772-a-quasioptic-ota-transmission-at-285-ghz-with-30-ghz-bandwidth.
2. "6G: Going Beyond 100 Gbps 1o 1 Tbps," *Keysight*, 2021, Web: https://www.keysight.com/zz/en/assets/7121-1152/white-papers/6G-Going-Beyond-100-Gbps-to-1-Tbps.pdf.

RF-LAMBDA

MADE IN USA

THE LEADER OF RF BROADBAND SOLUTIONS

EMC Broadband RF Power Amplifier

High Power Solid State

HUNDREDS IN STOCK

FAST SHIPPING

FREQUENCY UP TO 90GHZ

POWER UP TO 2KW CW

REMC06G18GG

6-18GHZ 300W

- AUTOMATIC BUILT IN SELF CALIBRATION AND BIAS ADJUSTMENT.
- OVER TEMPERATURE, CURRENT, INPUT POWER PROTECTION.
- VSWR MEASUREMENT AND OPEN CIRCUIT PROTECTION.
- USER FRIENDLY CONTROL INTERFACE.
- REMOTE ETHERNET CONTROL AND FIRMWARE UPDATE.
- HIGH POWER EFFICIENCY AND LIGHTWEIGHT.

RAMP42G47GA 42-47GHZ 8W

RAMP18G40GB-U 18-40G 20W

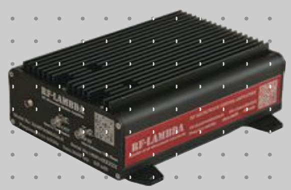

RAMP05M80GC 0.5-80GHZ

REMC02G06GE 2-6GHZ 500W

REMC08G11GE 8-11GHZ 400W

RF Amplifiers and Sub-Assemblies for Every Application

Delivery from Stock to 2 Weeks ARO from the catalog or built to your specifications!

- Competitive Pricing & Fast Delivery
- Military Reliability & Qualification
- Various Options: Temperature Compensation, Input Limiter Protection, Detectors/TTL & More
- Unconditionally Stable (100% tested)

ISO 9001:2000 and AS9100B CERTIFIED

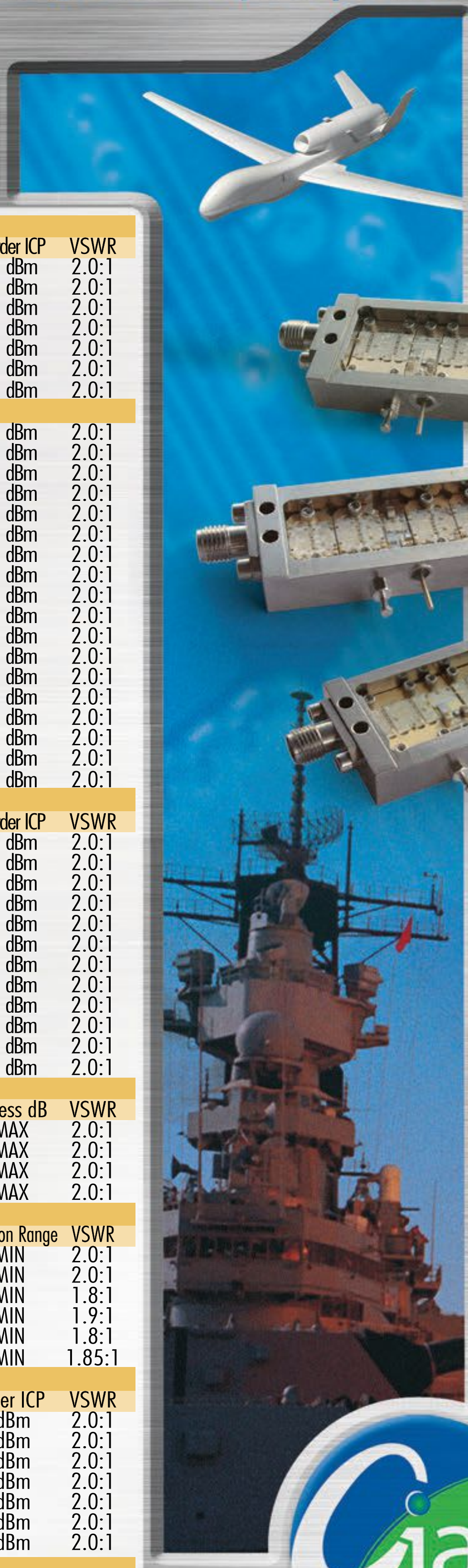

OCTAVE BAND LOW NOISE AMPLIFIERS

Model No.	Freq (GHz)	Gain (dB) MIN	Noise Figure (dB)	Power-out @ P1-dB	3rd Order ICP	VSWR
CA01-2110	0.5-1.0	28	1.0 MAX, 0.7 TYP	+10 MIN	+20 dBm	2.0:1
CA12-2110	1.0-2.0	30	1.0 MAX, 0.7 TYP	+10 MIN	+20 dBm	2.0:1
CA24-2111	2.0-4.0	29	1.1 MAX, 0.95 TYP	+10 MIN	+20 dBm	2.0:1
CA48-2111	4.0-8.0	29	1.3 MAX, 1.0 TYP	+10 MIN	+20 dBm	2.0:1
CA812-3111	8.0-12.0	27	1.6 MAX, 1.4 TYP	+10 MIN	+20 dBm	2.0:1
CA1218-4111	12.0-18.0	25	1.9 MAX, 1.7 TYP	+10 MIN	+20 dBm	2.0:1
CA1826-2110	18.0-26.5	32	3.0 MAX, 2.5 TYP	+10 MIN	+20 dBm	2.0:1

NARROW BAND LOW NOISE AND MEDIUM POWER AMPLIFIERS

Model No.	Freq (GHz)	Gain (dB) MIN	Noise Figure (dB)	Power-out @ P1-dB	3rd Order ICP	VSWR
CA01-2111	0.4 - 0.5	28	0.6 MAX, 0.4 TYP	+10 MIN	+20 dBm	2.0:1
CA01-2113	0.8 - 1.0	28	0.6 MAX, 0.4 TYP	+10 MIN	+20 dBm	2.0:1
CA12-3117	1.2 - 1.6	25	0.6 MAX, 0.4 TYP	+10 MIN	+20 dBm	2.0:1
CA23-3111	2.2 - 2.4	30	0.6 MAX, 0.45 TYP	+10 MIN	+20 dBm	2.0:1
CA23-3116	2.7 - 2.9	29	0.7 MAX, 0.5 TYP	+10 MIN	+20 dBm	2.0:1
CA34-2110	3.7 - 4.2	28	1.0 MAX, 0.5 TYP	+10 MIN	+20 dBm	2.0:1
CA56-3110	5.4 - 5.9	40	1.0 MAX, 0.5 TYP	+10 MIN	+20 dBm	2.0:1
CA78-4110	7.25 - 7.75	32	1.2 MAX, 1.0 TYP	+10 MIN	+20 dBm	2.0:1
CA910-3110	9.0 - 10.6	25	1.4 MAX, 1.2 TYP	+10 MIN	+20 dBm	2.0:1
CA1315-3110	13.75 - 15.4	25	1.6 MAX, 1.4 TYP	+10 MIN	+20 dBm	2.0:1
CA12-3114	1.35 - 1.85	30	4.0 MAX, 3.0 TYP	+33 MIN	+41 dBm	2.0:1
CA34-6116	3.1 - 3.5	40	4.5 MAX, 3.5 TYP	+35 MIN	+43 dBm	2.0:1
CA56-5114	5.9 - 6.4	30	5.0 MAX, 4.0 TYP	+30 MIN	+40 dBm	2.0:1
CA812-6115	8.0 - 12.0	30	4.5 MAX, 3.5 TYP	+30 MIN	+40 dBm	2.0:1
CA812-6116	8.0 - 12.0	30	5.0 MAX, 4.0 TYP	+33 MIN	+41 dBm	2.0:1
CA1213-7110	12.2 - 13.25	28	6.0 MAX, 5.5 TYP	+33 MIN	+42 dBm	2.0:1
CA1415-7110	14.0 - 15.0	30	5.0 MAX, 4.0 TYP	+30 MIN	+40 dBm	2.0:1
CA1722-4110	17.0 - 22.0	25	3.5 MAX, 2.8 TYP	+21 MIN	+31 dBm	2.0:1

ULTRA-BROADBAND & MULTI-OCTAVE BAND AMPLIFIERS

Model No.	Freq (GHz)	Gain (dB) MIN	Noise Figure (dB)	Power-out @ P1-dB	3rd Order ICP	VSWR
CA0102-3111	0.1-2.0	28	1.6 Max, 1.2 TYP	+10 MIN	+20 dBm	2.0:1
CA0106-3111	0.1-6.0	28	1.9 Max, 1.5 TYP	+10 MIN	+20 dBm	2.0:1
CA0108-3110	0.1-8.0	26	2.2 Max, 1.8 TYP	+10 MIN	+20 dBm	2.0:1
CA0108-4112	0.1-8.0	32	3.0 MAX, 1.8 TYP	+22 MIN	+32 dBm	2.0:1
CA02-3112	0.5-2.0	36	4.5 MAX, 2.5 TYP	+30 MIN	+40 dBm	2.0:1
CA26-3110	2.0-6.0	26	2.0 MAX, 1.5 TYP	+10 MIN	+20 dBm	2.0:1
CA26-4114	2.0-6.0	22	5.0 MAX, 3.5 TYP	+30 MIN	+40 dBm	2.0:1
CA618-4112	6.0-18.0	25	5.0 MAX, 3.5 TYP	+23 MIN	+33 dBm	2.0:1
CA618-6114	6.0-18.0	35	5.0 MAX, 3.5 TYP	+30 MIN	+40 dBm	2.0:1
CA218-4116	2.0-18.0	30	3.5 MAX, 2.8 TYP	+10 MIN	+20 dBm	2.0:1
CA218-4110	2.0-18.0	30	5.0 MAX, 3.5 TYP	+20 MIN	+30 dBm	2.0:1
CA218-4112	2.0-18.0	29	5.0 MAX, 3.5 TYP	+24 MIN	+34 dBm	2.0:1

LIMITING AMPLIFIERS

Model No.	Freq (GHz)	Input Dynamic Range	Output Power Range Psat	Power Flatness dB	VSWR
CLA24-4001	2.0 - 4.0	-28 to +10 dBm	+7 to +11 dBm	+/- 1.5 MAX	2.0:1
CLA26-8001	2.0 - 6.0	-50 to +20 dBm	+14 to +18 dBm	+/- 1.5 MAX	2.0:1
CLA712-5001	7.0 - 12.4	-21 to +10 dBm	+14 to +19 dBm	+/- 1.5 MAX	2.0:1
CLA618-1201	6.0 - 18.0	-50 to +20 dBm	+14 to +19 dBm	+/- 1.5 MAX	2.0:1

AMPLIFIERS WITH INTEGRATED GAIN ATTENUATION

Model No.	Freq (GHz)	Gain (dB) MIN	Noise Figure (dB)	Power-out @ P1-dB	Gain Attenuation Range	VSWR
CA001-2511A	0.025-0.150	21	5.0 MAX, 3.5 TYP	+12 MIN	30 dB MIN	2.0:1
CA05-3110A	0.5-5.5	23	2.5 MAX, 1.5 TYP	+18 MIN	20 dB MIN	2.0:1
CA56-3110A	5.85-6.425	28	2.5 MAX, 1.5 TYP	+16 MIN	22 dB MIN	1.8:1
CA612-4110A	6.0-12.0	24	2.5 MAX, 1.5 TYP	+12 MIN	15 dB MIN	1.9:1
CA1315-4110A	13.75-15.4	25	2.2 MAX, 1.6 TYP	+16 MIN	20 dB MIN	1.8:1
CA1518-4110A	15.0-18.0	30	3.0 MAX, 2.0 TYP	+18 MIN	20 dB MIN	1.85:1

LOW FREQUENCY AMPLIFIERS

Model No.	Freq (GHz)	Gain (dB) MIN	Noise Figure dB	Power-out @ P1-dB	3rd Order ICP	VSWR
CA001-2110	0.01-0.10	18	4.0 MAX, 2.2 TYP	+10 MIN	+20 dBm	2.0:1
CA001-2211	0.04-0.15	24	3.5 MAX, 2.2 TYP	+13 MIN	+23 dBm	2.0:1
CA001-2215	0.04-0.15	23	4.0 MAX, 2.2 TYP	+23 MIN	+33 dBm	2.0:1
CA001-3113	0.01-1.0	28	4.0 MAX, 2.8 TYP	+17 MIN	+27 dBm	2.0:1
CA002-3114	0.01-2.0	27	4.0 MAX, 2.8 TYP	+20 MIN	+30 dBm	2.0:1
CA003-3116	0.01-3.0	18	4.0 MAX, 2.8 TYP	+25 MIN	+35 dBm	2.0:1
CA004-3112	0.01-4.0	32	4.0 MAX, 2.8 TYP	+15 MIN	+25 dBm	2.0:1

CIAO Wireless can easily modify any of its standard models to meet your "exact" requirements at the Catalog Pricing.

Visit our web site at www.ciaowireless.com for our complete product offering.

Ciao wireless

Ciao Wireless, Inc. 4000 Via Pescador, Camarillo, CA 93012

Tel (805) 389-3224 Fax (805) 389-3629 sales@ciaowireless.com

RTX's Raytheon to Build Defensive Microwave Antenna Systems for U.S. Military

RTX's Raytheon business will design, build and test two high-power microwave (HPM) antenna systems that will use directed energy to defeat airborne threats at the speed of light. The systems are designed to be rugged and transportable for front-line deployment.

Under the three-year, $31.3 million contract from the Naval Surface Warfare Center Dahlgren Division, Raytheon will deliver prototype systems to the U.S. Navy and U.S. Air Force as part of the Directed Energy Frontline Electromagnetic Neutralization and Defeat (DEFEND) program.

The new HPM prototype systems build on Raytheon's decades of experience developing capabilities like the Counter-Electronic High-Power Microwave Extended Range Air Base Defense, known as CHIMERA.

Work on this contract is being conducted in Tucson, Ariz., in partnership with the U.S. Air Force Research Lab, Naval Surface Warfare Center Dahlgren Division and the Undersecretary of Defense for Research and Engineering. Prototypes are expected to be delivered in fiscal years 2024 and 2026.

HPM-Two Domains (Source: RTX)

LM, Verizon Demo 5G Streaming for Sustainment Applications

Lockheed Martin (LM) Skunk Works® and Verizon recently demonstrated 5G streaming for real-time visualization content on edge computing devices to advance Department of Defense sustainment missions.

As part of an ongoing strategic collaboration, the companies validated three key technology areas:

- 5G at the edge for latency-critical interactions of complex visualization applications such as augmented (AR), virtual (VR) or extended reality (ER) experiences
- Streaming of real-time, complex, 3D visualization content
- Streaming to edge compute devices including tablets, mobile, head mounted displays and more.

These technologies enable Lockheed Martin's "Maintainer as a Node" concept, by which a connected maintainer receives all the information where, when and how it is needed in a latency-critical environment.

In 2023, Lockheed Martin and Verizon focused on content streaming for sustainment use cases where advanced visualization capabilities are critical to supporting the maintainer with Resilient Logistics in a Contested Environment (RLCE). Examples of these use cases include:

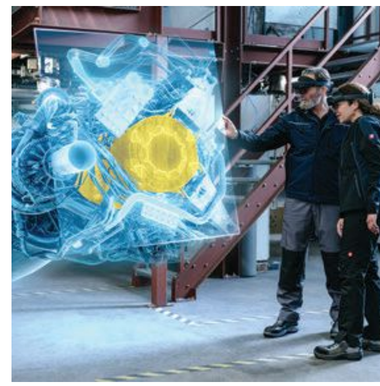

Hololight Raptor Engine (Source: Lockheed Martin)

- 3D step-based work instructions
- AR/VR/ER content deployment
- Remote desktop of high-end, real-time, 3D applications scenarios
- Remote assistance and other 3D graphically intensive applications.

The cases demonstrated a multi-user, AR experience across multiple geolocations streaming a large 3D CAD airspace engine in real-time. The target display device was a HoloLens, which used the project collaborator Holo-Light's streaming platform along with Verizon 5G Edge with AWS Wavelength over Verizon's 5G network.

RTX to Create Network of "Energy Webs" for DARPA

RTX's Raytheon business has received a $10 million contract from DARPA to design and develop a wireless airborne relay system to deliver energy into contested environments.

The Persistent Optical Wireless Energy Relay (POWER) program aims to revolutionize energy distribution by leveraging power beaming for near-instantaneous energy transport in a resilient, multi-path network.

Under the two-year contract, Raytheon will create an airborne relay design to enable "webs" capable of harvesting, transmitting and redirecting optical beams. These "webs" will transmit energy from ground sources to high altitude for the precision, long-range operation of unmanned systems, sensors and effectors. Harvesting energy will ultimately reduce the military's dependence on fuel as well as its delivery and storage.

The POWER program is part of DARPA's Energy Web Dominance portfolio, which aims to establish more

For More Information Visit mwjournal.com for more defense news.

Wireless Energy Transmission (Source: DARPA)

dynamic energy transport across air, space, maritime, land and undersea domains. By establishing energy web dominance, military commanders will be able to reroute energy in a matter of seconds or minutes, enabling them to pivot capability nearly instantaneously without reconfiguring supply lines.

U.S. Navy and LM Successfully Test Key Capabilities of Advanced Off-Board EW System

Lockheed Martin supported a successful government test of the Advanced Off-Board Electronic Warfare (AOEW) system's electronic attack capabilities while installed on a U.S. Navy MH-60R helicopter. This marked the first time in the program's development the system was able to perform engagement testing, demonstrate the ability to defeat threats and quantify system performance, while integrated and controlled by the target platform.

In partnership with the U.S. Navy at Naval Air Station Patuxent River in Maryland, this integration event tested the capabilities of the system and operability on the MH-60R helicopter platform. While the system is designed for both the MH-60R and MR-60S host platforms, only the MH-60R was used for this test.

MH-60R (Source: U.S. Navy)

AOEW is a pod-based EW missile defense system that will provide the U.S. Navy with enhanced electronic surveillance and attack capabilities against anti-ship missile threats. To date, the system has successfully undergone a series of incremental developmental and operational tests at Lockheed Martin's facility in Syracuse, N.Y.

Currently, AOEW is under a low-rate initial production contract and deliveries of the first AOEW units are expected in 2024.

Wireless Broadband Alliance – 10 Wi-Fi Predictions for 2024

Following the release of the Wireless Broadband Alliance (WBA) Annual Industry Report 2024, Tiago Rodrigues, CEO of the WBA, has revealed 10 predictions for 2024 and beyond that he believes will change the way wireless technology is used by communities and businesses across the world, including improved connectivity, efficiencies and new consumer experiences.

1. In the future 10 Gbps speeds will be commonplace. Fiber broadband deployments will continue to expand in most developed and developing markets, creating a need for an upgrade of home Wi-Fi networks to pass on the increased bandwidth to the device, which will drive the rapid adoption of Wi-Fi 6E and Wi-Fi 7. The rapid adoption of Wi-Fi 6E/7 will also be driven by its ability to access additional spectrum in the 6 GHz band as more countries open the band.

2. The capabilities of Wi-Fi 7 will drive immersive experiences and advance gaming and video content. In a sport where milliseconds count, networking equipment will be just as crucial to the game as the speed of the gaming rig. Wi-Fi 7 will be critical for speed and near-zero latency, and game developers will break new barriers with immersive experiences. Wi-Fi 7 client devices have already been released in 2023 with Qualcomm chipset with more to come in 2024.

> There has never been a more exciting time for Wi-Fi

3. OpenRoaming growth will continue and extend to integrate with private 5G and IoT networks in 2024, reaching a critical point of exponential growth by 2026 when tens of millions of hotspots will be enabled. Deployments of OpenRoaming (with Passpoint), continue to rise as more brands and identity providers recognize the value of the federation to enable seamless connectivity access across different networks.

4. Convergence will progress, enabling access to private and/or public 5G services over Wi-Fi. We expect network executives will continue deploying Wi-Fi and cellular in the coming years, with Wi-Fi 6E/7 for indoor, on-campus and fixed network situations and 5G/cellular for outdoor, off-campus and mobile environments. Rather than competing with 5G over emerging high performance use cases, the Wi-Fi community continues to work on coexistence with 5G, especially around identity management, authentication and policy management.

5. Network as a Service (NaaS) will rise beyond early adopters (e.g. managed Wi-Fi in multi-apartment units) spreading quickly to traditional enterprises where networks provide cloud-first, software-defined, application-centric environments. NaaS is attracting customers because it accelerates and simplifies the deployment of devices in today's shortened equipment replacement and improves security with the delivery of continuous security updates that prevent and reduce breaches and outages.

6. The role of artificial intelligence (AI) and machine learning cannot be overstated, with Adaptive AI set to explode on networks, from enabling automated frequency coordination (AFC) to predicting network resourcing needs. AI will help enterprises and ISPs speed up troubleshooting; streamline monitoring; and proactively anticipate outages, equipment failures and performance degradation.

7. Outdoor AFC will initially be successful in rural connectivity, in countries that have opened large portions of the 6 GHz spectrum to Wi-Fi. We expect 6 GHz low-power indoor devices with an average transmit power of 24 dBm to proliferate quickly for indoor applications such as residential mesh, indoor public venues and high-density enterprise networks. We also expect 6 GHz very low-power indoor devices with 14 dBm maximum transmit power to be quickly adopted for short-range indoor applications such as augmented (AR), virtual (VR) and extended reality, streaming and gaming. These device classes do not require AFC coordination with the incumbents.

8. New IoT technology will help unify connectivity across multiple home devices, transforming home users' experience with IoT devices. Matter — a new industry standard launched in 2023 provides reliable, secure connectivity across multiple device manufacturers. Given the weight of players involved (e.g., Apple, Amazon, Google, Samsung SmartThings), we expect the adoption of Matter-certified products will be exponential in the next three years, validating Wi-Fi's central role in smart connected homes and buildings.

9. Pilot projects and trials of Telecom Infra Project Open Wi-Fi will proliferate in developing countries and price-sensitive markets due to its cost-effectiveness and the benefits offered by an open disaggregated model. Well-established wireless local-area network vendors will continue working to make themselves more cost-effective in these markets through massive investment in ML and AI and an integrated Wi-Fi and 5G offering to enterprises.

10. AR and VR will gain a larger share of our daily lives at home and work, but it will require indoor broadband networks to adapt with improvements in user interfaces and network capabilities to cater to a larger group of users. According to Bloomberg, the metaverse's economy is expected to generate $800 billion by 2025 and $2.5 trillion by 2030. Thus, the metaverse is the universe of the future. Major brands are making substantial investments in this technology.

For More Information
Visit mwjournal.com for more commercial market news.

Direct-to-Phone Satellite Connectivity to Revolutionize the Satcom Industry

The latest edition of Euroconsult's "Prospects for Direct-to-Handheld and IoT Markets" unveils the developing potential of the satellite direct-to-device market, with projections indicating that direct-to-phone services could connect nearly 130 million average monthly users by 2032.

Satellite cellular IoT is a niche market enabling hybrid solutions via in-market unmodified IoT devices with a high market potential due to the ease of implementation. Non-geostationary orbit satellite constellations are playing an increasingly pivotal role in creating new opportunities to seamlessly integrate satellite connectivity into existing devices.

This surge in direct-to-device satellite connectivity is also being fueled by advancements in the 3rd Generation Partnership Project (3GPP) standards (specifically Release 17), facilitating the integration of terrestrial and non-terrestrial networks.

Consistent with a forecasted decline in-market demand and the cannibalization of competing services, Euroconsult's report asserts that traditional handheld phone users will decline by nearly half, while the direct-to-phone market will see a rising user count by 2032 to around 130 million. In addition, IoT devices are expected to triple over the coming decade, largely due to the increased accessibility of satellite IoT solutions offered by new market entrants.

Addressing the potential 'unconnected' population, the direct-to-phone segment eyes a total satellite connectivity market of over 2 billion subscribers in 2022. This segment targets individuals without terrestrial network coverage (1.9 billion) and mobile users encountering connectivity issues due to poor terrestrial network coverage or travel to areas without coverage (130 million).

> **Transformative shift due to the rapid rise of direct-to-device satellite solutions.**

Expanding the market's horizons further, the IoT segment is set to substantially increase its potential as a revenue-generating force with satellite cellular IoT anticipated to commence revenue generation in 2025. Key applications expected to drive this growth include 'connected cars' in transport/logistics, smart cities in natural resources (oil rigs, mining sites, utilities) and personal tracking assets like smartwatches. Projections forecast a substantial addressable market of 10.6 billion cellular IoT devices by 2032.

Around the **Circuit**

Barbara Walsh, Multimedia Staff Editor

MERGERS & ACQUISITIONS

PCTEL Inc., a global provider of wireless technology solutions, announced that it has been acquired by **Amphenol Corporation**, a provider of high-tech interconnect, sensor and antenna solutions. Under the terms of the previously announced agreement, PCTEL stockholders are receiving $7.00 in cash for each share of common stock they own. Following the acquisition, PCTEL is a wholly owned subsidiary of Amphenol and PCTEL shares are no longer publicly traded. PCTEL provides purpose-built industrial IoT devices, antenna systems and test and measurement products.

Mobix Labs Inc., a fabless semiconductor company developing disruptive next-generation connectivity technologies for 5G infrastructure, satellite communications and defense industries, announced that it has closed its previously reported acquisition of **EMI Solutions**, an Irvine-based manufacturer of electromagnetic interference filtering products for military and aerospace applications. This strategic move marks a significant milestone for Mobix Labs and positions the company for accelerated growth by gaining access to new high-reliability customers and markets. EMI Solutions has more than 20 years of acquired expertise and is recognized as the leading small business manufacturer of EMI filtering products for the military and aerospace supply chain.

CML Micro has acquired **MwT**, a leading MMIC and mmWave supplier based in California, U.S. The acquisition will bring together the capabilities of CML Micro and MwT, positioning the expanded company at the forefront of emerging markets and providing a broader and deeper RF and mmWave device portfolio for wireless communications. The strategic move expands CML Micro's product portfolio, bolstering the SμRF product brand with a broader range of GaAs and GaN MMICs as well as introducing discrete devices and hybrid amplifier products. This influx of new products and capabilities also strengthens CML Micro's ability to meet evolving needs in communication applications with higher frequency devices and increased module capabilities.

COLLABORATIONS

Richardson Electronics Ltd. announced a partnership with **Integrated Power Services (IPS)** in North America. This partnership allows IPS to supply and install Richardson's patented ULTRA3000® pitch energy module to key customers in North America. The IPS Renewables Business provides single-source capabilities for fleets operating wind turbines during warranty and after warranty for the asset life of the machines. IPS engineers repair, replace and remanufacture to minimize downtime and support run-time commitments. IPS is a distributor for key OEMs, with local, regional and national inventories, plus a network of used and surplus equipment suppliers.

NEW STARTS

Altum RF announced its expanded production and reliability testing infrastructure in Eindhoven, the Netherlands. The expansion supports growing business demands. This investment in both production and reliability testing includes equipment and infrastructure to automate low- to medium-volume series production testing, allowing quick response to customer interest in Altum RF's products. Also, Altum RF added more capability to do extensive over-temperature product reliability testing. This equipment includes an automated pick and place IC test system for RF and DC production test and high temperature operating life system for product reliability testing. Key features include a versatile teaching tool compatible with any oscilloscope manufacturer, built-in waveform generator for diverse signal demonstrations and advanced triggering capabilities for precise signal analysis.

ACHIEVEMENTS

On Tuesday, January 2, **Falcon 9** launched 21 Starlink satellites into low-earth orbit from Space Launch Complex 4 East (SLC-4E) at Vandenberg Space Force Base in California. This was the first flight for the first stage booster supporting this mission. This launch included the first six Starlink satellites with direct to cell capabilities that enable mobile network operators around the world to provide seamless global access to texting, calling and browsing wherever you may be on land, lakes or coastal waters without changing hardware or firmware. The enhanced Starlink satellites have an advanced modem that acts as a cellphone tower in space, eliminating dead zones with network integration similar to a standard roaming partner.

CONTRACTS

The **NATO Support and Procurement Agency (NSPA)** has awarded **COMLOG**, a joint venture between **Raytheon** and **MBDA**, their first contract under the European Sky Shield Initiative. With a total value of up to $5.6 billion, the NSPA contract supports a coalition of nations, including Germany, the Netherlands, Romania and Spain, with a combined quantity of up to 1,000 Patriot® GEM-T missiles, if all options are exercised. The contract includes the qualification of updated components, addition of new suppliers, test equipment and spares to support future sustainment. To support delivery, COMLOG will expand the production capacity of GEM-T missiles in Europe.

Viasat Inc. announced it will work with the **U.S. Air Force's Life Cycle Management Center (USAF's LCMC)** to transition and integrate new innovative technologies and capabilities as part of a $900 million ceil-

For More Information For up-to-date news briefs, visit mwjournal.com

DUAL or SINGLE LOOP
SYNTHESIZER & PLO MODULES

Up to 30 GHz*

Features:

- Proprietary digital Integer and Fractional PLL technology
- Lowest digital noise floor available -237 dBc/Hz figure of merit
- Output frequencies from 100 MHz locked crystal to 30 GHz
- Available with reference clean up dual loop, or single loop for very low noise reference
- Parallel fixed band stepping or SPI interface synthesized up to octave bandwidths
- Reference input range 1 MHz to 1.5 GHz
- Dual RF output or reference sample output available
- +12 dBm standard output power +16 dBm available
- Standard module size 2.25 X 2.25 X 0.5 Inches (LxWxH)
- Standard operating temperature -10 to 60 °C, -40 to +85 °C available

Applications:

- SATCOM, RADAR, MICROWAVE RADIO

* *16 - 30 GHz with added x2 module < 1" in height.*

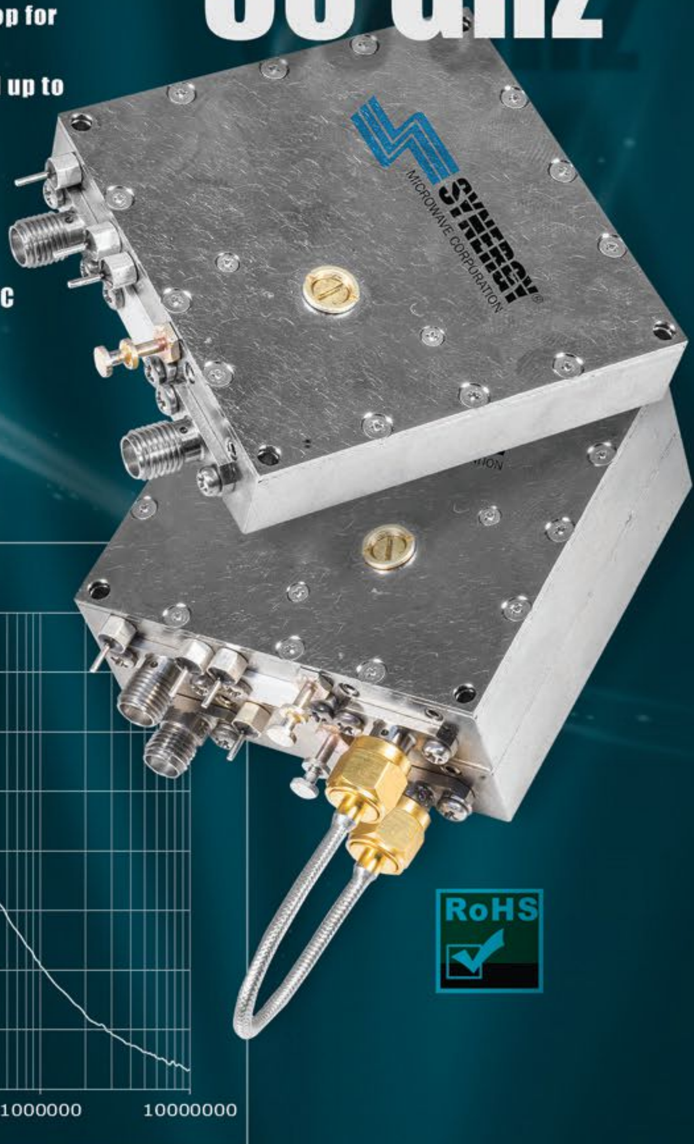

Talk To Us About Your Custom Requirements.

SYNERGY® MICROWAVE CORPORATION

Phone: (973) 881-8800 | Fax: (973) 881-8361
E-mail: sales@synergymwave.com
Web: WWW.SYNERGYMWAVE.COM
Mail: 201 McLean Boulevard, Paterson, NJ 07504

ing, indefinite delivery/indefinite quantity (IDIQ) contract. Under the multi-award contract, known by its initialism LCMC XA IDIQ, Viasat is expected to prototype and test systems, hardware, software and cybersecurity solutions to provide integrated, multi-domain capabilities for the USAF. Viasat experts will accelerate and expand technology integration across the USAF. The contract has an approximate five-year term, with options for up to an additional five years.

The **U.S. Department of Commerce** has announced approximately $35 million in initial funding for **BAE Systems** to modernize the Microelectronics Center (MEC) in Nashua, N.H. This is the first funding announcement as part of the CHIPS and Science Act, which was designed to strengthen American manufacturing, supply chains and national security. Modernizing BAE Systems' MEC helps support this vision and the continued development and manufacturing of cutting-edge technology to serve customers' missions. BAE Systems' MEC is a 110,000-square-foot, Department of Defense (DOD)-accredited, semiconductor chip fabrication and foundry facility that produces technology for DOD applications. The MEC develops advanced semiconductor technologies beyond those available commercially to meet demanding military requirements.

A major order for its AARTOS drone detection system highlights **AARONIA**'s 2023 financial statements. With a total volume of 20 million U.S. dollars, this is the largest single order for the AARTOS DDS to date. The system can be modularly adapted to a wide range of requirements and is currently the most powerful on the market. With AARTOS DDS, **AARONIA AG** offers particularly flexible, customizable solutions for all requirements and budgets. From the mobile laptop versions X2 and X5 for limited applications to the high-end solutions X7 and X9. AARTOS thus covers all civil and military areas in which drones can pose a threat.

Orbital Micro Systems (OMS), the instrument design and manufacturing subsidiary of **Weather Stream Inc.**, announced it was awarded a $1.7 million Small Business Innovation Research Phase II Other Transaction Authority agreement by the **U.S. Space Force's Space Development Agency**. The agreement was awarded to OMS for prototype design, production and testing of the Global Environmental Monitoring System – Passive and Exchangeable Advanced Radiometers for low earth orbit (GEMS-PEARL) microwave imager and sounder payloads. Under the agreement, OMS will build engineering prototypes of the GEMS-PEARL radiometers and perform extensive laboratory testing and characterization of key subsystems as well as validating the expected performance of retrieved environmental data products.

Sivers Semiconductors AB announced that its business unit, Sivers Wireless, has been granted €1.2 million (approximately 14 MSEK) EU Grant from **HORIZON Europe** as part of a larger consortium, to design mmWave building blocks for next-generation 6G technology. The grant

will cover 90 percent of Sivers funding for the 6G project and run for 3.5 years, 50 percent of the funding was paid out before year end by EU. Sivers Wireless will be responsible for the below 100 GHz front-end design and, in addition, Sivers will also co-design a wideband off-chip antenna with the front-end as part of the consortium.

Fort Lauderdale International Airport (FLL) has selected the **Rohde & Schwarz** R&SQPS Walk2000 walk-through scanner to increase security and provide a streamlined walk-through security experience at its employee screening checkpoints. Rohde & Schwarz will procure and deploy up to eight R&S QPS Walk2000 walk-through scanners to screen employees entering the secure area of the airport for metallic and non-metallic threats, weapons and contraband. The R&S QPS Walk was developed specifically to address high volume security screening in a wide range of operations requiring rapid and accurate screening for metallic and non-metallic threats, contraband, explosives, drugs, ceramic guns, blades and other prohibited items.

Israel Aerospace Industries (IAI) announced that it signed a contract with **Korea Aerospace Industries** to provide its adaptive defense antenna (ADA) system for light armed helicopter (LAH) second phase production during the Seoul ADEX 2023 exhibition. Under the contract, IAI will provide its ADA system, a GPS anti-jamming solution capable of suppressing interferences from multiple jammers from various directions, for serial installation on LAH platforms. In 2017, IAI's ADA system was selected by the Defense Acquisition Program Administration to be installed on various platforms of the Republic of Korea Air Force, Navy and Army.

Radar sensing and perception technology provide **Metawave Corporation** has been awarded a $1.7 million **U.S. Army** contract to enhance its defense application-proven Carson radar technology platform to support off-road perception sensing and other advancements for autonomous ground vehicles and systems. The resulting Hudson technology platform utilizes Metawave's unique long-range and all-weather detection, tracking and perception capabilities enabled by its patented phased array beamforming and steering front-end Marconi chips, highly integrated antenna-in-package (AiP) modules, and proven high-resolution and accurate radar algorithms. The new Hudson radar platform will also incorporate enhanced graphics processing units (GPUs) from NVIDIA.

PEOPLE

Aspinity, the leader in always-on processing and computation at near-zero power, announced that it has appointed semiconductor industry leader **Richard Hegberg** as chief executive officer. Hegberg will drive Aspinity's next phase of growth as its industry-leading AML100 processor enters volume production. Hegberg joins Aspinity with strong leadership and management experience, and a proven track record of guiding

Around the **Circuit**

▲ *Richard Hegberg*

companies through significant transition and growth periods. Most recently, he was the CEO at Vesper Mems, where he helped lead the company to a successful acquisition. He also served in various executive positions at NetApp, SanDisk, Qualcomm, Atheros, Numonyx, AMD and ATI Technologies.

▲ *Todd Hansen*

Stellant Systems Inc. continues to strengthen its executive leadership team with the selection of **Todd Hansen** as vice president and general manager of the Williamsport, Pa., facility. Hansen is responsible for driving operational performance and processing improvements at the Williamsport, Pa., site and reports to Stellant's Chief Operating Officer Steve Shpock. Hansen has 35 years of experience in the microwave electron tube industry with 20 years as a technologist and 15 years in manufacturing operations. Hansen began his career at Varian Associates in Beverly, Mass., and went on to be a tube engineer for Litton Electron Devices in Williamsport, Pa., and San Carlos, Calif. He also served as the U.S.-based technical liaison for Thales Electron Devices.

▲ *Anitra Simmons*

Apogee, a leading defense and security solutions provider, announced the promotion of **Anitra Simmons** to director of operations for its Mission Operations portfolio. Simmons will work closely with Apogee's leadership team and its federal government customers to ensure superior contractual delivery, employee engagement and customer relations. In this role, Simmons will lead program implementation and support federal government business development for Apogee's Mission Operations portfolio which is focused on U.S. DOD and Department of Homeland Security programs. The company's mission operations include 15 projects and 118 employees across Federal Agency Operations, Air Force Operations and Sustainment and AF Major Commands Staff programs.

REP APPOINTMENT

Modelithics® introduces **Maojet Technology Corp.**, an EDA tool and IP integrator and provider in Taiwan as a Modelithics reseller. Maojet Technology's mission is to make sure of the customer's success through successful integration, deep collaboration and professional service among technology partners, Maojet and customers. Maojet offers EDA tool solutions from system level, RTL, to GDSII, to manufacture and to PCB.

INVITED PAPER

Addressing Low Earth Orbit Satellite Communications System Design Challenges

Mike McLernon
MathWorks, Natick, Mass.

Interest and investment in commercial space satellite systems are booming. Private investors have injected more than $23.5 billion in private-sector funding into space-related companies since 2021.[1] Tech giants like SpaceX and Amazon (Kuiper) have launched space initiatives to increase global broadband access. Historically, satellite communications (satcom) have been used for voice communication, defense and space exploration; however, the introduction and proliferation of low earth orbit (LEO) satellites have lowered the financial barrier required to launch satellites and opened the door for new use cases. This economic benefit is due to two factors. The first benefit relates to the size of the satellites; the latest Starlink LEOs from SpaceX are as small as a kitchen table. The second benefit revolves around the ability to launch multiple LEOs simultaneously, which helps control launch costs. However, while LEOs make satcom systems more economically viable, they introduce complexity and require engineers to manage higher Doppler shifts, interference and network complexities. A representative LEO satellite is shown in ***Figure 1***.

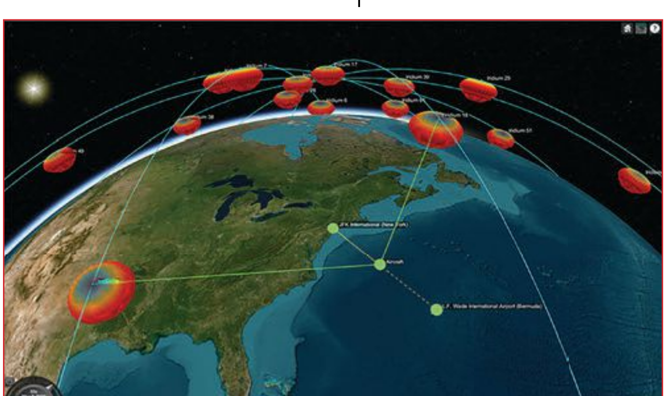

Fig. 1 **Rendition of a LEO satellite.**

TRENDS DRIVING SATCOM SYSTEMS ADOPTION

Ubiquitous connectivity, an environment where devices can create, share and process data from virtually anywhere, is one of the key trends driving the adoption of LEOs. Despite progress in building the terrestrial wireless communications infrastructure, significant portions of the world, such as rural communities and oceans, remain devoid of cellular connectivity due to cost or geography. Satellites are a critical enabling technology in the wireless industry's work toward closing the connectivity gaps between urban and rural areas.

In addition to cellular accessibility, LEOs can also improve cellular capacity. Consider the following market data from Statista: there are currently 4.6 billion smartphone users worldwide[2] and the number of Internet-connected devices is expected to reach more than 29 billion worldwide by 2030.[3] More and more people are using the internet, increasing the global cellular system demand. Wireless companies continue to invest in terrestrial infrastructure, as commercial satellites have not always been cost-effective; however, the cost of LEOs is decreasing, making them a viable option to address the increasingly limited bandwidth, especially in remote areas.

Finally, disaster recovery communications are a key trend driving satcom adoption, as extreme weather events are becoming more powerful and frequent.[4] Cellular infrastructure is frequently knocked out during these events, prompting satellite activation to ensure first responders, government officials and residents can broadcast and receive critical safety information. This use case was validated when Starlink positioned 120 satellites over Southwest Florida and other areas affected by Hurricane Ian[5] when terrestrial cellular infrastructure was destroyed.

SIGNAL LATENCY AND POWER AMPLIFICATION

Before LEOs, satcom systems primarily used geostationary earth orbit (GEO) satellites. Three GEO satellites, properly spaced in longitude and revolving at the same rate as the rotation of Earth, can provide virtually full Earth coverage. Three GEO satellites can cover the planet with a few crosslinks but, unfortunately, are more expensive to build and launch than LEOs. Furthermore, the distance of GEO satellites from the ground and each other introduces latency in their signals. While GEO satellites are acceptable for email and other non-real-time communications, phone and video calls experience significant delays that impede natural communication.

Signal delays are much shorter with LEOs because they are closer to Earth's surface. However, transmitters need more power to communicate with LEOs than terrestrial networks. This is because terrestrial network signals travel between 5 and 10 km, while LEO signals travel up to 2000 km and suffer more signal loss.

The diminutive size of LEO satellites is both a boon and a design challenge. The LEO power amplifiers (PAs) must be physically small yet have enough power to transmit a signal to their intended target. In an ideal world, satellite engineers want PAs to have a linear characteristic even when driven with high-power inputs. However, when a PA is driven too hard, it will go into compression and that can significantly distort the signals. ***Figure 2*** shows a representative PA characteristic illustrating the effects of both nonlinearity (compression) and memory.

One method to counteract and improve these distortions is to use digital predistortion (DPD) subsystems in the transmitter. DPD applies an "inverse PA" characteristic to the signal that causes the output signal of the PA to be more linear. DPD tools, such as those in the MathWorks Communications Toolbox®, are increasingly using AI to improve results. Figure 2 also shows the gain characteristics of a representative DPD circuit and it becomes clear how the DPD inverse characteristics help compensate for the amplifier nonlinearity.

RF LINKS, OPTICAL LINKS AND PHASED ARRAYS

Interference also presents a challenge when using LEOs for satellite communications systems. The main reason for this is the simple fact that there are nearly 6000 LEOs in orbit currently.[6] Traditional RF links have long been used in satcom systems, but engineers increasingly choose optical links when possible. Optical beam patterns are more narrow than traditional RF links, whose broad beams can spill over into other receivers and cause interference.

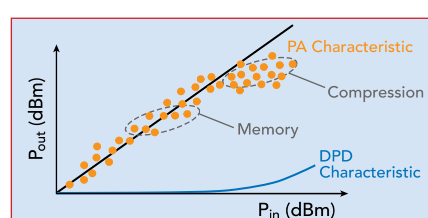

Fig. 2 Power amplifier and DPD measured data.

Interference from optical systems is significantly reduced due to limited signal spreading.

Finally, satellite engineers can also use phased arrays, which are groups of computer-controlled antennas that create a beam that can be electronically steered to point in different directions. Phased arrays can spatially null out interference and direct energy at a particular spot on the ground. Phased array systems maximize beam energy in the direction of the signal of interest and insert beam nulls in the direction of interference, maximizing signal-to-interference plus noise ratio (SINR).

DOPPLER EFFECT AND FREQUENCY SHIFT

Unlike GEOs, LEOs do not revolve around Earth at the same rate as the planet's rotation. This means that they are constantly moving either toward or away from receivers.

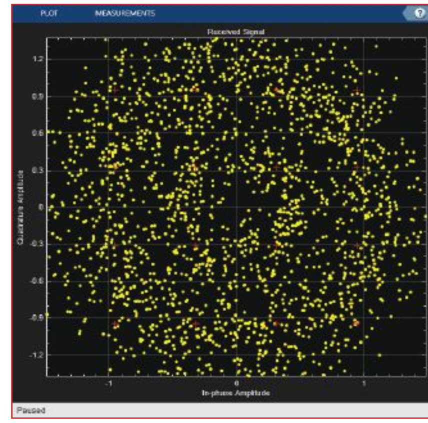

Fig. 3 **Representative received signal data.**

This movement creates a Doppler effect that satellite engineers must manage. In engineering terms, the Doppler effect refers to the difference in frequency between the transmitted wave and the received wave due to transmitter or receiver motion. Doppler challenges require satellite engineers to acquire and track the continually changing center frequencies of LEO satellites.

The frequency and phase of the transmitter and receiver must be completely locked in to ensure the waveforms are successfully demodulated. However, large Doppler shifts cause the frequency, phase and timing to be out of sync. As a result, multiple closed loops must be implemented in these receivers to eliminate Doppler-induced frequency offsets. Synchronization must happen at the frame, symbol timing, carrier frequency and carrier phase levels. ***Figure 3*** shows representative received I/Q data plotted on a constellation diagram and specific constellation points cannot be identified.

Figure 4 shows the constellation diagram with a frequency-corrected signal and while the constellation diagram is becoming clearer, the received signal can be only partially identified.

Figure 5 shows the constellation diagram when the timing and frequency have been synchronized and the signal aligns with the expected 16-QAM constellation points. Products from MathWorks can help designers model and understand these effects and how to successfully close the link for a satcom network.

CONCLUSION

Many satellite engineers use refmenlomicro

High Intermod, Low Insertion Loss

Current equipment is too big, too heavy, and too power hungry. Saving on size, weight, and power is critical to mission success. Menlo Micro offers a field of technology that is smaller, more efficient and more capable. The Ideal Switch® increases agility, functionality and delivers on long life capability for every device.

See more of our Aerospace and Defense product portfolio at menlomicro.com/markets/aerospace-and-defense

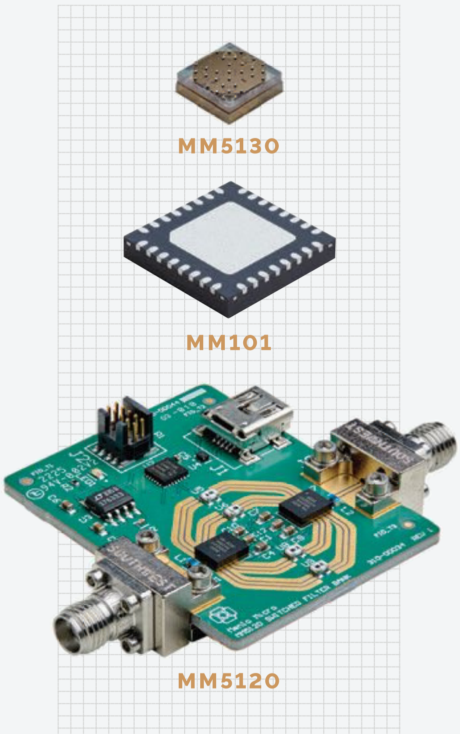

erence receiver designs from products such as MATLAB™ so they do not need to constantly reinvent the wheel. With minor customization from the reference designs, satellite engineers can design robust receivers that can operate in challenging RF environments.

LEOs have received their fair share of attention because of their compelling short- and long-term use cases. Companies like Apple are already tapping into satcom networks and that is only the start. As satcom continues influencing the wireless industry, engineers should familiarize themselves with the uses, challenges and enabling technologies for these satellite networks. ■

References

1. "Space Tech Funding Comes Back Down To Earth," *Crunchbase*, July 2023, Web: news.crunchbase.com/venture/space-tech-funding-drops-spacex-relativity.

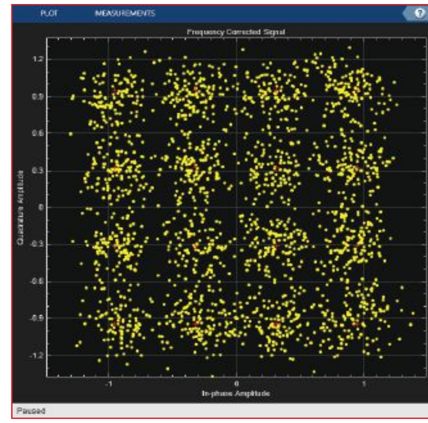

Fig. 4 Frequency-corrected signal.

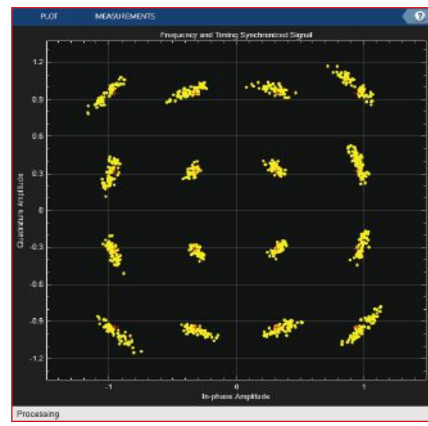

Fig. 5 16-QAM constellation data with frequency and timing synchronization.

2. "Number of Smartphone Users Worldwide from 2013 to 2028," *Statista*, August 2023, Web: www.statista.com/forecasts/1143723/smartphone-users-in-the-world.
3. "Number of Internet of Things (IoT) Connected devices worldwide from 2019 to 2023, with Forecasts from 2022 to 2030," *Statista*, July 2023, Web: www.statista.com/statistics/1183457/iot-connected-devices-worldwide.
4. "Explaining Extreme Events from a Climate Perspective," *American Meteorological Society*, Web: www.ametsoc.org/index.cfm/ams/publications/bulletin-of-the-american-meteorological-society-bams/explaining-extreme-events-from-a-climate-perspective/.
5. "Elon Musk to Provide Florida with Starlink Satellites in Response to Hurricane Ian," *Reuters*, October 2022, Web: www.reuters.com/world/us/elon-musk-provide-florida-with-starlink-satellites-response-hurricane-ian-2022-10-01.
6. "UCS Satellite Database," *Union of Concerned Scientists*, December 2005, Web: www.ucsusa.org/resources/satellite-database#:~:text=Total%20number%20of%20operating%20satellites%3A%206%2C718%20United%20States%3A,Russia%3A%20174%20China%3A%20590%20Other%3A%201%2C425%20LEO%3A%205%2C938.

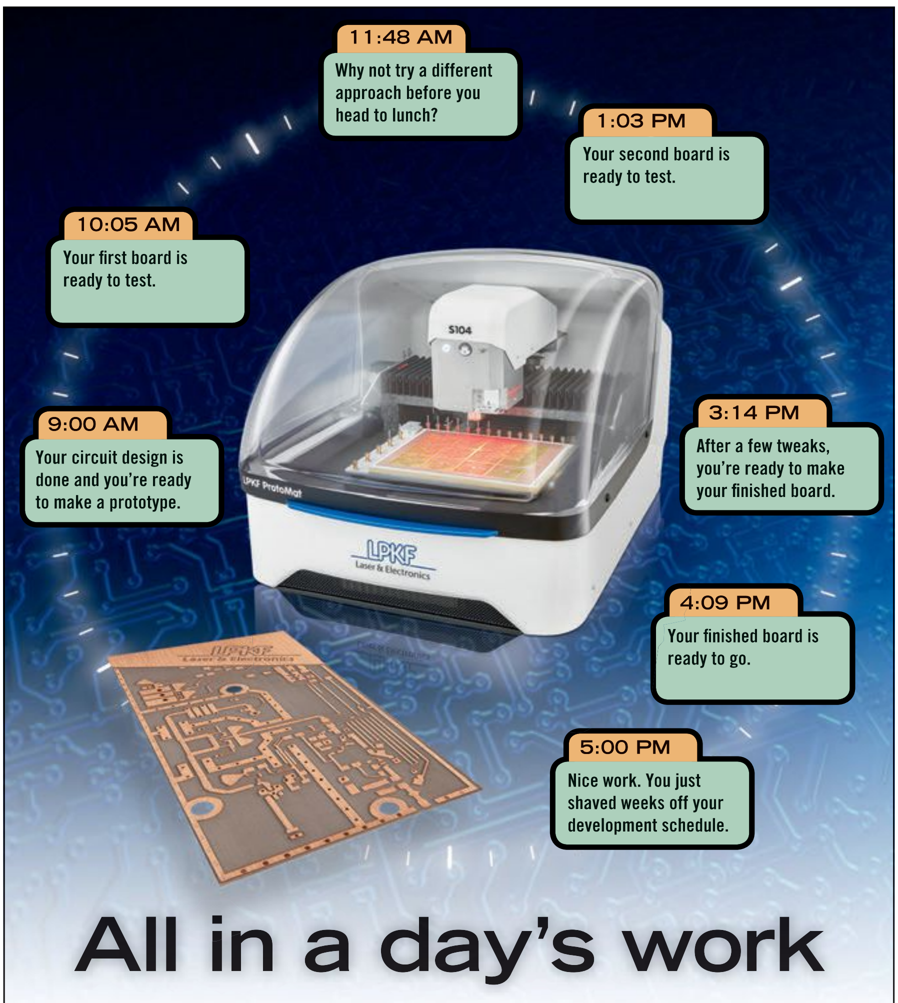

Revolutionizing Wireless Coverage With DAS Integrated Solutions

Hamed M. Sanogo
Analog Devices, Wilmington, Mass.

This article presents a comprehensive solution for distributed antenna systems (DAS), which are essential for extending cellular coverage and capacity within buildings. It outlines the benefits of highly integrated system designs that include an RF transceiver coupled with bidirectional amplifier (BDA) or remote access unit (RAU) equipment. By exploring this solution through the proposed block diagrams, readers can better understand how these elements work together.

Modern environments, such as commercial buildings and sports venues, often require excellent cellular coverage to provide seamless connections. However, the steel, concrete and energy-efficient glass walls in today's large commercial buildings, hospitals and sports venues can easily prevent cellular signals from reaching the mobile devices of the people inside. The fortified construction and highly-tinted windows, among other construction materials, make buildings act like an RF shield.[1] High-rise structures may also experience elevated levels of RF interference from nearby cellular towers, which can further degrade service. Overcapacity, with too many people occupying a small space, is another cause of poor mobile device reception. These factors combine to cause poor cellular device reception. An integrated DAS solution is essential to enabling quality cellular service and accelerating the future growth of wireless networks.

WHAT IS A DAS?

A DAS is an in-building wireless enhancement system that provides building occupants with reliable cellular device coverage. A DAS is a network of spatially separated antenna nodes that expand the cellular range and boost signal strength. The DAS helps to achieve superior cellular connectivity in high-density indoor or outdoor venues. Although no two DAS implementations are the same, a typical deployment may involve direct connections between a donor antenna, an RF signal BDA or booster, a wireless carrier's base transceiver station (BTS), a fiber distribution headend, RAUs and many strategically placed in-building ceiling antennas. In some cases, multiple BTSs are installed with each carrier that serves the building supplying one.

Often, multiple RF feeds are combined and then transmitted to the headend, which

is the primary distribution unit. The donor antenna, placed on the roof of the building, sends and receives signals from a cell carrier and brings the wireless signal into the building through an optimally-located RF signal BDA. The headend equipment then feeds the RAUs via a variety of fiber-optic cabling. The RAUs, in turn, feed the antenna systems via coax cables. Multiple ceiling antennas can be fed from a single RAU. This provides voice and data services to devices inside the building, much like a cell site provides coverage in a cellular network. ***Figure 1*** shows a typical full implementation of a hybrid DAS architecture in a building.

There are two main methods of improving in-building wireless coverage. The first uses only an RF booster or BDA, which are simple repeaters for signals. This is known as passive DAS. The second method is to use a fully active DAS system. Both passive and active DAS signal distribution systems are used to improve wireless coverage and capacity inside a commercial building, depending on the situation. When a distribution system has both passive and active aspects, it is known as a hybrid DAS architecture.

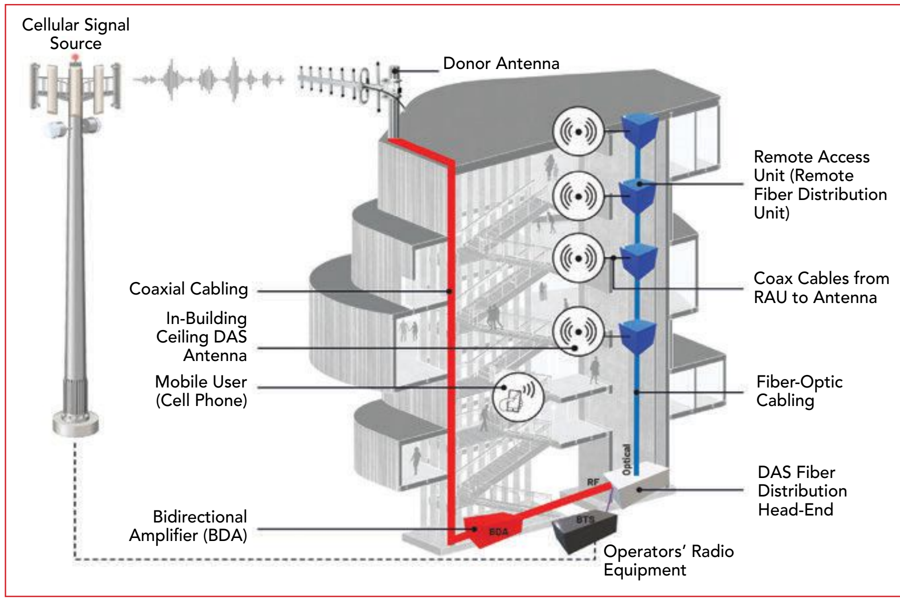

Fig. 1 **A hybrid DAS architecture.**

THE BIDIRECTIONAL AMPLIFIER

The RF signals will grow weaker in response to the coaxial cable attenuation as the distance these signals travel from the donor antenna increases. To mitigate this loss, a passive DAS offers a wide variety of multi-band RF repeaters to amplify and rebroadcast the signals. The BDA front-end consists of a filter, LNA and sometimes an automatic gain control (AGC) circuit. The AGC components are designed to limit the RF power level and protect the BDA from damage or distortion. The BDA amplifies the RF signals in two directions simultaneously. They do not modulate, modify or otherwise distort the actual radio signal. Their main purpose is to keep the RF signal strong throughout the building. Most BDA modules are designed to amplify multiple carriers at the same time and their use does not require an agreement with the carriers. ***Figure 2*** shows the high-level block diagram with some suggested electronic components for a BDA for RF signal amplification and rebroadcasting.

THE DAS REMOTE ACCESS UNIT

The DAS headend equipment performs analog-to-digital conversions and can convert RF signals from one or multiple carriers. This is why carrier approval is usually need-

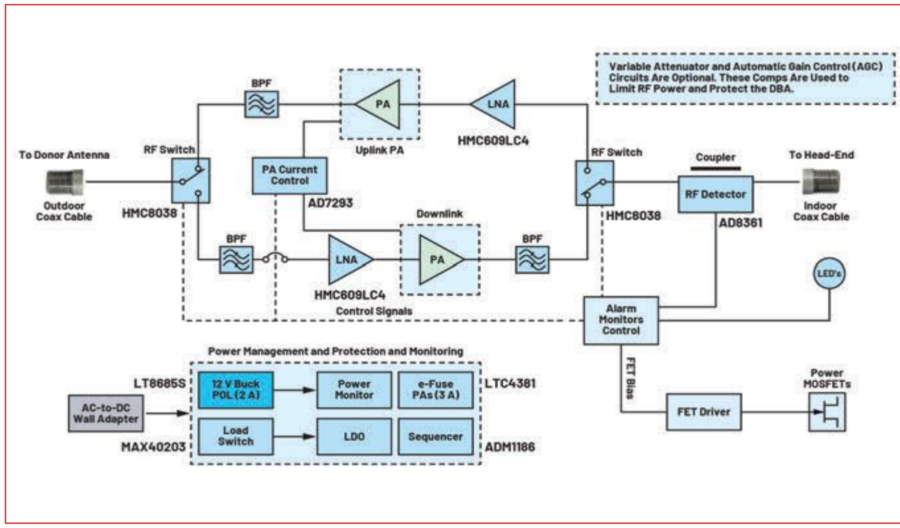

Fig. 2 A BDA/RF booster block diagram.

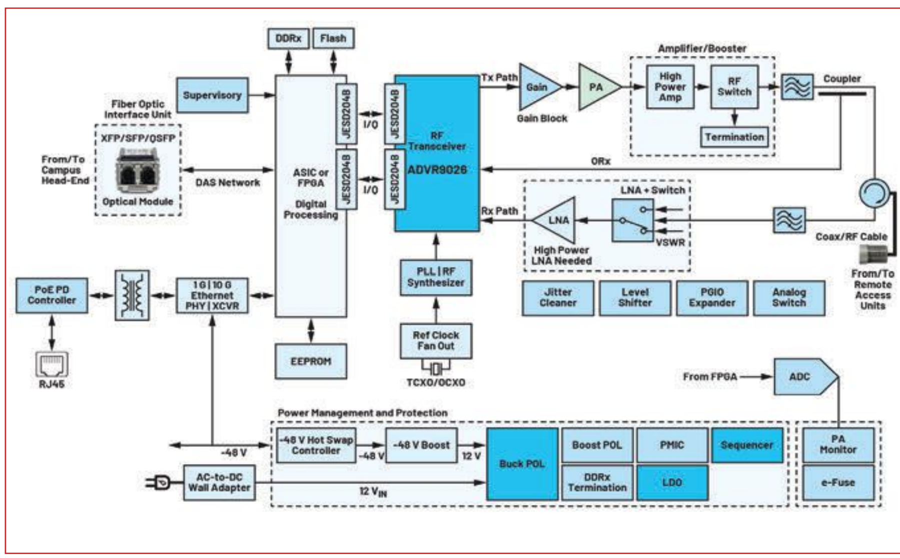

Fig. 3 A block diagram of a typical RAU with the ADRV9029 RF transceiver.

ed from each provider to install an active DAS. Digitizing the RF signal and transporting it on fiber-optic cabling results in a high bandwidth signal that can be transmitted over much longer distances with minimal losses. This allows the signal to be distributed to all the RAUs strategically placed on each floor throughout the commercial building.[1] With this process, signals are much less susceptible to interference.

The RAUs convert the digital fiber signals back to analog RF and feed them to the DAS ceiling antennas. The RAU is connected to the remote ceiling antennas via coaxial cables providing more coverage and range, which allows all users to experience good levels of cellular connectivity. Figure 1 shows the optical fiber cabling

TABLE 1

ADI COMPONENTS FOR RAU DESIGN

Function	ADI Part Number
Gain Block	HMC788A
RF Transceiver	ADRV9029
RF Switch	ADRF5160
PLL/VCO	ADF4351
Clock Jitter Cleaner	AD9528
Buck POLs	LT8625S, LT8627SP
LDOs	LT1761, ADM7172
PMIC	ADP5055
Sequencer	ADM1166
PA Monitor, e-Fuse	AD7393, LTC4381
PoE PD Controller	MAX5969A


ANALOG
DEVICES
AHEAD OF WHAT'S POSSIBLE™
ANALOG DEVICES
AD9081
ANALOG DEVICES
AD9082
Highly Integrated High-Speed Converters

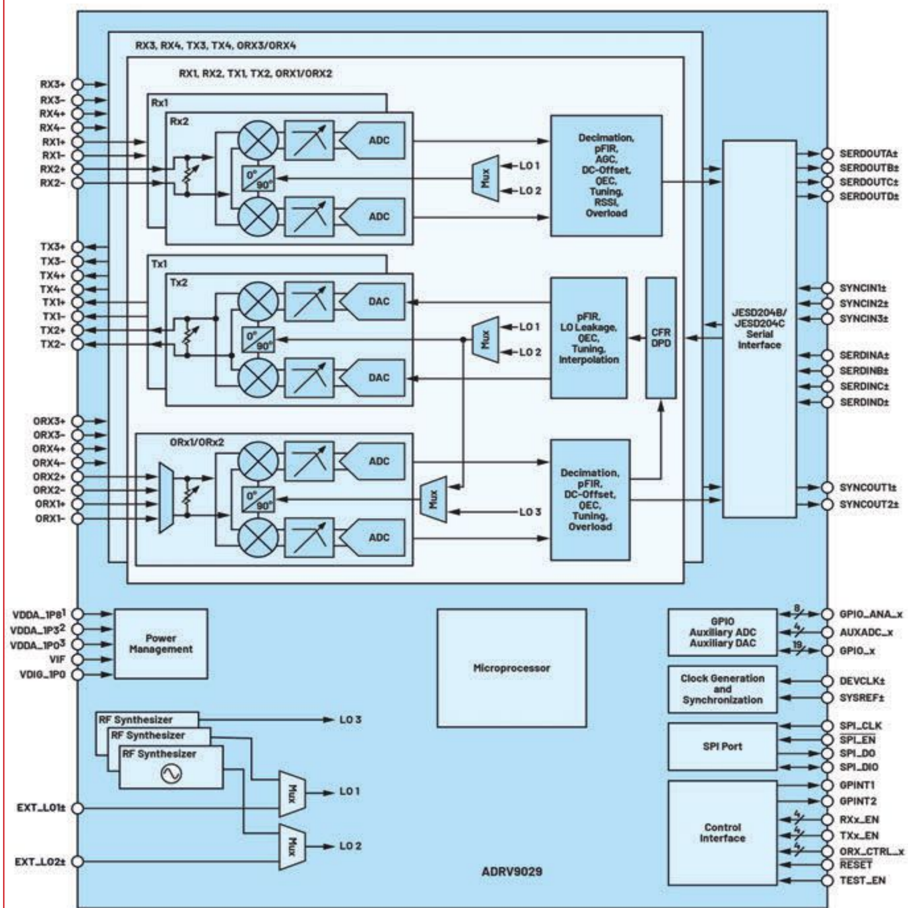

Fig. 4 **ADRV9029 functional block diagram.**

between the headend and all the RAUs.

The RAU in a DAS facilitates the expansion of RF capacity and this is a very important function. The main purpose of the RAU is the digital-to-RF and RF-to-digital conversions. To support the requirements of the RAU, Analog Devices, Inc. (ADI) supplies highly integrated and agile RF transceiver solutions, like the ADRV902x family. These integrated circuit components enable the RAU to take on complex tasks.

Figure 3 shows a high-level block diagram of a typical DAS RAU. ***Table 1*** lists some possible ADI part numbers for functional components that can be used in an RAU design. While the RAU function can be realized with the discrete part number recommendations shown in Figure 2, the rest of this article addresses the integrated ADRV9029 RF transceiver and a few of the external power components that are necessary to complete the design.

ENHANCING DAS PERFORMANCE WITH THE ADRV9029

The ADRV9029 is a highly integrated zero-IF sampling analog transceiver, capable of synthesizing and digitizing wideband signals. The device can be programmed for usage in both frequency-division duplex (FDD) and time-division duplex (TDD) applications. The device provides the performance demanded by DAS cellular infrastructure applications, especially within the RAU. The device includes a digital predistortion (DPD) adaptation engine and a crest factor reduction (CFR) engine. For cases where the DAS system has stringent latency requirements, the CFR can be bypassed. The functional block diagram of the ADRV9029 is shown in ***Figure 4***.

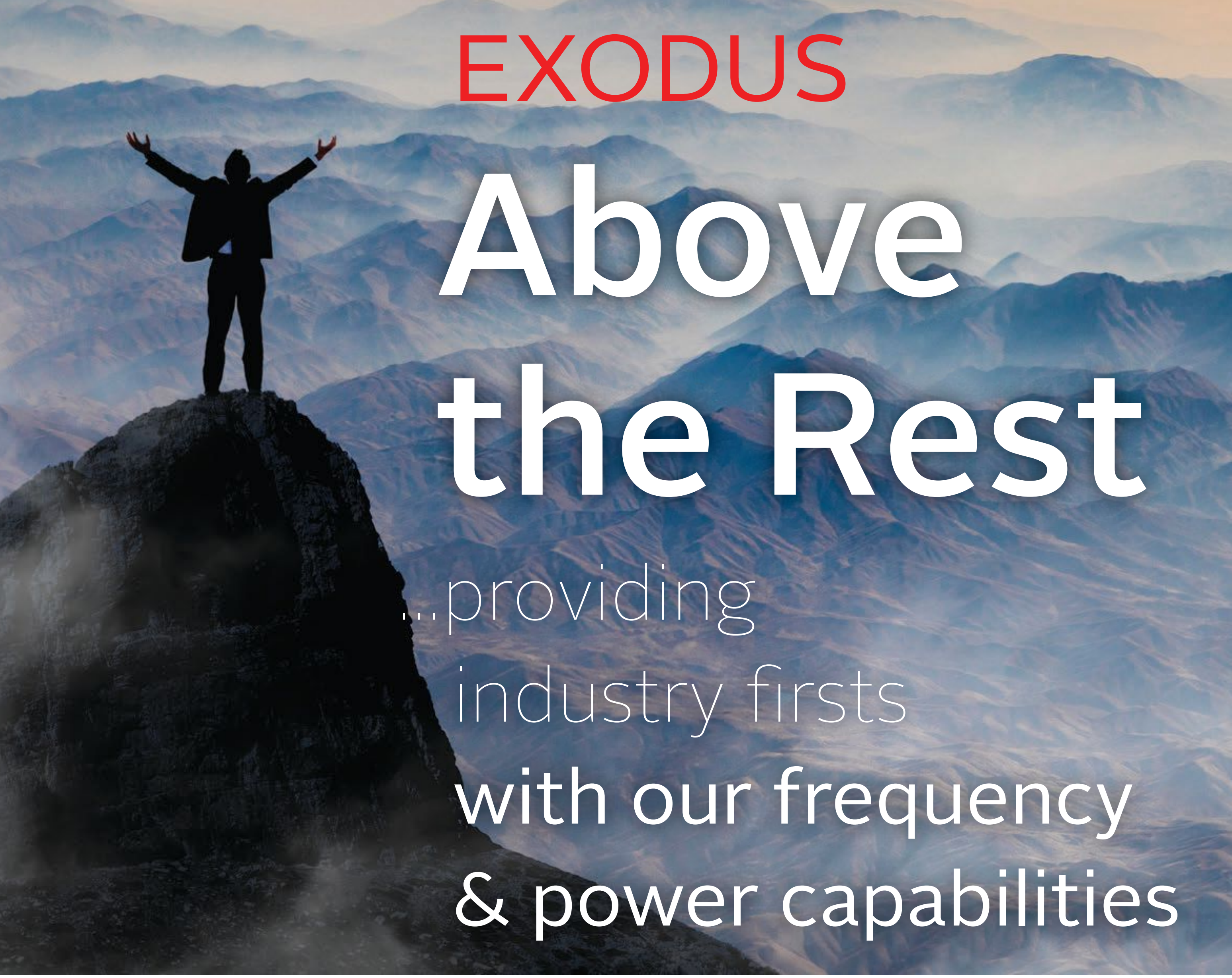

AMP4066A-1LC, **26.5-40GHz, 100W**

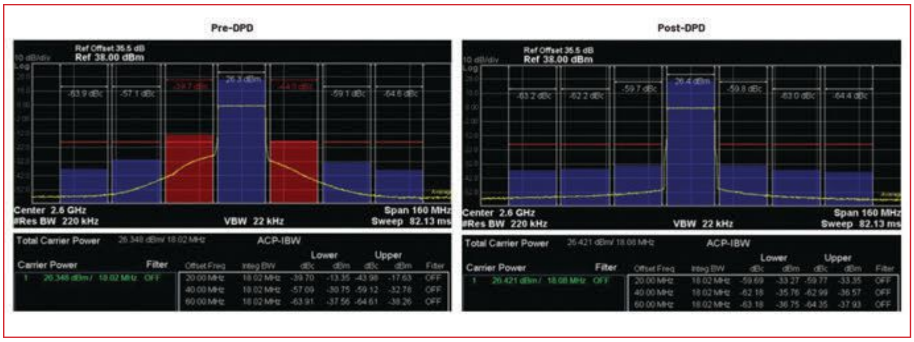

Fig. 5 Power spectral density before and after DPD application.

Digital Predistortion Function

The DPD function allows a wireless system to drive its power amplifiers (PAs) closer to saturation to enable higher efficiency in the PA, while still maintaining the amplifier linearity. The DPD function enables the RAUs to achieve higher PA efficiency by extending the linear operating region of the PA, while still meeting adjacent channel leakage ratio (ACLR) requirements in the transmit signal chain. A PA in the remote DAS node also helps to reduce its overall power consumption. The ADRV9029's observation receiver paths connect to the DPD actuator and the coefficient calculation engine to help the system PAs operate at high efficiency levels.

The DPD algorithm in the ADRV9029 supports a carrier bandwidth of up to 200 MHz. ADI has calculated that the integration of the DPD function into the ADRV9029 results in significant system-level cost, space and power savings when compared to a discrete implementation that uses an RF transceiver with a field-programmable gate array-based DPD solution. When a specific application calls for it, the DPD engine in the ADRV9029 can be completely bypassed through GPIO control.

In addition to the savings mentioned above, the DPD engine improves the ACLR performance. ACLR is the ratio of the transmitted power on the assigned channel to the power leaked into the adjacent radio channel. ***Figure 5*** shows how ACLR performance improves following the application of DPD to a 20 MHz LTE signal baseband. These power spectral density plots illustrate how the out-of-band nonlinearities, caused by intermodulation products of the LTE 20 MHz signal, are reduced from 15 to 20 dB after the application of DPD.

Crest Factor Reduction Block

Many of the current wireless multiplexing schemes, especially multicarrier waveforms such as orthogonal frequency-division multiplexing (OFDM), require a signal that can have a high peak-to-average power ratio (PAPR). A high PAPR can adversely impact the efficiency of the PAs. The main concern is that the signal may have

Nxbeam™

Ka / V / E - Band GaN MMIC Power

Ka

- NPA2001-DE | 26.5-29.5 GHz | 35 W
- NPA2002-DE | 27.0-30.0 GHz | 35 W
- NPA2003-DE | 27.5-31.0 GHz | 35 W
- NPA2004-DE | 25.0-28.5 GHz | 35 W
- NPA2020-DE | 24.0-25.0 GHz | 8 W
- NPA2030-DE | 27.5-31.0 GHz | 20 W
- NPA2040-DE | 27.5-31.0 GHz | 10 W

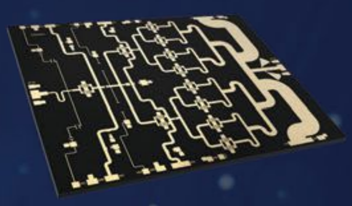

V

- NPA4000-DE | 47.0-52.0 GHz | 1.5 W
- NPA4010-DE | 47.0-52.0 GHz | 3.5 W

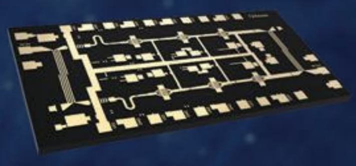

E

- NPA7000-DE | 65.0-76.0 GHz | 1 W
- NPA7010-DE | 71.0-76.0 GHz | 4 W*

* In Fabrication

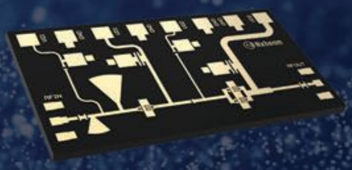

4388 Cerritos Avenue
Los Alamitos, CA 90720

www.nxbeam.com
info@nxbeam.com

Phone: 949-656-2883
info@nxbeam.com

peaks that exceed the linear operating range of the PA. A CFR scheme ensures that the range required by the signal is within the linear range of the PA. Meeting this requirement helps to mitigate or eliminate the issues created by a high PAPR in a system.

The ADRV9029 comes with an onboard CFR engine that helps reduce the PAPR. With reduced PAPR, the PAs in the RAU can operate at a higher output power, which increases the power-added efficiency in the transmit lineup. The ADRV9029 has three CFR engines to assist the DPD engine which will improve the linearity and efficiency of the RAU transmit architecture. The ADRV9029 implements CFR using a variation of the pulse cancellation technique by subtracting a pre-computed pulse from the detected peaks to bring the signal within the PA's linear range. Therefore, a pulse needs to be generated and loaded for each carrier combination. For these and other reasons, the CFR block adds latency. In many cases, DAS systems have stringent latency requirements. When this is the case, the CFR function can simply be bypassed or a companion part like the ADRV9026 that does not have the DPD and CFR functions can be used.

Power Supplies

After taking all the precautions to achieve the highest possible EVM and ACLR performance, the RAU power supply design must also be considered. During operation, supply currents can vary significantly, especially when operating in TDD mode. If noise from the power supply is not controlled, it could affect the JESD204B/JESD204C link performance.

ADI has developed a switched-mode power supply and the packaging technologies necessary to support all its RF transceivers and other 5G RF SoC parts, like the ADRV9029. The Silent Switcher® 3 family of ICs features low RMS output noise, fast transient response, low EMI emissions and high efficiency. ADI has several products in this family that can provide benefits in the power management and control function of the DAS RAU shown in the block diagram in Figure 3. In many cases, the ADI third-generation Silent Switcher devices eliminate the need for the LDO regulator shown in Figure 3.

CONCLUSION

A DAS helps deliver effective RF coverage and capacity, which facilitates seamless connectivity to support today's needs for reliable voice and data transmission. A fully active DAS or a passive DAS/BDA solution can improve cellular signals within building structures to ensure that users have robust wireless connections throughout the building. The RAU is an integral part of a fully active DAS communication solution and ADI's ADRV9029 can be an integral part of the DAS node solution, helping to improve both the performance and the cost of the system. ■

Reference

1. "Designing Distributed Antenna Systems (DAS)," *Advantage Business Media*, 2016.

INVITED PAPER

6G and The Long RF Journey Ahead

Stefan Pongratz
Dell'Oro Group, Redwood City, Calif.

We have not reached half-time yet with 5G, but the 6G clock is already ticking. Research on 6G is gaining momentum, and governments worldwide are contemplating how this next-generation mobile standard aligns with their broader technology roadmaps. China outlined its vision in a 6G white paper published back in 2021 titled, "6G Vision and Candidate Technologies," targeting a 2030 launch. In 2023, the government of India announced plans to prepare the operators for commercial 6G by 2030. Meanwhile, the South Korean government aims to have commercial 6G networks operational by 2028, two years ahead of the International Telecommunication Union's scheduled approval for the 6G standard. As the industry grapples with defining the roles of AI, Cloud radio access network (RAN), automation and ESG in the 6G era, we will stay away from the shiny objects and focus on the basics: what spectrum will be utilized for 6G and why ongoing RF innovation is crucial for transforming 6G from a concept into reality within the next five to six years.

To begin, we need to assess the current state of 5G. Recent estimates indicate that the 5G RAN market has experienced rapid growth during the initial five years of commercial operation, surpassing the developmental pace of previous mobile technologies. One contributing factor to this remarkable rise is the diminished regional gap between advanced and less advanced mobile broadband (MBB) markets. During the LTE era, there was a five- to seven-year disparity between the development in the U.S. and China/India, respectively. However, with the advent of 5G, China took the lead and the Indian RAN market already reached its peak in 2023, just a year after North America's RAN peak in 2022. Widespread small cell adoption has also contributed to the market distinction between 4G and 5G, in part because the LTE small cell market was negligible in the first half of the 4G era while 5G New Radio (NR) small cell revenues already account for more than 10 percent of the combined 5G NR macro plus small cell market. ***Figure 1*** shows Dell'Oro Group's most recent estimate on the 5G status.

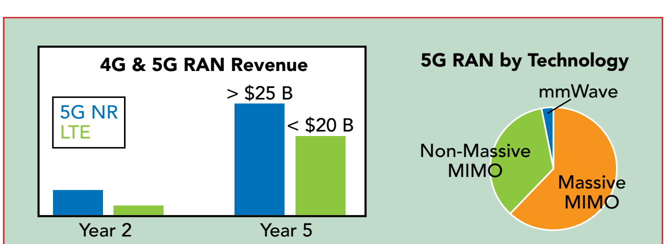

Fig. 1 **5G revenue and technology segmentation.**

One of the key drivers behind the success of existing mobile broadband (MBB)/fixed wireless access (FWA) use cases and a major contributor to the 5G ramp is the widespread adoption of sub-6 GHz massive MIMO (mMIMO). Initially seen as primarily suitable for hotspot scenarios, mMIMO has made significant strides over the past five years. Apart from its capacity benefits, mMIMO has played a crucial role in extending the range and compensating for the higher carrier frequencies typically associated with the upper mid-band. This enables operators to leverage their exist-

01005 0201 0402 0603 0805

ing 4G grid without the need for substantial incremental cell site investments.

Not surprisingly, mmWave NR comprises a low, single-digit share of total 5G NR investments to date. This is largely due to the less favorable RAN economics associated with the high-band relative to the upper mid-band. This is especially true with the current mmWave approach that relies on small cell infrastructure and "lower" EIRP levels.

The journey toward 5G-Advanced and eventually 6G will not be trivial. It depends on a confluence of factors, with the type of spectrum being one of the more critical unknowns that can completely change the trajectory and velocity of the entire 6G ramp. After all, the 5G capital expenditure (capex) envelope would look entirely different if not for the large swaths of spectrum in the upper mid-band, coupled with mMIMO.

Presently, the prevailing notion is that the 6 GHz band and the centimeter wave (cmWave) spectrum will play pivotal roles as anchor bands in the 6G era with frequencies spanning from 6.4 to 15.3 GHz. This band will be akin to the functions carried out by the C-Band in the 5G era. Concurrently, the mmWave spectrum transitions from a backseat position in 5G to a potential passenger seat with 6G in this multi-layered spectrum approach, encompassing new and existing sub-7 GHz, cmWave and mmWave spectrum. ***Figure 2*** shows the details for these particular spectrum bands.

However, achieving economic viability for the broader 6G coverage layer complicates the situation and poses challenges with small cell infrastructure. Consequently, the 6 to 15 GHz base stations will need to make use of the existing macro grid. Ideally, future mmWave systems will also increasingly leverage the macro infrastructure for MBB applications.

As the saying goes, nothing in this world can be said to be certain, except death, taxes and the inevitability of greater propagation losses with rising frequencies. According to the Hata model for a medium-sized city, the received power drops by approximately 7 dB when comparing the 6 GHz band with the C-Band. Another loss of approximately 7 dB occurs at 12 GHz in comparison to 6.5 GHz.

	New/Refarm	Bandwidth	Coverage
Sub-7 GHz			
Sub-1 GHz	Refarm	<0.1 GHz	#1
2 GHz	Refarm	<0.1 GHz	#2
2.5 to 4.2 GHz	Refarm	~0.5 GHz	#3
4.4 to 5.0 GHz	New	~0.6 GHz	#4
6.4 to 7.1 GHz	New	~0.7 GHz	#5
cmWave			
7.1 to 8.5 GHz	New	~1.4 GHz	#6
10.7 to 11.7 GHz	New	~1 GHz	#7
11.7 to 12.7 GHz	New	~1 GHz	#8
12.7 to 13.2 GHz	New	~0.5 GHz	#9
14.0 to 14.8 GHz	New	~0.8 GHz	#10
14.8 to 15.3 GHz	New	~0.5 GHz	#11
mmWave	New	~1.2 GHz	#12
THz	New	>2 GHz	#13

Tentative based on Nokia, Ericsson, Samsung papers.

Fig. 2 **5G/6G spectrum chart.**

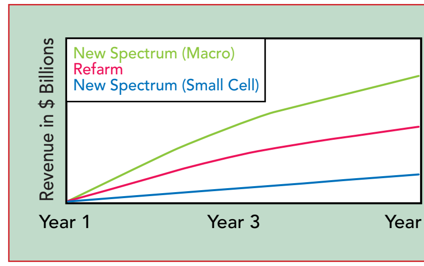

Fig. 3 **6G RAN spectrum.**

In essence, RF innovation becomes crucial for operators aiming to deploy large bandwidth and wide area 6G in new spectrum. At a broader level, there are three main efforts already part of the 5G journey, including boosting the RF output power, adding more transceivers and incorporating more antenna elements. For 6G deployments within the upper 6 to 15 GHz range, advancing mMIMO becomes indispensable to achieve equivalent upper mid-band coverage. Leading vendors are currently exploring configurations such as 128T/128R or 256 transceiver channels to compensate for different loss parameters. Though it is still early days, preliminary testing shows promise. For instance, Huawei has verified in small-scale tests that the propagation delta between the 6 GHz and C-Band is manageable with higher-order MIMO.

So far, mmWave deployments have primarily centered around FWA and low-mobility MBB applications, partly due to challenges related to coverage and performance degradation in higher-mobility scenarios. In response, technology leaders are now boosting the EIRP to tackle coverage limitations. One of the suppliers has already verified that co-site deployments with macros using 70 dBm+ EIRP and intra-band coordination with sub-6 GHz spectrum, can deliver Gbps performance throughout the cell. More innovation is also required to smooth out the handovers. Notably, the UL is typically the limiting factor and more work is needed to address the approximately 20 dB gap between the mmWave bands and the C-Band.

SUMMARY

From a spectrum perspective, three high-level 6G "anchor" options present themselves, each with vastly different capex considerations: 1) re-farmed spectrum, 2) new spectrum using the macro grid as primary and 3) new spectrum using the small cell grid as primary. The base-case scenario currently leans towards new spectrum (upper 6 GHz to 15 GHz) with the macro grid playing a leading role. ***Figure 3*** shows Dell'Oro' Groups thoughts on the relative importance of these different spectrum options to the overall 6G market revenue going forward. However, there remains a considerable RF journey ahead to transform this vision into reality. ■

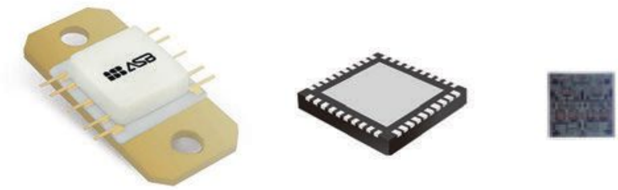

Metal-flange / QFN / Die

ASX
AGN family
ABX

HPA

SatCom, up to 35 W

Internally Matched MMIC

S-, C-band

AGN0343MC	3.2~4.2	20 W
AGN0540MC	4.2~5.2	12 W
AGN0542DC/Q/MC	4.4~5.6	20 W
AGN0642DC/MC	5~7	18 W
AGN0743MC	5.8~8.5	22 W

Ku-, Ka-band

AGN1440DC/MC	13~16.5	12 W
ASX1436	13.75~14.5	3 W
ASX1437	13.5~14.5	5 W
ASX1536	13.5~16	5 W
ASX2731D/Q35P	27.5~31	3 W

X-band

ASX0837HG	7.5~8.5	4 W
ASX1037HG	8.5~10.5	4 W
ASX1037	8.5~10.5	5 W
AGN0940DC	7.7~10.7	12 W
AGN0942D/Q	7.7~10.7	14 W
AGN0943DC/Q	7.7~10.7	20 W
AGN0944DC/Q/MC	8.5~10	25 W
AGN0945DC/Q	8.5~10.5	35 W

Wide-band

ABX0618Q	6~18	1 W

ISO 9001
ISO 14001
IATF 16949
www.asb.co.kr

ASB

INVITED PAPER

MMIC Filter Advancements Drive New Tools

Doug Jorgesen
Marki Microwave, Morgan Hill, Calif.

Integrated circuits have redefined electronics in many areas, but not microwave filters until recently. Bringing the power of MMIC fabrication technology to bear on filtering applications has inspired the development of new tools and new ways of thinking about classic problems. This article discusses advancements in software tools and filter hardware, along with applications where both are valuable.

TOOLS OF THE TRADE: THE MMIC FILTER SOFTWARE STACK

In contrast to most broadband components, fixed filters are generally custom-designed for a system with sometimes vaguely defined performance specifications that may shift frequently. Increasingly, customer requirements are driven more by size than rejection requirements. Frequently, filters solve an unanticipated design problem, often stemming from the frequency plan or previous component choices. The filter business and manufacturing process require speed at every step. Once specifications are agreed upon, the design, fabrication and characterization of the filter must happen quickly. However, since fixed filters are passive and linear, the characterization consists of measuring a single two-port S-parameter. To address this new paradigm with maximum speed, new tools are required. Software tools that automate key steps in the design and commercialization processes are necessary to prevent repetitive and time-consuming work.

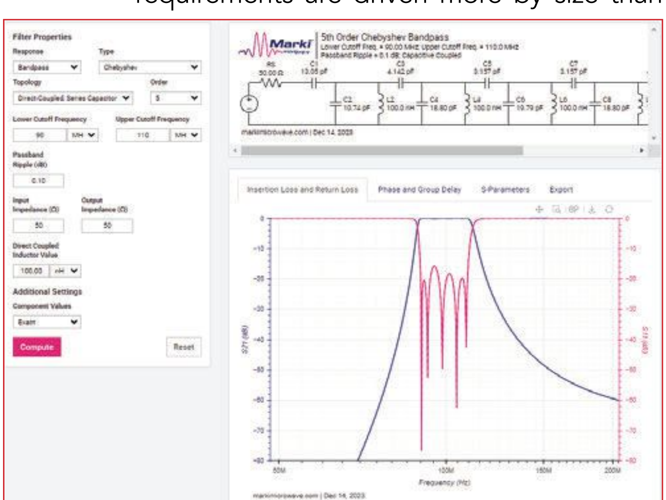

Fig. 1 **Fifth-order Chebyshev bandpass filter synthesis.**

Step 0: Theoretical Definition with LC and Microstrip Filter Design Tools

Before initiating a MMIC filter design, filter designers investigate what is theoretically possible and what kind of inductances and capacitances are necessary to realize these filters. Marki Microwave does this with analytical filter design tools that the company has made publicly available. The LC filter design tool uses equations from fundamental filter research to calculate the theoretical performance of many different types of filters (Chebyshev, Butterworth, Elliptical, etc.) of different orders at given cutoff frequencies. A representative output of this design tool is shown in ***Figure 1***.

The microstrip filter design tool goes a step further and calculates the actual layout of a planar microstrip filter in a more limited

number of topologies (Chebyshev and Butterworth). It calculates the scattering parameters for this structure using mathematical models. Tools like these allow a designer to quickly develop an intuition for what is possible in the filter space.

While powerful and fast, the drawback of these tools is that they only provide theoretical results. When fabricated, the filters created by the microstrip and LC filter design tools will not match the design tool results. The design tools do not account for parasitics of the inductors and capacitors, loss in the components and transmission lines and especially, coupling between different structures. The real-world performance of the filter will not match the simplistic simulation. To achieve better results, further design optimization in a more realistic circuit solver is necessary. For optimal performance, retuning with a sophisticated circuit solver may be required.

Step 1: Topology Definition

Once the theoretical possibilities are understood, the next step is to find the best physical layout to implement in a MMIC structure. This requires researching previously published filter designs, experimenting with different coupling structures and possible circuits in a schematic-level circuit solver, along with exploring different implementations of the circuit in a 3D finite element method (FEM) electromagnetic solver. While standard optimization tools can be used, this is mostly a manual, analog process. The result of this process is not a specific filter design, however, but a topology. A filter topology is the essential, scalable geometry of a filter circuit implemented in a MMIC structure that can be scaled and re-optimized to change the center frequency and bandwidth while maintaining the basic artwork. A given topology will have 10 to 20 design variables that can be continuously varied, leading to millions of potential geometries. Only a small number of these geometries yield a useful filter. Beyond a specific constrained solution space of these design variables, the design is not viable due to unmanufacturable geometries or unacceptably high unit-to-unit variance. Within that useful filter range, however, many designs can be realized with first-pass success.

Step 2: Automatic Design

To realize a specific filter geometry, a designer starts with the base topology and a rough calculation to estimate a seed value for the 10 to 20 design variables. The designer then solves using the seed values in 3D and takes the output to iterate closer to the optimal filter design. This iterative process uses a combination of software tools to refine initial estimates.

Marki uses HOTMESS, a combination of an automatic 3D filter optimizer and a proprietary machine learning algorithm, to automate and optimize the process of creating a set of filters to meet requirements. There are two keys to this tool:

- The 3D FEM solver is relatively slow, taking minutes to hours to solve, so automating the process allows around-the-clock optimization of filters.
- The optimization routine is not blind. It uses the "incorporating prior knowledge" machine learning concept. Unlike a simple gradient solver, HOTMESS solves for the required circuit effect first, improving with each cycle.

Due to these properties, HOTMESS can solve for every achievable percentage bandwidth and center frequency for a given filter topology. ***Figure 2*** illustrates that a filter design should more appropriately be thought of as a matrix of center frequency and passband combinations.

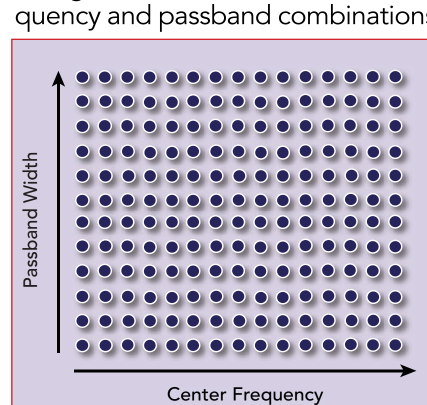

Fig. 2 **Filter topology matrix.**

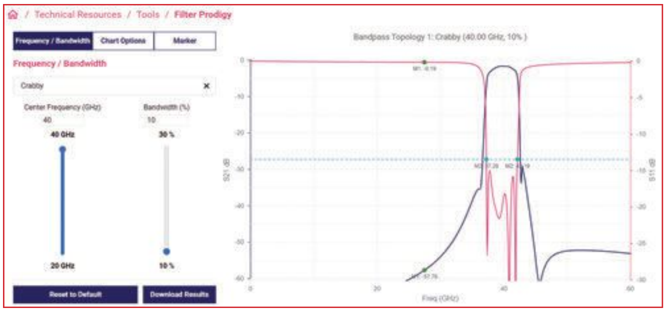

Fig. 3 Prodigy™ Filter Designer user interface.

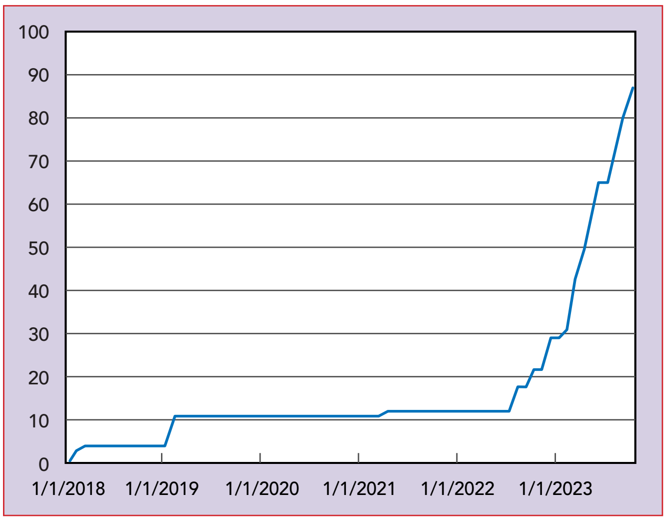

Fig. 4 Marki MMIC filter catalog.

Step 3: Design a Filter Instantly

HOTMESS can provide a solution for nearly every filter topology, but this only addresses the design aspect of the problem. To address the manufacturing aspect, HOTMESS is paired with Prodigy™ Filter Designer to arm filter designers with as much information as early as possible before they develop a filter procurement specification. The publicly available Prodigy™ Filter Designer allows a user to design a filter at any center frequency and bandwidth within the operating range of a given topology. The Prodigy™ Filter Designer interface is shown in ***Figure 3***.

In the Prodigy™ Filter Designer interface, a user selects the desired filter topology, center frequency and bandwidth. The interface then shows an insertion loss and return loss simulation for the selected filter design. This interface is very similar to the LC filter and microstrip filter solvers described earlier, but the underlying math is very different.

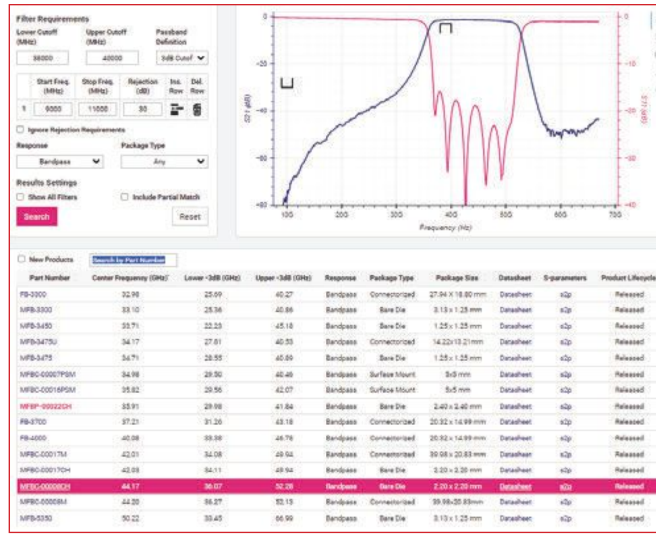

Fig. 5 Filter search tool and the results.

In contrast to the ideal filter prediction given by the mathematical models, Prodigy™ Filter Designer creates a real filter, with known design variables and size. Most importantly, Prodigy™ Filter Designer uses machine learning to calculate the real S-parameters of the filters with all the effects like metal loss, parasitics and cross-coupling. This design and its Touchstone file are immediately available to system designers so they can incorporate actual filter performance at the initial stages of a system design.

While Prodigy™ Filter Designer can display every achievable filter for a given topology, it does not display the best achievable performance for a given filter specification. Where the performance of the filter is sufficient, the Prodigy solution will be a cost-effective solution. When the Prodigy solution does not meet the requirements, there are trade-off techniques among rejection, size and insertion loss that can be considered.

Step 4: Optimize Cost and Prototyping Speed

Since implementing these new MMIC filter models that allow filter designs to be developed quickly and at scale, the library of in-stock filter designs at Marki has grown quickly. This can be seen in ***Figure 4***. The anticipation is that there will be hundreds of filter designs in production by the end of 2024.

Since each filter has its unique combination of center frequency and rejection shape, finding the optimum filter for a given requirement becomes challenging. This challenge is further compounded for applications

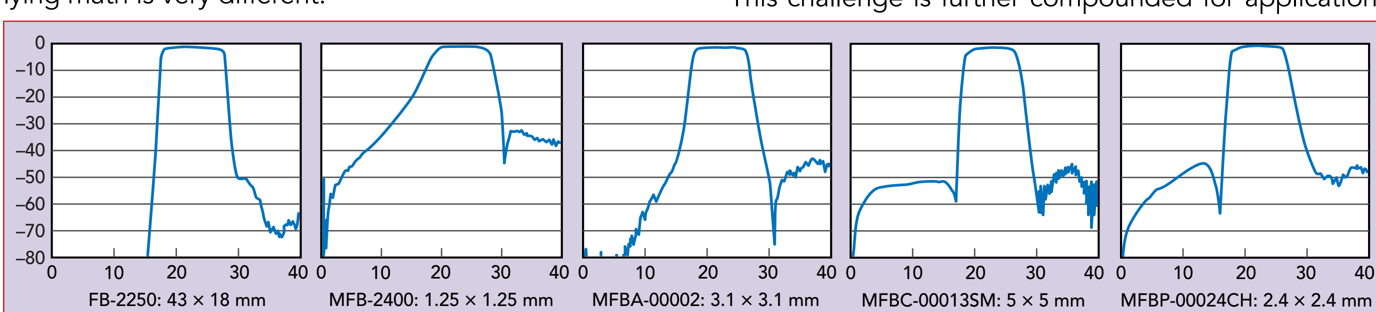

Fig. 6 Filter trade-offs affect performance.

TABLE 1
FILTER DETAILS

Part Number	Package	Size (mm)	Insertion Loss (dB)	40 dBc Rejection Offset (%)
FB-2250	Module	43 x 18	1.5	8
MFB-2400	Chip	1.25 x 1.25	1.3	63
MFBA-00002CH	Chip	3.1 x 3.1	1.7	16
MFBC-00013SM	QFN	5 x 5	1.4	10
MFBP-00024CH	Chip	2.4 x 2.4	1.4	12

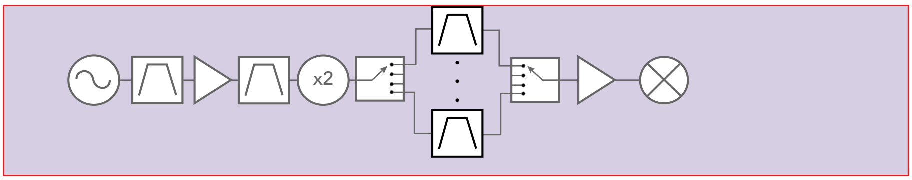

Fig. 7 **SFB in a transmit lineup.**

that need a series of filters for harmonic cleanup or switched filter banks. A filter search tool has been developed to address this issue. A user inputs passband and rejection performance requirements and the filter search tool cycles through all available catalog products and displays the best match. If no filter is found that meets the desired specifications, the closest available match can be found using the "partial match" match option. While the type (lowpass, highpass or bandpass) of filter can be a selection criterion, leaving this option generic can expand the pool of possible solutions. ***Figure 5*** shows the user interface and the output of the filter selection search tool.

FILTER APPLICATIONS

Figure 6 shows the performance of filters with a similar center frequency and bandwidth, but different trade-offs in terms of size, insertion loss, close-in rejection and far-out rejection. The first result in Figure 6 is a legacy laminate filter in a connectorized module and the rest are MMIC filters released after 2020. Each of the MMIC filters utilizes a new topology developed to meet a new system requirement. ***Table 1*** shows selected characteristics of the filters in Figure 6.

Switched Filter Banks

Switched filter banks (SFBs) are a common application for MMIC filters. An SFB is commonly found in wideband receivers and wideband LO generators and synthesizers. MMIC filters are particularly well suited for use in SFBs for two reasons. First, SFBs use many filters, so the size advantage of a MMIC filter is multiplied by the number of filters in the bank. A reduction of 100 mm^2 on a single filter translates to a size reduction of 8 cm^2 on an 8-channel SFB and that is significant. Secondly, the cost of creating a new MMIC filter is dominated by the mask for the reticle and the first wafers. Mask production is a slow, serial and expensive process performed with electron beam lithography. Since four to eight filters can share a single mask, the major cost of developing the filters is split among the entire bank of filters.

The most straightforward application of MMIC filters for SFBs is the filtering of harmonics following a frequency multiplication block. ***Figure 7*** shows the lineup for an SFB after a frequency doubler, along with the placement of the filters. With applications going higher in frequency, the multiplication block could be a doubler, tripler or quadrupler.

Marki doublers achieve harmonic suppression performance of 40 to 60 dBc across several octaves of bandwidth, however, this performance may not meet the requirements of high performance electronic warfare and instrumentation LO generators. Because the harmonic spurs are always separated from the desired tone by a fixed ratio and not a fixed frequency, a constant percentage bandwidth filter

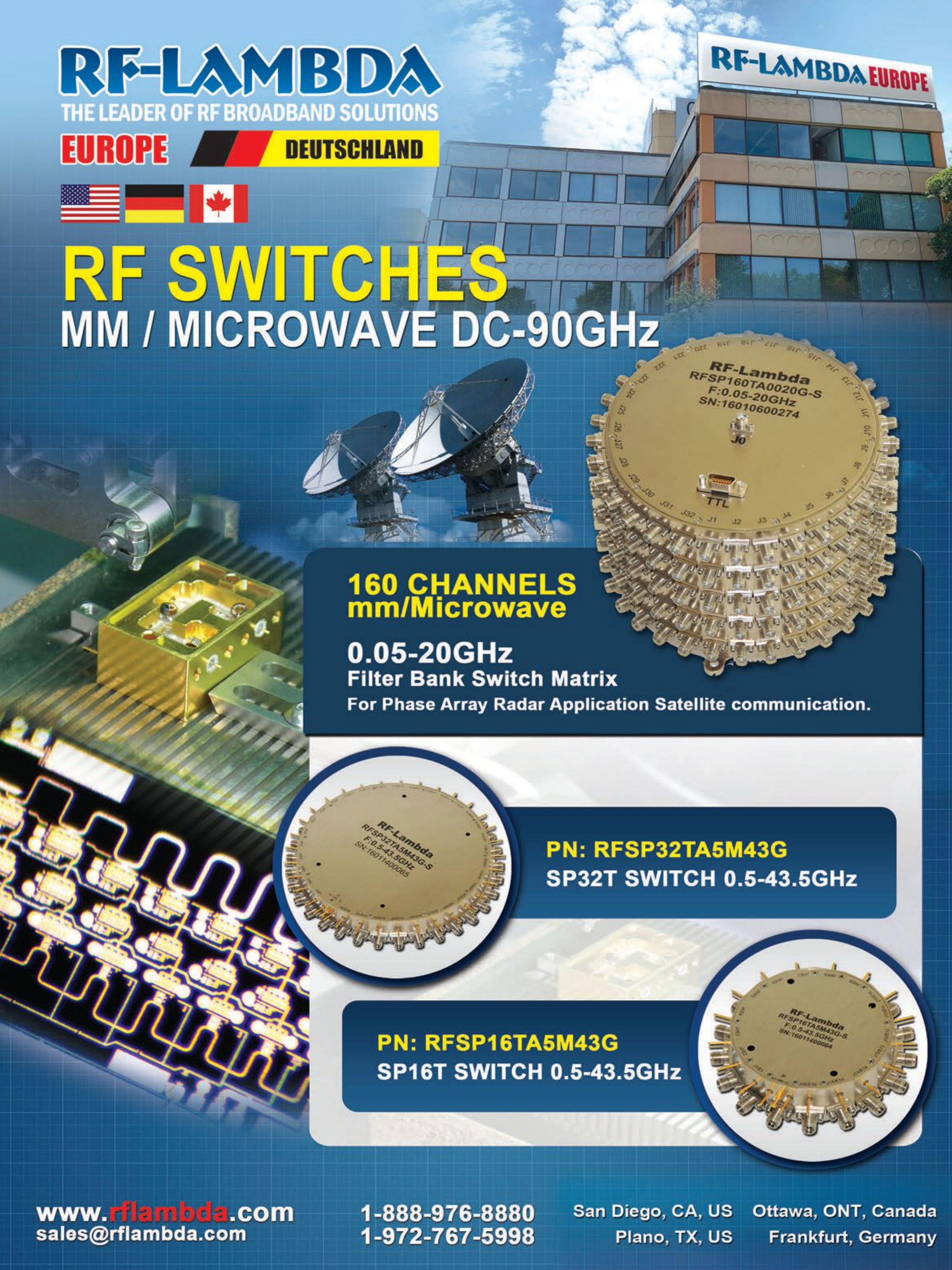
RF-LAMBDA
THE LEADER OF RF BROADBAND SOLUTIONS
EUROPE
DEUTSCHLAND
RF-LAMBDA EUROPE
RF SWITCHES
MM / MICROWAVE DC-90GHz
RF-Lambda
RFSP160TA0020G-S
F:0.05-20GHz
SN:16010600274
160 CHANNELS
mm/Microwave
0.05-20GHz
Filter Bank Switch Matrix
For Phase Array Radar Application Satellite communication.
PN: RFSP32TA5M43G
SP32T SWITCH 0.5-43.5GHz
PN: RFSP16TA5M43G
SP16T SWITCH 0.5-43.5GHz
www.rflambda.com
sales@rflambda.com
1-888-976-8880
1-972-767-5998
San Diego, CA, US
Plano, TX, US
Ottawa, ONT, Canada
Frankfurt, Germany

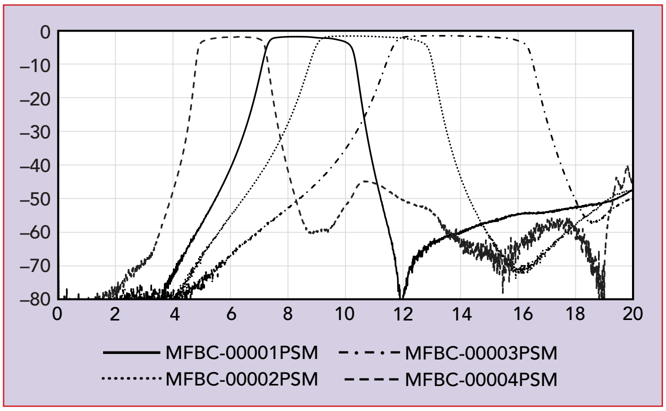

Fig. 8 Retuning filter designs for different bands.

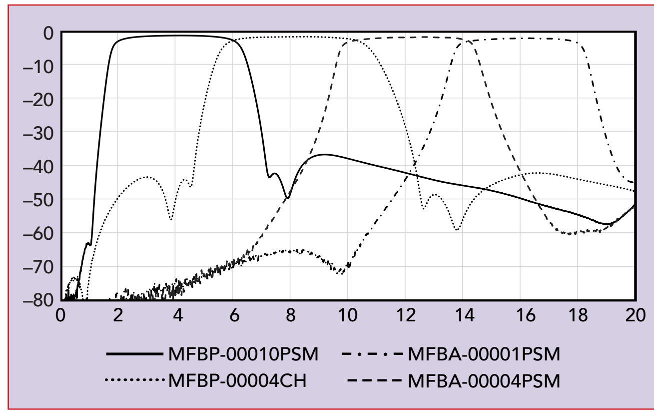

Fig. 10 2 to 18 GHz SFB performance.

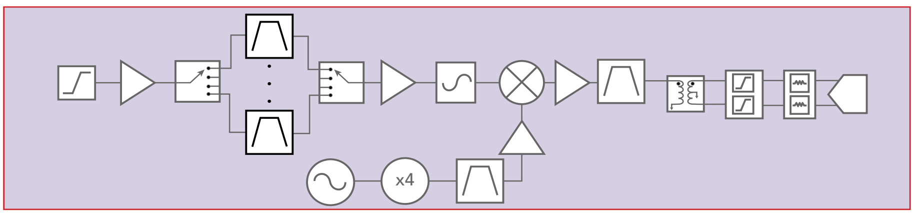

Fig. 9 SFB used as a pre-selection filter.

bank is required. Fortunately, this design is straightforward in a MMIC filter using a single filter topology since the basic design can be scaled and retuned to move the center frequency as shown in ***Figure 8***.

Pre-selection Filter

The pre-selection filter is another common SFB application. This function appears at the front end of a wideband receiver as shown in ***Figure 9***. These filters typically come after the limiter and low noise amplifier (LNA) or they may be switched with the LNA to reduce the nonlinear harmonics created by the signal before frequency conversion or further signal processing. While these pre-selection filters can be constant percentage bandwidth when second-order intermodulation distortion (IP2) is a major limitation, frequently they are a fixed bandwidth to maximize the Nyquist zone of the ADC at the end of the receive chain. ***Figure 10*** shows a series of four GHz filters that can be combined with SP4T switches on either side to create a four-channel 2 to 18 GHz pre-selection filter. While constant percentage bandwidth filters can easily be realized as MMICs by scaling the circuit, constant bandwidth filters offer a different set of challenges. This is particularly evident at low frequencies where filter bandwidths can be more than an octave. The performance of this 2 to 18 GHz pre-selection SFB is shown in Figure 10.

CASCADING FILTERS

A solution for multi-octave filters is to cascade lowpass and highpass filters. This sounds straightforward, but not all filters can be cascaded and maintain satisfactory performance. A key attribute to success is ensuring that the lowpass and highpass filters have good out-of-band performance. Lowpass filters must have good high frequency response, which means a flat passband. Highpass filters must have good out-of-band performance, maintaining good rejection out to 40 GHz and beyond without bandpass filter reentrant mode issues.

There are several advantages to

creating bandpass filters from highpass/lowpass filter combinations. The technique allows for arbitrarily wide percentage bandwidths, making 2 to 18 GHz filters as easy as 2 to 6 GHz filters. The highpass and lowpass filters can be designed and optimized independently, allowing for rapid design of a complete set of filters at regular steps. Lumped elements can be used in MMIC highpass and lowpass filters, allowing for a small die size. In theory, the combination highpass/lowpass filter can be in separate, well-matched packages placed close to each other.

However, not all filters can be cascaded. This technique is useful for improving the rejection of bandpass filters. When a requirement calls for a steeper rejection than a single filter can provide, a cascade filter may be the solution. However, precautions need to be taken because bandpass filters are reflective. This and other challenges can be addressed with reflectionless filters.

REFLECTIONLESS FILTERS

Classic filters function as mirrors outside of the passband. This may present an issue for frequency conversion functions like mixers, doublers and nonlinear transmission lines (NLTLs) because the strongest tone, (the LO, image or the fundamental input) is not the desired tone. Reflections of these high-power tones back into a frequency conversion device may cause unpredictable responses due to nonlinearities in the device. There are at least two solutions that may be appropriate for these issues. The best choice will depend on the specifics of the application:

Terminated Diplexers: A diplexer is a device that routes signals to specific output ports based on frequency. A bias tee is a simple and extreme example of a diplexer; most diplexers have a higher crossover frequency. When one side is terminated in a 50 Ω load, it will function as a highpass or lowpass filter where the common port has good return loss across the band. The diplexer design will determine the return loss performance of the highpass and lowpass ports. This approach can be an excellent termination for an NLTL or other multiplier chain since the low frequency fundamental tones can be eliminated. ***Figure 11*** shows a block diagram of a diplexer terminating an NLTL to reduce reflections.

Balanced Filters: To create a reflectionless, balanced circuit requires two identical subcircuits connected with quadrature hybrids. By combining MMIC filter technology

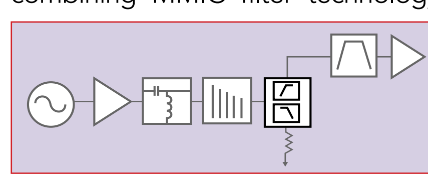

Fig. 11 NLTL terminated with a diplexer.

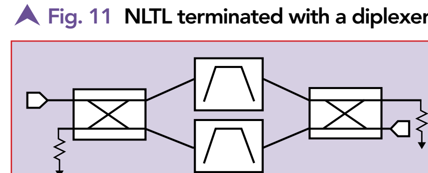

Fig. 12 Balanced filter block diagram.

MiCable

0.3~18GHz High Power

Directional & Dual-Directional Coupler

- High power handling **600W CW**
- Excellent coupling, flatness and directivity which will significantly improve the signal acquisition accuracy
- Environment conditions meet MIL-STD-202F
- Low VSWR & insertion loss
- Custom-design & narrow band is available
- Arbitrary customization of 30-40dB nominal coupling

Stock~4WKS
1 ~ 9 pcs

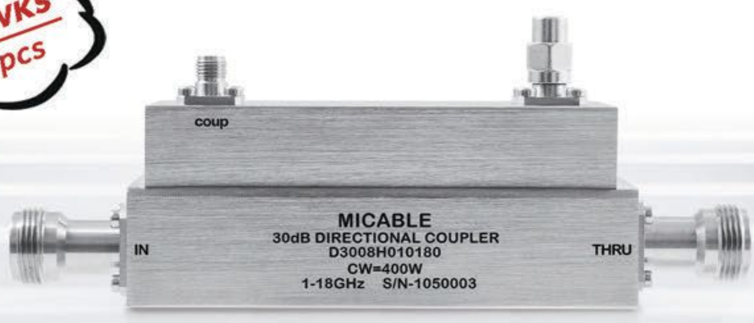

—— Test Curve of D3008H010180 ——

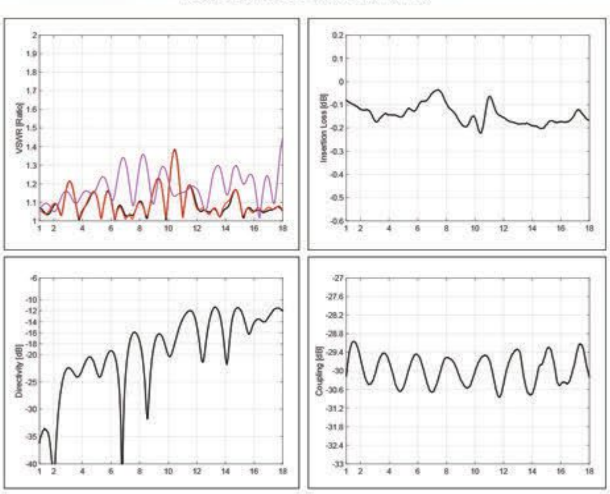

Freq. Range (GHz)	P/N	Coupling Max.(dB)	Main Line VSWR Max.(:1)	Coupling VSWR Max.(:1)	Insertion Loss* Max.(dB)	Flatness Max.(dB)	Directivity Min.(dB)	Power Max.(W)
High Power Directional Coupler								
0.3-6	D3012H003060	30±0.9	1.4	1.4	0.6	±1.2	15	600
	D4012H003060	40±1.0	1.4	1.4	0.6	±1.3	15	600
0.5-6	D3012H005060	30±0.7	1.3	1.3	0.4	±1.0	15	600
	D4012H005060	40±0.8	1.3	1.3	0.4	±1.1	15	600
0.5-18	D3008H005180	30±1.2	1.5	1.6	1.0	±1.2	10	400
	D4008H005180	40±1.2	1.5	1.6	1.0	±1.4	10	400
0.7-8	D3012H007080	30±0.8	1.4	1.4	0.5	±1.0	14	600
	D4012H007080	40±0.8	1.4	1.4	0.5	±1.0	14	600
1-8	D3012H010080	30±0.8	1.4	1.4	0.4	±0.9	14	600
	D4012H010080	40±0.8	1.4	1.4	0.4	±0.9	14	600
1-18	D3008H010180	30±1.2	1.5	1.6	0.6	±1.0	10	400
	D4008H010180	40±1.2	1.5	1.6	0.6	±1.0	10	400
6-18	D3008H060180	30±1.0	1.5	1.6	0.5	±0.7	10	400
	D4008H060180	40±1.0	1.5	1.6	0.5	±0.7	10	400
High Power Dual-Directional Coupler								
0.3-6	D3012HB003060	30±0.9	1.4	1.4	0.7	±1.5	15	600
	D4012HB003060	40±1.0	1.4	1.4	0.7	±1.6	15	600
0.5-6	D3012HB005060	30±0.7	1.3	1.3	0.6	±1.2	15	600
	D4012HB005060	40±0.8	1.3	1.3	0.6	±1.3	15	600
0.5-18	D3008HB005180	30±1.2	1.5	1.6	1.0	±1.5	10	400
	D4008HB005180	40±1.2	1.5	1.6	1.0	±1.7	10	400
0.7-8	D3012HB007080	30±0.8	1.4	1.4	0.6	±1.2	14	600
	D4012HB007080	40±0.8	1.4	1.4	0.6	±1.2	14	600
1-8	D3012HB010080	30±0.8	1.4	1.4	0.6	±1.1	14	600
	D4012HB010080	40±0.8	1.4	1.4	0.6	±1.1	14	600
1-18	D3008HB010180	30±1.2	1.5	1.6	0.8	±1.2	10	400
	D4008HB010180	40±1.0	1.5	1.6	0.6	±1.0	10	400
6-18	D3008HB060180	30±1.0	1.5	1.6	0.5	±0.9	10	400
	D4008HB060180	40±1.0	1.5	1.6	0.5	±0.9	10	400

*Theoretical Insertion Loss Included

More Information-
Scan the QR Code

MIcable Inc.

www.micable.cn sales@micable.cn +86-591-87382856

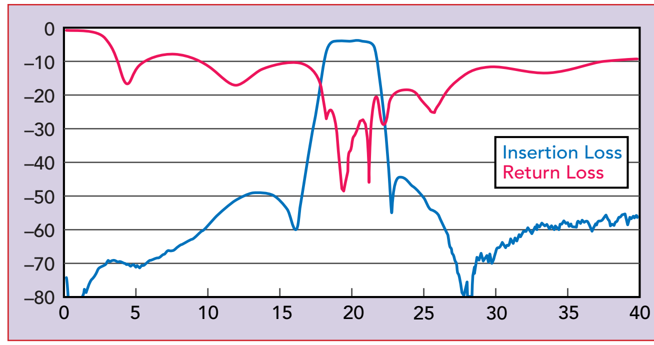

Fig. 13 **MFQH-00001CH performance plots.**

and quadrature hybrid designs, designers can create reflectionless bandpass filters with good return loss across a wide bandwidth. The major benefit of this technique is that it is simple and can be realized on a single chip, with only a slight increase in chip area. The block diagram of this design approach is shown in ***Figure 12*** and ***Figure 13*** shows the actual performance of a Marki MMIC reflectionless bandpass filter.

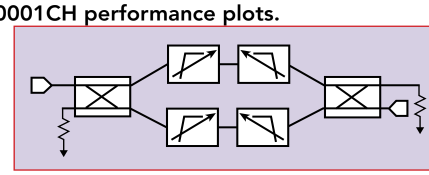

Fig. 14 **Varactor-tunable bandpass filter.**

VARACTOR-TUNABLE FILTERS

The ideal solution for many RF systems has long been tunable filters. If an ideal tunable filter were available, it would dramatically reduce the complexity, size and cost of many RF systems. There are many types of tunable or switchable filters available using various techniques. Varactor-tuned filters use fixed inductors with varying capacitors to move the values of the resonators. While these filters have found wide acceptance, tunable bandpass filters are only capable of fixed percentage bandwidth tuning, which creates challenges. Also, the return loss of varactor-tuned filters tends to suffer across the tuning range due to the detuning of the filter structures.

To overcome these limitations, many of the previously described techniques can improve the state-of-the-art in varactor-tuned filters. Marki solves the challenge of fixed percentage bandwidth tuning by designing separate highpass and lowpass filters that are tuned independently. Without these separate, independent tuning voltages, the best result is roughly fixed percentage bandwidth filters.

To overcome the challenge of detuning filters that degrade return loss, Marki designers embed a highpass/lowpass cascade in a balanced structure to provide good return loss regardless of the tuning state. This approach results in a versatile and effective filter for size-constrained applications that can sacrifice some rejection and insertion loss performance. ***Figure 14*** shows the block diagram of this varactor-tunable bandpass filter approach.

The following charts show the performance of Marki's MFBT-00003PSM varactor-tuned bandpass filter and they illustrate some of the concepts previously discussed. ***Figure 15a*** and ***Figure 15b*** show the insertion loss as the

independent control voltages are swept. ***Figure 15c*** and ***Figure 15d*** show insertion loss for constant percentage bandwidth and constant bandwidth applications. ***Figure 16*** shows the return loss for different bias conditions.

CONCLUSION

Size and channel density requirements for high performance RF circuits pressure designers to minimize the footprint without sacrificing performance. When size is the primary concern, MMIC fixed and tunable filters offer significant size reductions and improved economics for applications where multiple filtering states are necessary. Innovation from companies like Marki in both automated design flows and filter performance enables a viable business model for high performance MMIC filters in the low volume and high-mix market applications. ■

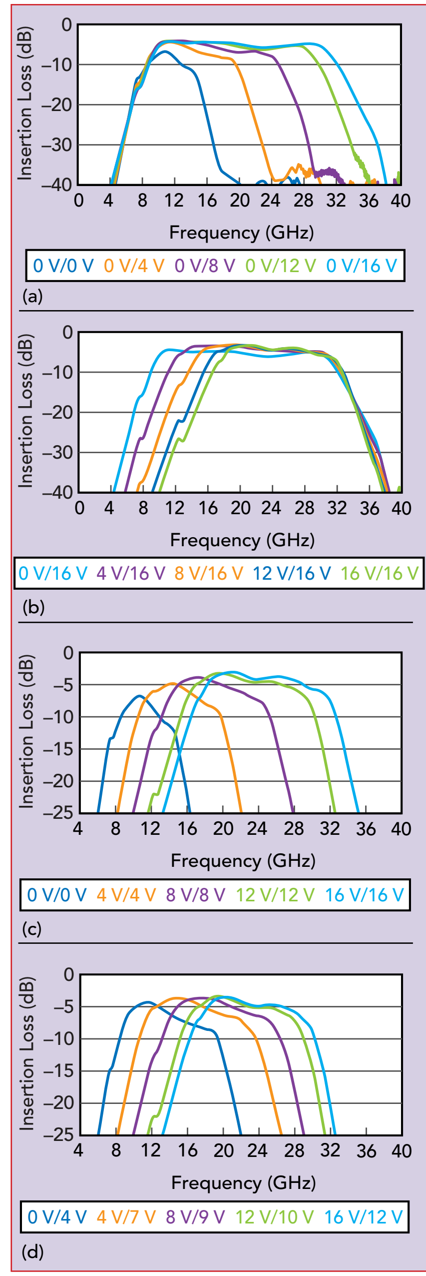

Fig. 15 **(a) Insertion loss sweeping lowpass. (b) Insertion loss sweeping highpass. (c) Insertion loss constant percentage bandwidth. (d) Insertion loss constant bandwidth.**

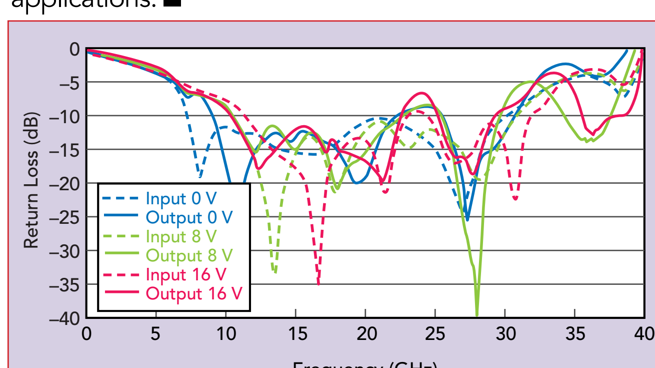

Fig. 16 **Insertion loss constant bandwidth.**

INVITED PAPER

Unlocking the Potential: A Guide to Electronically Steered Antennas

Eran Agmon
Pacific Grove Consulting

In recent years, we have observed a rapid evolution in the field of satellite communications (satcom). The decreasing cost of accessing space has led to the emergence of new satellite constellations, particularly non-geostationary systems, designed to deliver high speed data connectivity worldwide. In-flight connectivity is becoming increasingly prevalent as coverage areas expand and data rates continue to improve with geostationary (GEO) satellites and planned low earth orbit (LEO) constellations. This shift has necessitated fundamental changes to satellite terminal equipment, as the pointing vector to and from the satellite is no longer fixed. Tracking antennas are a crucial technology for implementing these advancements, ensuring a continuous line of sight to the satellite when the satellite and the terminal are in motion relative to each other.

For some, antennas have traditionally been the least understood part of the communication system. The process in which microwave energy is radiated into free space and shaped in a specific radiation pattern seemed like the ultimate "black magic." This article aims to demystify the operation of electronically steered antennas (ESAs) for those tasked with integrating these advanced antennas into their satcom solutions. Anticipating the challenges with antenna technologies, this article provides a simple yet comprehensive explanation of how ESAs work, while delving into their inherent characteristics. It also highlights key considerations in the design of satcom solutions that feature these antennas.

WHAT IS AN ESA?

In simple terms, an ESA is an antenna that can electronically move its beam pattern in both azimuth and elevation planes without moving physical parts. While ESAs have been in existence for several decades, their prohibitive cost made them most suitable for defense applications. However, the emergence of low-cost RFIC technology, coupled with advanced simulation capabilities, has made it possible to lower the cost of ESAs and extend their utility to commercial applications.

WHY USE AN ESA?

Antenna beam steering has been a mechanical process for many years in radar applications and earth stations for LEO observation satellites. The first commercial satellite in-flight connectivity system, Connexion by Boeing, used a mechanically steered tracking antenna in 2003.[1] In addition to improving reliability by eliminating moving parts, ESA technology provides several fundamental advantages over mechanically steered antennas. The ability to independently track more than one satellite and to switch between satellites in less than one millisecond are just two of these advantages. These and other characteristics are not possible with mechanically steerable antennas and are critical to unlocking the full potential of newer LEO constellations.

FUNDAMENTALS OF ESA

This section explains antenna and phased array operating principles. This understanding is essential to ESA functions, capabilities and limitations.

Antenna Arrays and Phased Arrays

An antenna array consists of several radiating elements, arranged in a certain configuration to create a desired radiation pattern. A phased array is an antenna array that can electronically steer its radiation pattern by changing the phase of the signal that feeds each element of the array. In a simple antenna array, two identical isotropic radiating elements are placed with a half-wavelength separation from each other and fed with identical power and phase. The radiated power from these two elements will be the sum of the power of each element in the direction perpendicular to the plane of the elements, called boresight and zero in the direction parallel to the plane. The beam created by these two elements is narrower than that of the individual isotropic radiators.

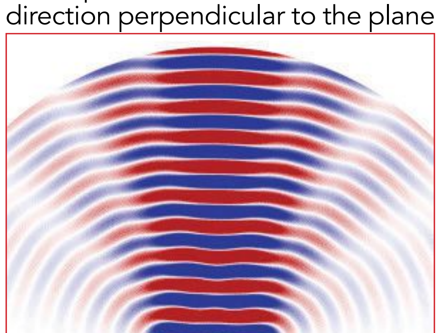

▲ Fig. 1 Radiation pattern of a line array.[2]

Adding more elements to the array increases the equivalent aperture size of the array and the beam gets narrower in the plane perpendicular to the row of elements. In antenna terminology, the gain of the antenna increases, or more accurately, the directivity that increases. ***Figure 1*** shows the radiation pattern of a line array. The dark area along the centerline of the radiation pattern is the main lobe and the lighter areas are the side lobes.

This pattern is the result of the constructive and destructive interference between these elements. The radiation pattern of this simple array is the product of the radiation pattern of the individual element and the array factor. The array factor describes the effect of placing multiple radiating elements at a certain configuration and spacing.

Electronic Beam Steering

Figure 2 shows the effect on the waveform of adding a time delay to the input of each element in an array. The time delay matches the time difference of the wavefront emitted from each element. The applied delay causes the four signals to combine in phase in a specific spatial direction that is related to

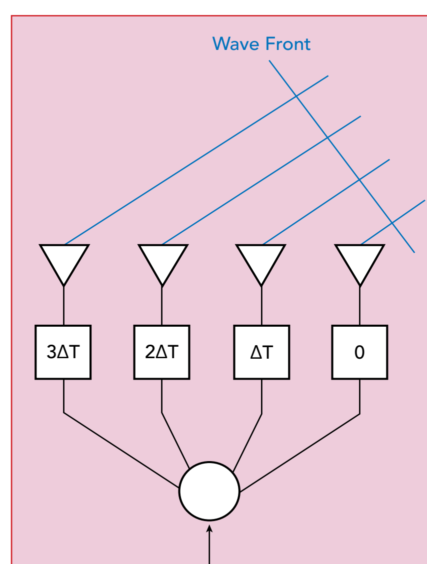

▲ Fig. 2 Electronic beam steering using time delay.

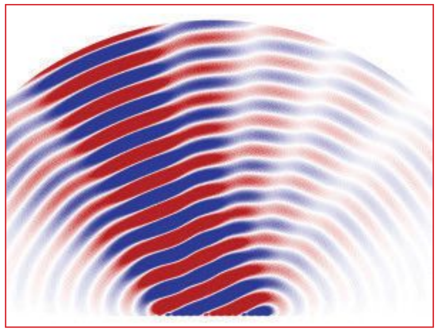

Fig. 3 Steered radiation pattern with time delay.[3]

the time delay magnitude. ***Figure 3*** shows the steered radiation pattern of the array shown in Figure 1.

In many practical implementations of phased array antennas, time delay is implemented using phase shifters. However, time delay and phase shift are not equivalent. This difference will be discussed, along with how this affects beam squint later in the article. The analysis to this point has assumed a one-dimensional (1D) array for simplicity. ESAs used for satcom are two-dimensional (2D) arrays that create a pencil-like pattern. These next sections discuss some of the features and challenges of 2D ESA arrays.

Beam Shaping, Forming and Sidelobe Level Control

Controlling the phase of the signal to each array element steers the radiation pattern in space. If all array elements are fed with the same power level, it creates a uniform aperture illumination. Uniform illumination yields maximum aperture efficiency, however, feeding different array elements with different power levels can lower sidelobe levels and create nulls in directions of interference. Depending on the specifics of the implementation, this can be done dynamically to reduce interference, as an example.

A useful feature of phased arrays is that they can be used to create and steer multiple beams simultaneously and independently of each other. A set of complex amplitude and phase weighting functions can be fed to each element of the array to shape the radiation patterns and steer it to the desired spatial location. Since the array elements are linear devices, different sets of complex weights can be applied simultaneously to the array to create multiple beams, by the principle of superposition.

While a phased array antenna can rapidly switch pointing between satellites, this capability comes at the cost of reducing the satellite duty cycle, which translates to reduced capacity. Multiple simultaneous beams allow communication with multiple satellites at the same time. However, this capability results in a more complex antenna implementation.

The Effect of Scan Angle on Antenna Performance

Since phased array antennas steer beams without physically moving the array, the line of sight between the antenna and the satellite is often not normal to the plane of the array. This means that the effective area of the antenna is reduced, as only a projection of the full area is exposed to the satellite. This creates a scan loss, reducing the overall gain of the antenna. This is a fundamental difference between phased array antennas and other antenna designs.

This loss is approximately 10 log (cos (θ)), with θ being the angle between a line normal to the array's plane and the line of sight to the satellite. At θ=60 degrees, for example, the scan loss is 3 dB. Depending on the specific design of the array, scan losses tend to be slightly higher than 10 log (cos (θ)), especially at higher values of θ.

Time Delay Versus Phase Shift

As shown in Figure 2, steering an antenna beam depends on delaying the wavefront between elements. This delay is commonly implemented with phase shifters. However, a phase shifter creates a frequency-dependent time delay, making this approach most useful for a narrow band of frequencies. Newer satcom systems use wideband waveforms, meaning that the time delay will not be constant for a fixed phase shift. As a result, the beam changes direction as a function of frequency. This change in the beam's pointing vector with frequency is called beam squint. Beam squint is also a function of the scan angle θ and is more pronounced at higher values of θ.

Grating Lobes

The concept of grating lobes is derived from a mathematical description of a phased array antenna and is beyond the scope of this article. However, an example helps with the concept. ***Figure 4*** shows the array factor of a 32-element array with element spacing of 0.5λ and 0.7λ. Element spacing of 0.7λ yields a narrower main beam and a tighter sidelobe pattern. This improvement results from a larger aperture area, where the same number of elements have more spacing between them. However, this configuration also produces another full gain beam at -70 degrees. This is a grating lobe and this beam may transmit power to or receive power from an undesired direction. This will interfere with other satellites or terminals and it may pick up undesired signals and noise. However, this phenomenon does not necessarily mean that element spacing must always be kept below a half-wavelength.

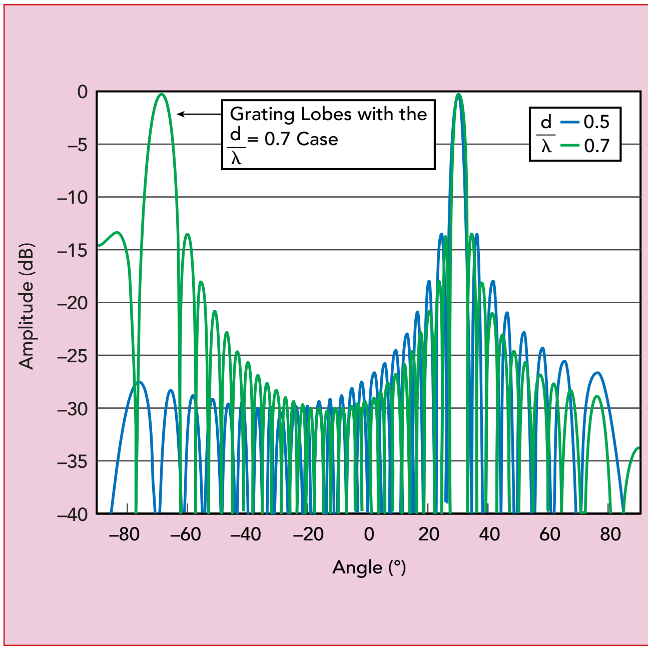

Fig. 4 Normalized array factor of a 32-element linear array.[1]

ESA-BASED SATCOM SOLUTIONS

There are several important design considerations when integrating an ESA into a satcom solution. This section and the article concentrates on active flat arrays, which have gained popularity thanks to their design flexibility, low-profile and cost-effectiveness. Active flat arrays for two-way satcom typically feature two separate apertures; one for receive and one for transmit. The dual aperture configuration significantly simplifies the design of the antenna.

Each flat array aperture is built with unit cells and each unit cell contains several radiating elements and an RFIC. The unit cell is tiled in two dimensions to create the desired aperture area. This structure is easy to implement on a single printed circuit board (PCB) and the result is a very compact, low-profile antenna. In this design, printed radiating elements are on top of the PCB, as shown in ***Figure 5a***, and RFICs are placed on the back, as shown in ***Figure 5b***. Each of the receive antenna elements feeds a low noise amplifier and each transmit element is driven by a power amplifier (PA). This antenna architecture is different from traditional satcom antenna designs and has several aspects that should be carefully evaluated.

Unlike traditional dish antennas, ESAs do not have standard sizes. ESA-based terminals are usually customized to the application with aperture size as the primary customization feature. Separate receive and transmitted apertures provide

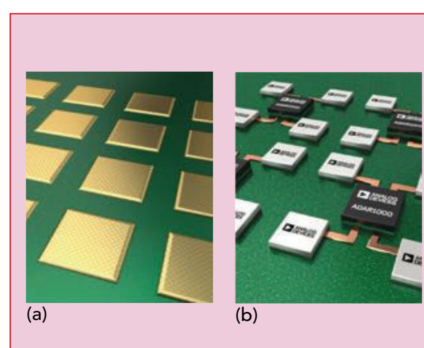

Fig. 5 (a) Flat panel array antenna patches and (b) flat panel array ICs on the back of the antenna PCB.[5]

a degree of freedom, allowing the satellite link designer to optimize aperture size based on link performance in each direction. Since the aperture is built from multiple unit cells, aperture size directly impacts cost, power consumption and heat dissipation.

As described earlier, the effective aperture area decreases as the scan angle increases. This scan loss, based on the look angle to the satellite should be factored into the link budget design. For example, the elevation angle to a GEO satellite from an antenna onboard a commercial aircraft crossing the Atlantic Ocean at latitudes between 40 degrees and 50 degrees is between 40 degrees and 30 degrees. This is a simplified result since the orbital location of the satellite also affects the elevation angle. However, the result is a scan angle of 50 degrees to 60 degrees from boresight. The scan loss at a 60-degree scan angle is 3 dB, which is significant and applies to both receive and transmit apertures. The analysis indicates that the minimum antenna performance should be specified at the maximum anticipated scan angle.

The receive aperture size will be determined by the antenna gain to noise temperature ratio (G/T) required to satisfy the downlink performance requirements. This ratio is directly proportional to the aperture area. Determining the transmit aperture size is more complicated. In a traditional terminal design, the effective isotropic radiated power (EIRP) is determined by two independent quantities: antenna gain and block up-converter or HPA power. In an ESA, these two quantities are both a function of aperture size. Antenna gain is directly proportional to the aperture area. Transmit power is the sum of all contributions of power from each radiating element and the antenna gain and transmit power increase with increasing aperture area.

Antenna gain is proportional to 10log (N), where N is the number of elements. Multiplying the number of receive aperture elements by two increases the G/T by 3 dB/°K. Multiplying the number of transmit aperture elements by two increases the EIRP by 6 dB, as both gain and power double.

The aperture size of the ESA must satisfy several requirements, including link budget and adjacent satellite interference requirements. The antenna pattern must be narrow enough to meet the interference performance. If the aperture size must increase beyond what the link budget requires, power throttling may be considered.

Since an ESA contains two apertures, it has a larger footprint. Depending on the implementation technology, this may result in a lower profile. The mechanical configuration shown in Figure 5a and Figure 5b creates heat dissipation challenges, since these RFICs mount on the bottom side of the antenna PCB, which is not optimal for heat removal. Proper heat analysis and cooling methods must be considered to remove the heat from that area. In certain applications, like aircraft fuselage-mounted antennas, the operating time of the antenna on the tarmac may be limited without the cooling provided by airflow during flight.

To an extent, any ESA is customized by replicating a predesigned antenna unit-cell to create the required aperture size. The mechanical design, RF channel gain, frequency conversion and IF interface with the modem may also be adapted for a specific application. However, designing a user terminal as part of an integrated satcom system allows the terminal ESA to be optimized and simplified by accommodating the characteristics of the satellite constellation and air interface.

To this point, the antenna architecture has assumed a separate receive and a transmit aperture. A notable exception to this architecture is the Starlink terminal antenna. This architecture features a single transmit and receive aperture. The Starlink system is a proprietary closed system, without much publicly available information. The available information suggests that the Starlink air interface is half-duplex, eliminating the need for isolation between receive and transmit signal paths. This simplifies the unit cell design

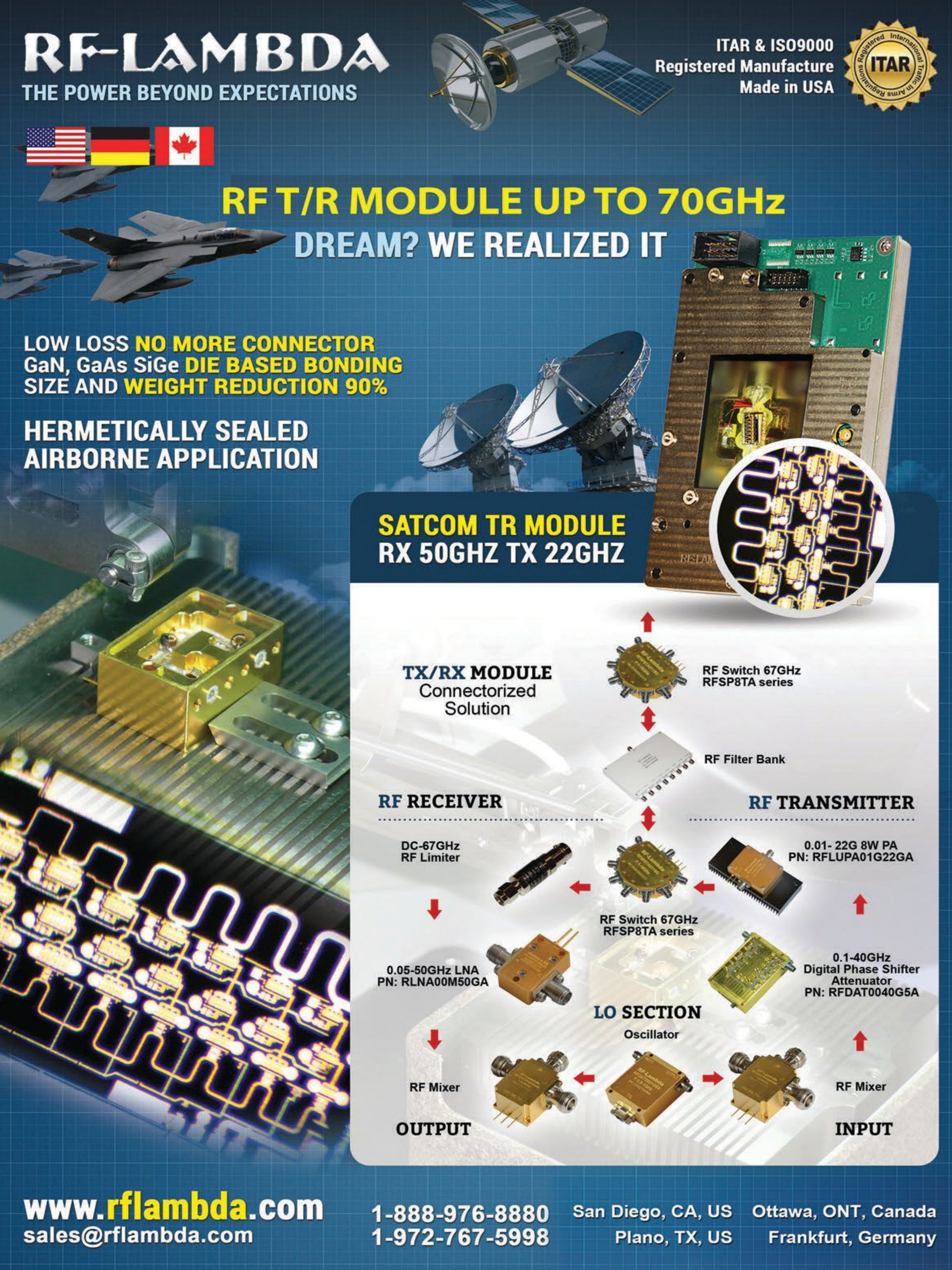
RF-LAMBDA
THE POWER BEYOND EXPECTATIONS
ITAR & ISO9000
Registered Manufacture
Made in USA
ITAR
Registered International Traffic In Arms Regulations
RF T/R MODULE UP TO 70GHz
DREAM? WE REALIZED IT
LOW LOSS NO MORE CONNECTOR
GaN, GaAs SiGe DIE BASED BONDING
SIZE AND WEIGHT REDUCTION 90%
HERMETICALLY SEALED
AIRBORNE APPLICATION
SATCOM TR MODULE
RX 50GHZ TX 22GHZ
TX/RX MODULE
Connectorized
Solution
RF Switch 67GHz
RFSP8TA series
RF Filter Bank
RF RECEIVER
RF TRANSMITTER
DC-67GHz
RF Limiter
0.01- 22G 8W PA
PN: RFLUPA01G22GA
RF Switch 67GHz
RFSP8TA series
0.05-50GHz LNA
PN: RLNA00M50GA
0.1-40GHz
Digital Phase Shifter
Attenuator
PN: RFDAT0040G5A
LO SECTION
Oscillator
RF Mixer
RF Mixer
OUTPUT
INPUT
www.rflambda.com
sales@rflambda.com
1-888-976-8880
1-972-767-5998
San Diego, CA, US
Plano, TX, US
Ottawa, ONT, Canada
Frankfurt, Germany

and allows the same array element to be used for non-simultaneous receive and transmit.

Another characteristic of this terminal is that during installation the antenna panel is mechanically tilted towards the sky at a certain elevation angle. This hints that the antenna is not required for large scan angles. This is supported by an angular separation between satellites in each orbital plane of about 20 degrees and an angular separation between orbits of only 5 degrees. These small angular separations allow for a limited scan range, which means lower scan loss. This means antenna performance barely degrades as it scans. This also allows element spacing greater than a half-wavelength and this means fewer unit cells to achieve the required gain, no grating lobes, reduced power consumption and lower cost.

In the earlier analysis, the ability to generate multiple independent beams was touted as an ESA advantage. When implementing an ESA for multi-beam applications, close collaboration with an antenna vendor becomes important. This collaboration is necessary for both sides to understand the specific antenna architecture and the multi-beam implementation. The details of multi-beam operation can easily affect both the cost and power consumption of the antenna.

Implementing beamforming techniques to create multiple beams allows for simultaneous communication with multiple satellites. Effective beamforming enables the formation of multiple beams, with each beam fully utilizing the entire antenna aperture, thereby maintaining consistent antenna gain across all beams. This is distinct from creating multiple beams by using only sections of the array, which would result in each beam having a reduced gain.

For multi-beam transmit antennas implemented with unit cells incorporating a PA, the EIRP per signal is reduced similarly. The formula for calculating EIRP is shown in Equation 1:

$$\text{EIRP} = \text{Power}_{\text{transmitter}} + \text{Gain}_{\text{antenna}} \quad (1)$$

where all values are in dB and dBm.

While antenna gain remains the same for multi-beam operation, the PA output is finite and splits between two or more signals, assuming a single PA. In addition, the EIRP reduction might be more than 10log (number of beams) if the operating point of the PA must be backed off further to meet spectral regrowth requirements.

CONCLUSION

Recent advancements in phased array antenna and RFIC design are enabling more affordable ESA technology for commercial applications. ESAs can revolutionize satcom with their ability to electronically steer beams to provide connectivity to mobile platforms. This article has presented the fundamentals of ESAs, explaining the principles of phased array antennas and beamforming, as well as the advantages of flat phased arrays compared to traditional antenna designs. ESAs allow multiple satellites to be tracked simultaneously, which contributes to the development of the industry. These developments are enabling more commercial and defense space applications, but as this article has described, some challenges remain when designing and implementing ESA-based satcom solutions. ■

References

1. "Connexion by Boeing," *Wikipedia*, Web: https://en.wikipedia.org/wiki/Connexion_by_Boeing.
2. "Phased array," *Wikipedia*, Web: https://en.wikipedia.org/wiki/Phased_array.
3. P. Delos, B. Broughton and J. Kraft, "Phased Array Antenna Patterns—Part 2: Grating Lobes and Beam Squint," *ADI Analog Dialogue*, Vol. 54, June 2020, Web: https://www.analog.com/en/analog-dialogue/articles/phased-array-antenna-patterns-part2.html.
4. "Phased array beamforming ICs simplify antenna design," *eeNews Wireless*, Web: https://www.eenewseurope.com/en/phased-array-beamforming-ics-simplify-antenna-design/.

MMIC Power Amplifier for LEO Satellite Downlinks

mmTron Inc.
Redwood City, Calif.

The achievement of relatively low-cost rocket launches has enabled the commercialization of low earth orbit (LEO) satellite constellations, aiming to provide broadband internet connectivity anywhere on the planet. Starlink, OneWeb and Project Kuiper are three of the many systems vying to capture business in consumer, industrial, government and military markets. A network comprising hundreds to thousands of LEO satellites and millions of ground terminals faces significant technical challenges for the high data rate links that constantly switch among the satellites and terminals for both users and gateways. The most practical architecture for these links is a beam-steered antenna array, enabling the satellite or ground terminal to follow the receiver or transmitter as the satellite traverses the sky. The satellite-to-earth downlink and earth-to-satellite uplink use different frequency bands. With the current generation of systems, the gateway uplinks use the 27.5 to 30 GHz band and the downlinks use the 17.7 to 20.2 GHz band. Project Kuiper plans to use these same bands for their users, while OneWeb and Starlink use Ku-Band for the user links.

TABLE 1

MMTRON SATCOM MMICS

Satellite Downlink: 17.3 to 21.2 GHz		
	Performance	**Availability**
TMC261 PA	1.1 W output, 35% PAE at 13 dB NPR	Available Now
TMC173 LNA	1.2 dB NF, 23 dB gain, 3 V/17 mA bias	Engineering Release
Satellite Uplink: 27.5 to 30 GHz		
	Performance	**Availability**
TMC253 PA	26.5 to 31.5 GHz, 28 dBm output at 4% EVM, 36 dBm P_{1dB}	Available Now
TMC174 LNA	1.5 dB NF, 21 dB gain with 2 V, 15 mA bias	Engineering Release

FAMILY OF MMICS FOR LEO SYSTEMS

To serve these LEO systems, mmTron is developing a family of MMIC power amplifiers (PAs) and low noise amplifiers (LNAs) for both the satellites and gateway terminals. The TMC261, mmTron's latest PA MMIC, was developed for the gateway downlink and covers 17.3 to 21.2 GHz. The performance and availability of this family is shown in ***Table 1***.

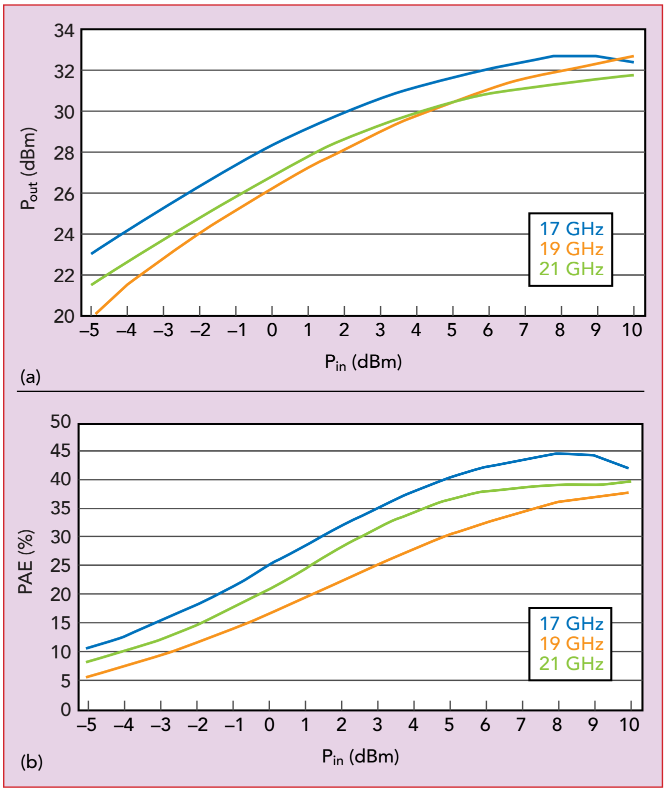

Fig. 1 **(a) TMC261 measured output power. (b) TMC261 measured PAE.**

Based on customer link budgets, mmTron designed the TMC261MMIC to provide 31 dBm output power at 1 dB compression with high linearity and power-added efficiency (PAE). High PAE is essential to minimize a satellite's DC power and thermal load. ***Figure 1a*** shows the PA output power and ***Figure 1b*** shows PAE versus input drive at 17, 19 and 21 GHz.

Linearity is also a key requirement for transmitting high data rates and satellite system engineers typically use noise power ratio (NPR) to specify the required performance. At an NPR of 13 dB, the TMC261 provides 1.1 W output power and 35 percent PAE. The small-signal gain of the TMC261 is greater than 20 dB across the band, typically 24 dB mid-band as shown in ***Figure 2***, with input and output return loss better than 10 dB. The PA was designed for an operating bandwidth from 17.3 to 21.2 GHz.

The TMC261 was designed to be biased at +18 V on the drain and draws 74 mA, set with a negative gate supply. The drain bias can be increased to +24 V to increase the output power to 2 W while maintaining good PAE and NPR performance. The TMC261 is available as a 3.5 × 2.5 mm, 0.004 in. thick die or in a 6 × 6 mm air-cavity ceramic QFN package. Production quantities of the die are available for immediate delivery.

PA DESIGN

To ensure sufficient gain with satellite temperature variations, the TMC261 is a three-stage, class AB design. While either GaAs or GaN would achieve the design goals, GaN is the more attractive option. The higher supply voltage of GaN enables more efficient power distribution and higher system efficiency than would be achievable with a GaAs PA.

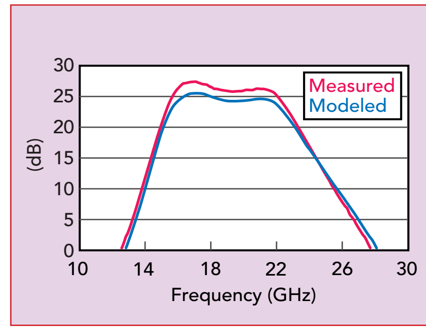

Fig. 2 **TMC261 measured versus modeled small-signal gain.**

Simultaneously optimizing the output power, linearity and PAE of a PA is quite challenging and the process gets more challenging as the bandwidth increases. Historically, many applications have focused on achieving two of the three parameters, but not all three. One of the challenges of designing a 1 W PA with a GaN device biased at +18 V is transforming the impedance up within each stage. This makes achieving the PAE difficult over the wide bandwidth.

After choosing GaN and specifying the epitaxial structure and fabrication process steps to maximize device performance, mmTron's designers determined the output device periphery to meet the output power and linearity specifications. Then, they performed a detailed analysis of possible transistor quiescent points and associated matching impedances to identify the best load targets that would meet the design bandwidth. The "secret sauce" was optimizing the matching networks to minimize the AM/AM and AM/PM distortion at the chosen bias points.

Given the importance of the thermal design, the designers paid close attention to minimizing the power dissipation of each device. This also included accounting for losses in the matching networks. To complete the circuit design, a thorough stability analysis was performed to ensure stability over process, temperature and loading variations.

READY FOR SPACE

Designed to fly on a LEO satellite, the TMC261 is fabricated in a foundry using GaN processes that have built other MMICs flying in space. The TMC261 was designed for maximum reliability and it includes on-chip ESD protection. Consistent with industry standards, bond pad and backside metallization are Au-based and compatible with eutectic or high conductivity epoxy die attach processes as well as ribbon and wedge bonding.

With the TMC261, mmTron has expanded its MMIC satellite amplifier portfolio. The mmTron team has designed the TMC261 to have a unique combination of power, linearity and efficiency performance over a 20 percent bandwidth at K-Band. The company has not seen a higher efficiency, higher linearity three-stage GaN PA commercially available or published in the literature.

mmTron Inc.
Redwood City, Calif.
www.mmtron.com

New Waveguide Power Sensor Products

LadyBug's LB5975W, V-Band, Power Meter provides accurate measurements from 50 to 75 GHz. The Power Meter is the first in the company's new line of waveguide power sensors designed for defense, satcom, automotive and security scanner applications. Additional sensors will be introduced, including E- and W-Band products. Customers using waveguide adaptors with coaxial power sensors can increase the accuracy of their measurements by using the fully characterized sensors.

The RMS-responding two-path diode-based sensors deliver fast settling times and a high dynamic range. This allows customers to accurately test and characterize a variety of products and systems quickly. LadyBug's patented thermal stability provides additional value by eliminating user zeroing and adding the ability to make continuous measurements with no drift or interruption.

The products are all delivered with the company's PMA-12 software. The software includes a strip chart for graphical analysis, tabular logging, two sensor analysis, plus detailed control of the sensor's settings such as triggering, storage, averaging and analog recorder out. Data from the logger or strip chart can easily be exported in various file formats. Internal sensor capability such as simple offsets and frequency dependent offset tables can be setup and controlled using the software.

The sensors are also ideal for ATE users. They feature a composite USB interface that includes either USBTMC or USB-HID interfaces. In addition to LabVIEW® drivers, drivers and support for a variety of programming languages are provided. Optional SPI or I2C connectivity is available. This option allows customers to directly connect to the sensor using microprocessors, microcontrollers or FPGAs, eliminating the need for a computer and its operating system.

VendorView

LadyBug Technologies
Boise, Idaho
www.LadyBug-Tech.com

Wideband mmWave Testing Solution

As the demand for mmWave chipsets, modules and devices continues to surge, the production and testing landscape is seeing formidable challenges. The intricacies of frequency and port count pose significant hurdles, necessitating innovative solutions for seamless and efficient testing processes. TMY Technology Inc. (TMYTEK), a leading provider of mmWave solutions, introduced a wideband mmWave production testing solution covering FR2 to FR3 for 5G/6G, satcom and radar sensor testing. This solution upgrades existing sub-6 GHz testing capabilities, ensuring a streamlined and efficient production process for mmWave chipsets, modules and devices.

The UD Box series, featuring the UD Box 5G, with a frequency range of 24 to 44 GHz for FR2 and the UD Box 0630 with a frequency range of 6 to 30 GHz for FR3, improves production testing by seamlessly managing frequency up-conversion and down-conversion from 6 to 44 GHz. This capability helps reduce high frequency testing equipment costs. Combined with the TMYTEK Matrix Switch, a flexible and multi-port RF switch supporting SP72T and frequencies up to 52 GHz, this integrated solution meets high frequency measurement demands while enhancing testing throughput, eliminating manual control and mass cabling limitations. The Matrix Switch and UD series are integrated into a versatile broadband testing solution. UD models feature a programmable local oscillator and both devices offer a control API for seamless automation. This bundled solution improves testing efficiency, transforming high frequency testing challenges.

TMYTEK delivers mmWave solutions for 5G/6G and satellite communication applications. TMYTEK transforms the mmWave RF front-end with innovative devices, develops beamforming development kits, implements phased arrays with antenna-in-package technology and redefines the over-the-air testing methodology, TMYTEK empowers industrial innovations to go to market faster.

VendorView

TMY Technology, Inc.
New Taipei City, Taiwan
tmytek.com

Tunable Notch YIG Filters Operate to 20 GHz

Micro Lambda Wireless, Inc. has developed a new Yttrium Iron Garnet-based filter that provides superior notch depths over the 6 to 18 GHz and 6 to 20 GHz frequency ranges. This new filter provides a tunable notch of 80 MHz minimum at 40 dBc down. The 3 dB bandwidth is 250 MHz maximum with a typical passband insertion loss of 2.2 dB. These filters target EW and ECM applications.

The frequency of the filter can be adjusted by changing the current across the tuning coil which has a sensitivity of 19 MHz/mA. The filter uses an internal heater that operates from either a +28 VDC supply or ±12 to ±14 VDC supplies. Surge current typically is 300 mA maximum and less than 100 mA steady state.

Over the temperature range of 0°C to +60°C, the frequency drift is 15 MHz while the linearity is ±5 MHz over the frequency range. Extended temperature models are available over the -40°C to +85°C range. Units can also be ordered with analog or digital drivers.

Micro Lambda Wireless was founded to supply the microwave community with technically superior products at reasonable prices with the highest regard for customer service and quality. Products include YIG oscillators, YIG bandpass and band-reject filters, frequency multipliers and frequency synthesizers. Micro Lambda Wireless is the largest independent supplier of YIG components in the world with over 20,000 YIG-based components and assemblies delivered annually.

Micro Lambda Wireless, Inc.
Fremont, Calif.
microlambdawireless.com

Martin Cotter Discusses Intelligent Edge Automations

Unlocking higher efficiency in energy usage, particularly in factories and buildings, is crucial for meeting net zero goals. Listen in as ADI's Martin Cotter details this and more in a recent interview.

Analog Devices, Inc.
www.youtube.com/watch?v=zF1mvF0XQis

Eravant Receives Patent for Revolutionary Uni-Guide Waveguide Connector

Eravant announces the issuance of U.S. Patent No. 11,804,681. This patent relates to a novel series of electrical connectors used in the rapidly growing field of mmWave electronics.

Eravant
www.eravant.com

Importance of Signal Monitoring and Analysis for Today's SIGINT Systems

Read Anritsu's Test Talk blog to learn how this makes signal monitoring and analysis crucial for today's SIGINT systems.

Anritsu
https://bit.ly/3Szwu6f

Channelizing High-Power SMT Couplers to Optimize Coupling, Directivity & Isolation

This application note examines form-in-place gasketing for two distinct bidirectional coupler styles: the core and wire and the stripline SMT.

Mini-Circuits
https://bit.ly/40ZjLvR

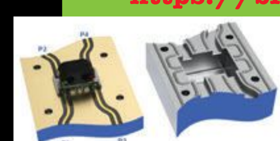

The Transition from Si to SiC in Power Electronics

Qorvo explores why SiC is becoming a breakthrough power electronic technology of the future.

Qorvo
https://bit.ly/3TQN5mA

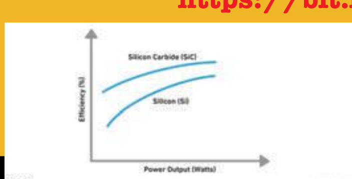

Impedance Measurements using R&S LCX200 & MFIA

The LCR Meters and Impedance Analyzers from Rohde & Schwarz are ideal for measuring impedance at a fixed frequency as well as for determining the best operating point for the component under test.

Rohde & Schwarz
www.youtube.com/watch?v=RzeCB6KiJxc

SIX DAYS ■ THREE CONFERENCES ■ ONE EXHIBITION

EUROPE'S PREMIER MICROWAVE, RF, WIRELESS AND RADAR EVENT

EUROPEAN MICROWAVE WEEK
PORTE DE VERSAILLES
PARIS, FRANCE
22-27 SEPT. 2024
www.eumweek.com
Waves Connecting Europe

THE EUROPEAN MICROWAVE EXHIBITION

PARIS EXPO PORTE DE VERSAILLES PARIS, FRANCE
22 – 27 SEPTEMBER 2024

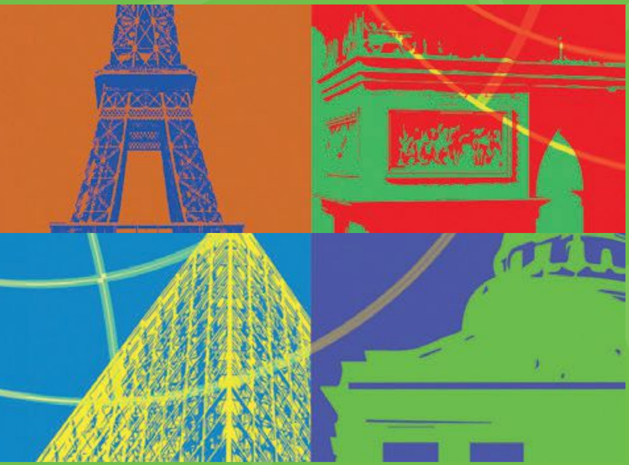

- 10,000 sqm of gross exhibition space
- Around 5,000 attendees
- 1,700 - 2,000 Conference delegates
- In excess of 300 international exhibitors (including Asia and US as well as Europe)

INTERESTED IN EXHIBITING?

Please contact one of our International Sales Team:

Richard Vaughan,
International Sales Manager
rvaughan@horizonhouse.co.uk

Gaston Traboulsi, France
gtraboulsi@horizonhouse.co.uk

Mike Hallman, USA
mhallman@horizonhouse.com

Brigitte Beranek, Germany, Austria & Switzerland
bberanek@horizonhouse.com

Katsuhiro Ishii, Japan
amskatsu@dream.com

Young-Seoh Chinn, Korea
corres1@jesmedia.com

CALL +44(0) 20 7596 8742 OR VISIT WWW.EUMWEEK.COM

NEW PRODUCTS

FOR MORE NEW PRODUCTS, VISIT WWW.MWJOURNAL.COM/BUYERSGUIDE
FEATURING VENDORVIEW STOREFRONTS

DEVICES/ COMPONENTS/MODULES

Up/Down-Converter IC

The AWMF-0218 is a highly integrated silicon frequency-conversion IC for 5G phased array applications. When used together with Anokiwave's beamformer IC products, this device enables low-cost, high performance and feature-rich 5G phased array systems. The half-duplex IC integrates Tx single-side-band up-conversion and Rx image-reject down-conversion functionality. An on-chip frequency multiplier simplifies board-level integration with external PLLs. The IF up/down-converter ICs are fully compatible with the respective Anokiwave beamformer ICs, sharing common mechanical and electrical interfaces and designed for cascade integration from IF to antenna and back.

Anokiwave Inc.
www.anokiwave.com

Ferrite Junction Waveguide Isolators

Cernexwave's Ferrite Junction Waveguide Isolators are great solutions for protecting sensitive equipment from excessive signal reflection. These compact units handle high power and can be tailored to a narrow or broad frequency range at any microwave or mmWave band. The precision internals provide high isolation with the lowest possible insertion loss to allow systems to operate at peak efficiency.

Cernexwave
www.cernexwave.com

Broadband Resistive Power Divider

The HL9479 is a 6 dB power divider that provides outstanding amplitude and phase symmetrical power division from DC to 110 GHz. This ROHS-compliant product is designed using a three-resistor network resulting in outputs that are nominally attenuated to 6 dB, and all ports are impedance-matched to 50 Ohms when the ports are terminated. They are suitable for use in 224 Gbps PAM4 communications systems, high speed analog-to-digital conversion, frequency response testing for differential devices and many other applications.

HYPERLABS
www.hyperlabs.com

Drop-in and Surface-Mount Bi-Directional Coupler

MIcable released the new drop-in and surface-mount bi-directional couplers. The coupling covers 5 to 30 dB, frequency covers 0.5 to 6.2 GHz. It has 200 W power handling capability with excellent stability and heat dissipation ability in a small package. It can realize the functions of power dividing and combining, signal acquisition. It is suitable for active phased array radar, power amplifier, radio and satellite communication, etc.

MIcable Inc.
www.micable.cn

MRFXF0025 5 to 1220 MHz Balun

The MRFXF0025 has been recently characterized and specified down to 5 MHz. This makes this balun an ideal choice for input devices in both forward and return path applications. Its low insertion loss (< 0.8 dB typical), flat RF response and excellent return loss (24 dB typical) has made it popular for Qorvo's QPL-88xx series amplifiers. Excellent phase and amplitude balance, low frequency return loss and a flat response are highly desirable features when running circuits at high output levels for both forward and return path CATV signal applications.

MiniRF
www.minirf.com

Miniature Bi-Phase Modulator/ Phase Shifter

Quantic PMI Model PS-90-6012-HS15NS-OPT6D1G is a high speed 6.1 GHz, 0 to 180 degrees, miniature bi-phase modulator/phase shifter with TTL control logic. ECL logic is available. Specifications include an insertion loss of 2.5 dB typical, 3.0 dB maximum; phase accuracy of ±0.05 degrees; VSWR 2.0:1; operating input power of 20 dBm; and 15 ns switching speed. Package size is 1.0 × 1.0 × 0.5 in. with SMA female connectors.

Quantic PMI
www.quanticpmi.com

Sky5® 2.4 to 8.3 GHz SPDT Switch

Richardson RFPD, Inc. announced the availability and full design support capabilities for a single-pole, double-throw switch from Skyworks Solutions, Inc. The SKY59608-711LF SPDT uses advanced switching technologies to maintain low insertion loss and high isolation for all switching paths. The high linearity performance and low insertion loss achieved by the SKY59608-711LF make it an ideal choice for low-power transmit/receive applications. The SKY59608-711LF is intended for mode-switching in WLAN applications.

Richardson RFPD
www.richardsonrfpd.com

EMI Capacitors

Special Hermetic Products' EMI capacitors are designed to minimize stress/strain on both the internal components and the external solder joints, which connect them to their host housing. The stress/strain considerations of these devices are crucial to their long-term reliability. It is critical that the recommended housing design geometry be followed and that the appropriate device be chosen for the host housing material. SHP supplies free assistance for ensuring the consideration of all relative factors in the selection of the optimum device for any given application.

Special Hermetic Products
www.shp-seals.com

CABLES & CONNECTORS

Patented Waveguide Connectors

Uni-Guide™ waveguide connectors are ideal for realizing hermetically sealed waveguide ports. The patented connectors are compatible with the glass beads and threaded holes used by standard 2.4 mm and 1.85 mm coaxial connectors. By attaching directly to component packages designed for coaxial connectors, Uni-Guide™ connectors eliminate the need for separate coaxial-to-waveguide adapters.

Eravant
www.eravant.com

New**Products**

AMPLIFIERS

Solid-State Broadband Amplifier

VENDORVIEW

Exodus AMP2055DB-750-200LC is a rugged, compact dual-band 80 MHz to 6.0 GHz solid-state broadband amplifier. Class A/AB design for all applications and industry standards. This amplifier produces $>$ 750 W 80 MHz to 1.0 GHz and $>$ 200 W 1.0 to 6.0 GHz with 58 dB gain. Simplified, elegant and reliable testing, optional forward/reflected power monitoring in dBm and watts, VSWR, voltage/current/temperature sensing for extreme reliability. Nominal 45 kg in a compact 10U chassis.

Exodus Advanced Communications
www.exoduscomm.com

GaN Power Amplifiers

The GaN power amplifiers are some of the most popular and best candidates for output power from CW 2 W to 200 W or pulsed 100 W to 1 kW. Suitable for TWT replacement, IPA, driver amplifier, transmitter, radar, electronic warfare, RPV, unmanned aerial vehicle, point-to-point and datalink communications.

Kratos General Microwave
www.kratosdefense.com

5 GHz MMIC LNA

VENDORVIEW

Mini-Circuits' model TSS2-53LNB+ is a low-noise amplifier (LNA) with bypass switching for high-level input signals. The MMIC amplifier has 1.3 dB or better typical noise figure from 0.5 to 5.0 GHz with 21 dB typical gain at midband. A good fit for 5G backhaul radio systems, the amplifier features high dynamic range with typical third-order intercept of +47 dBm IP3 in bypass mode. The 50 Ω amplifier is supplied in an eight-lead QFN style package measuring 2 × 2 mm.

Mini-Circuits
www.minicircuits.com

24.2 to 26.5 GHz, 2 W PA

Qorvo QPA4536 is a K-Band power amplifier (PA) with integrated power detector. The QPA4536 operates from 24.2 to 26.5 GHz and is designed using Qorvo's power pHEMT production process. The QPA4536 typically provides 33 dBm of saturated output power and 31.5 dBm output power at 1 dB gain compression. The small signal gain is 18 dB and third-order intercept is 43 dBm at 23 dBm SCL. To simplify system integration, the QPA4536 is fully matched to 50 Ω with integrated DC clocking caps on both I/O ports.

Qorvo
www.qorvo.com

SDM Hybrid Amplifiers

VENDORVIEW

With a frequency range of 1805 to 4100 MHz and fully-integrated micro-strip GaN modules, experience unparalleled performance in mobile infrastructure, small cells and low-power radio heads. Discover the future of wireless technology with RFHIC's latest SDM hybrid amplifiers, meticulously designed for a multitude of applications. Whether you're working on 4G LTE or 5G mMIMO systems, TDD/FDD configurations, mobile infrastructure, small cells or low-power remote radio heads, we have the perfect solution to elevate your projects.

RFHIC
www.rfhic.com

GaN HEMTs

Teledyne e2v HiRel announces the addition of new space screened versions of its popular 100 V, 90 A and 650 V, 30 A high reliability gallium nitride high electron mobility transistors (GaN HEMTs). The new parts go through NASA Level 1 or ESA Class 1 screening flow and can be brought up to full Level 1 conformance with extra qualification testing if desired. Typical applications include battery management, DC-DC converters and space motor drives.

Teledyne e2v HiRel
www.teledyne-e2v.com

NewProducts

ANTENNAS

Broadband Horn Antennas

VENDORVIEW

NSI-MI's line of broadband horn antennas are suitable for a wide variety of applications that require stable antenna performance over extremely broad frequency bandwidths. The best-in-class radiation patterns remain consistent across the operating frequency band for applications that require broadband performance. Each model is also designed to maintain VSWR across the complete frequency bandwidth.

AMETEK NSI-MI Technologies
www.nsi-mi.com

Horn Antennas

VENDORVIEW

Fairview Microwave announced the launch of its newest product line: quad-ridge, dual-polarized, broadband gain horns. These gain horns range from 0.8 GHz to 95 GHz waveguide and are available in gain varieties of 6, 10, 12, 15 and 20 dBi. Designed to perform in broadband test and measurement applications, these gain horns are instrumental in characterizing antennas and wireless systems.

Fairview Microwave
www.fairviewmicrowave.com

Advanced Rubberduck and Whip-Style Antennas

VENDORVIEW

Pasternack announced a new series of rubberduck and whip-style antennas. Designed to elevate wireless applications, these antennas exemplify Pasternack's dedication to producing top-tier, high-efficiency solutions. The newly-minted rubberduck and whip-style antennas by Pasternack epitomize portability and performance. Ideal for diverse scenarios, they act as lightweight, compact enhancers for radios. Impeccably engineered, these antennas are adjusted to specific frequency brackets, ensuring maximum operational proficiency.

Pasternack
www.pasternack.com

TEST & MEASUREMENT

USB Real-Time Spectrum Analyzers

VENDORVIEW

The SPECTRAN® V6 ECO series is Aaronia's latest generation of cost-effective real-time spectrum analyzers. The entry-level model SPECTRAN® V6 ECO 100XA-6 is already equipped with a real-time bandwidth of 44 MHz. The V6 ECO 150XA-6 version has an additional 44 MHz Tx output. The top model V6 ECO 200XA-6 of this analyzer family has two separate inputs (dual Rx) with 2 x 44 MHz RTBW, which can be configured independently.

Aaronia AG
www.aaronia.com/en/

Spectrum Analyzer

Signal Hound announced its new spectrum analyzer, the SP145, is now in stock and available to order. Customers can add an SP145 analyzer to their RF analysis toolkits for just $9,950 U.S. retail. The compact format, coupled with remarkable frequency accuracy, make this product an excellent option for field, test or even aerial applications. The SP145 is specialized for accurate remote spectrum monitoring and analysis in a portable, durable format.

Signal Hound
www.signalhound.com

MICRO-ADS

High-Power Microwave Sources and Technologies Using Metamaterials

Review by: Ajay Poddar

Bookend

Edited By J. W. Luginsland, J. A. Marshall, A. Nachman, E. Schamiloglu

Metamaterials (MTMs) are very interesting, yet not many books cover the broad applications focusing on high-power microwave (HPM) sources using artificial composite material. The content of this book is very diverse, authored by a team of university researchers who emphasize the application of MTMs in the broadest definition of terms, as well as in HPM antennas and related passive structure components. Previous books have mostly concentrated on split ring resonator-based composite structures as a part of MTMs.

The book consists of 11 chapters, Chapter 1 gives the prerequisite to MTMs for those in research work on artificial composite material structure and related applications manipulating the DNG space dimensions. Chapters 2 and 3 explain a typical multi-transmission line model for a beam-wave interaction structure and a comprehensive Pierce model from the Lagrangian. Chapters 4 and 5 bring dispersion engineering for slow wave structure design and perturbation analysis of Maxwell's Equations. Chapter 6 defines an assessment of the properties of conventional periodic structures with corrugated MTMs. Chapter 7 explains the group theory approach for designing MTMs for HPM devices. Chapters 8 and 9 discuss the temporal evolution of microwave EM fields in MTM structures and the survivability of MTM in the HPM environment. Chapter 10 reports experimental results of beam-wave interaction with MTM structures and the authors explain the advantages of MTM slow wave structures. The last chapter highlights the summary and future direction of MTM-inspired slow wave structures in the HPM background.

This book will appeal to a broad audience, ranging from students to engineers of all experience levels. This book can be a very useful guide to building the first simulation model of an MTM slow wave structure for HPM sources related to practical circuits and validating the results. The authors have advanced the understanding of a new generation of direct energy microwave capability that introduces MTMs into their beam-wave interaction structures. Conventional microwave vacuum electronics have advanced enormously from continuous research for nearly a century. MTM-based devices have been explored for less than a decade, so one can only imagine what advances will be realized in the future.

ISBN: 978-1-119-38444-1
Pages: 304
To order this book contact:
Wiley (December 2021)
wiley.com/en-us

Advertising**Index**

Advertiser	Page No.
3H Communication Systems	19
Aaronia AG	COV 3
Analog Devices	27
Anritsu Company	56
Artech House	110
ASB, Inc.	69, 89
Avtech Electrosystems	109
B&Z Technologies, LLC	11
CentricRF	78
Cernex, Inc.	94
Ciao Wireless, Inc.	30
Coilcraft	23
COMSOL, Inc.	15
Dalian Dalicap Co., Ltd.	65
EDI CON Online 2024	101
Empower RF Systems, Inc.	50
ERAVANT	41
ERZIA Technologies S.L.	73
ET Industries	90
EuCAP 2024	64
EuMW 2024	97, 105
Exceed Microwave	40
Exodus Advanced Communications, Corp.	61
Fairview Microwave	85
Flann Microwave	49
GGB Industries, Inc.	3
Greenray Industries, Inc.	37
HASCO, Inc.	47
Herotek, Inc.	92
HYPERLABS INC.	43
IEEE International Symposium on Phased Array Systems & Technology 2024	82
IEEE MTT-S International Microwave Symposium 2024	99
IEEE WAMICON 2024	44
iNRCORE	83
KR Electronics, Inc.	109
KRYTAR	48
LadyBug Technologies LLC	28
Logus Microwave	24
LPKF Laser & Electronics	52
Marki Microwave, Inc.	13
Master Bond Inc.	109
Menlo Micro	51
MIcable Electronic Technology Group	81, 93
Microwave Components Inc.	32
Microwave Journal	84, 96, 103, 107, 108
Microwave Products Group (a Dover Company)	36
Miller MMIC	COV 2
MilliBox	71
Millimeter Wave Products Inc.	57
Mini-Circuits	4-5, 16, 34, 113
MiniRF Inc.	55
Networks International Corporation	6
Norden Millimeter Inc.	76
Nxbeam	63
Passive Plus	67
Pasternack	8
Q Microwave	79
QML Inc.	42
Quantic PMI	53
Quarterwave Corporation	72
Reactel, Incorporated	33
Remcom	45
Remtec	88
RF-Lambda	9, 29, 77, 95
RFMW	13, 55, 87
Richardson RFPD	59
RLC Electronics, Inc.	21
Rosenberger	25
Satellite 2024	111
Sigatek LLC	58
SignalCore, Inc.	40
Signal Hound	75
Special Hermetic Products, Inc.	62
Spectrum Control	7, 87
Synergy Microwave Corporation	39, 91
Tabor Electronics	80
Taitien Electronics Co., LTD	26
Tecdia, Inc.	60
Weinschel Associates	22
Wenteq Microwave Corporation	109
Werlatone, Inc.	COV 4
West Bond Inc.	96
Withwave Inc.	42

Sales Representatives

Eastern and Central Time Zones
Carl Sheffres
Group Director
(New England, New York, Eastern Canada)
Tel: (781) 619-1949
Cell: (781) 363-0554
csheffres@horizonhouse.com

Michael Hallman
Associate Publisher
(NJ, Mid-Atlantic, Southeast, Midwest, TX)
Tel: (301) 371-8830
Cell: (781) 363-0338
mhallman@mwjournal.com

Pacific and Mountain Time Zones
Brian Landy
Western Reg. Sales Mgr.
(CA, AZ, OR, WA, ID, NV, UT, NM, CO, WY, MT, ND, SD, NE & Western Canada)
Tel: (831) 426-4143
Cell: (831) 713-9085
blandy@mwjournal.com

Submitting ad material?
Visit: www.adshuttle.com/mwj
(866) 774-5784
outside the U.S. call
+1-414-566-6940

Ed Kiessling
(781) 619-1963
ekiessling@mwjournal.com

International Sales
Richard Vaughan
International Sales Manager
Tel: +44 207 596 8742
rvaughan@horizonhouse.co.uk

Zena Coupé
Tel: + 44 207 1506737
Cell: +44 7887 874074
zena@expomedia.biz

Germany, Austria, and Switzerland (German-speaking)
Brigitte Beranek
Tel: +49 7125 407 31 18
bberanek@horizonhouse.com

France
Gaston Traboulsi
Tel: +44 207 596 8742
gtraboulsi@horizonhouse.com

Korea
Jaeho Chinn
JES MEDIA, INC.
Tel: +82 2 481-3411
corres1@jesmedia.com

China
Shanghai
Linda Li
ACT International
Tel: +86 136 7154 0807
lindal@actintl.com.hk

Wuhan
Phoebe Yin
ACT International
Tel: +86 134 7707 0600
phoebey@actintl.com.hk

Shenzhen
Annie Liu
ACT International
Tel: +135 9024 6961
anniel@actintl.com.hk

Beijing
Cecily Bian
ACT International
Tel: +86 135 5262 1310
cecilyb@actintl.com.hk

Hong Kong
Floyd Chun
ACT International
Tel: +852 28386298
floydc@actintl.com.hk

Taiwan, Singapore
Simon Lee
ACT International
Tel: +852 2838 6298
simonlee@actintl.com.hk

Japan
Katsuhiro Ishii
Ace Media Service Inc.
Tel: +81 3 5691 3335
amskatsu@dream.com

Corporate Headquarters: 685 Canton Street, Norwood, MA 02062 • Tel: (781) 769-9750

FABS and LABS

TÜV Rheinland®: Precisely Right.

Founded in 1872 in Germany, the initial focus of TÜV Rheinland was on ensuring the safety of steam boilers and pressure vessels. The company pioneered the concept of technical inspections and over the years, they have expanded their scope. TÜV Rheinland has diversified its services to encompass a wide spectrum of industries, including automotive, manufacturing, healthcare, energy, information technology and more. With this diversification, the company has become one of the world's leading testing service providers with more than 20,870 employees and annual revenues of around 2.3 billion euros.

TÜV Rheinland believes in the sustainable development of safety and quality in the interaction between man, technology and the environment in nearly all aspects of daily life and the economy. In its role as independent third party testing, inspection, and certification body, its experts test technical systems and products around the world, support innovations in technology and business, train people in numerous professions and certify management systems according to international standards. Operating as more than a test lab, these independent experts generate trust in products as well as processes across global value and supply chains. As an example of these activities, TÜV Rheinland has been a member of the United Nations Global Compact to promote sustainability and combat corruption since 2006.

To facilitate this broad range of activities, the company is committed to excellence and innovation. This is exemplified through TÜV Rheinland's global network of state-of-the-art laboratories, testing facilities and education centers that are all staffed by teams of highly skilled experts. These experts utilize innovative technology and rigorous testing methodologies to assess the quality, safety and compliance of products, systems and services.

Providing this broad range of services to an increasing set of market applications requires constant attention to the latest tools, technologies and machinery. It also involves investment. The company has just constructed and opened its Northeast Technology and Innovation Center in Boxborough, Mass. This brand new, multi-million-dollar, 65,000 sq. ft. sustainable mixed-use laboratory/office space is located on 350 acres of land. With an eye toward their stated goal of sustainability, the campus has 200 acres of conservation land and a State of Massachusetts-recognized park within the campus.

TÜV Rheinland's Northeast Technology and Innovation Center will be able to perform a wide range of tests and certifications for its global customer base. These tests will include electrical product safety, medical device testing, EMC testing, product safety, environmental testing, IP testing, laser testing, salt spray, dust testing, power electronics, research and development testing, robotics, semiconductor manufacturing, photo voltaic inverter and energy storage. As part of their solutions-based offering, TÜV Rheinland will offer efficient full market access to all these services for all regions of the world. This will be true for industrialized countries to emerging markets and developing regions. The Center will be a hub for clients and partners with TÜV Rheinland offering end-to-end solutions while providing space for collaboration, troubleshooting, training sessions, meetings and customer space.

Everyone knows TÜV Rheinland; the brand is registered. For many, its name is synonymous with neutrally tested quality and safety. The points of the triangle in the TÜV Rheinland logo symbolize the interaction between man, technology and the environment, and the wave represents a technical examination. For years, the logo has inspired trust and is recognized around the world as a symbol of safety and quality tested by an independent and neutral organization from facilities like the new TÜV Rheinland Northeast Technology and Innovation Center. When you need it, Precisely Right.

TÜV Rheinland
www.tuv.com/usa/en/

WERLATONE
ENGINEERING EVOLVED

RADIAL COMBINERS

Multi-kW Power Levels · **Low Loss Circuits** · **Custom Designs Available**

Model	Type	Frequency (MHz)	Power (W CW)	Peak Power (W) 10% DC	Insertion Loss (dB)	VSWR	Connector Type
D9816	8-Way	330-530	10,000	50,000	0.25	1.30:1	3 1/8” EIA, N-Female
D8454	8-Way	370-450	10,000	50,000	0.25	1.30:1	3 1/8” EIA, N-Female
D5320	12-Way	470-860	500	5,000	0.30	1.30:1	All N-Female
D10119	4-Way	700-4200	2,000	15,000	0.30	1.35:1	13-30 DIN-Female, N-F
D10603	32-Way	900-925	50,000	150,000	0.15	1.25:1	WR975, 7/16-Female
D10795	32-Way	900-930	25,000	150,000	0.25	1.20:1	WR975, 4.3-10-F
D9710	8-Way	1000-2500	2,000	10,000	0.30	1.40:1	1 5/8” EIA, N-Female
D8182	5-Way	1175-1375	1,500	25,000	0.40	1.35:1	1 5/8” EIA, N-Female
D6857	32-Way	1200-1400	4,000	16,000	0.50	1.35:1	1 5/8” EIA, N-Female
D11896	4-Way	2000-2120	4,000	40,000	0.25	1.40:1	WR430, 7/16-Female
D11828	4-Way	2400-2500	3,000	25,000	0.20	1.25:1	WR340, 7/16-Female
D10851	8-Way	2400-2500	8,000	50,000	0.20	1.25:1	WR340, 7/16-Female
D11433	16-Way	2700-3500	2,000	20,000	0.30	1.35:1	WR284, N-Female
D11815	16-Way	2700-3500	6,000	40,000	0.30	1.35:1	WR284, N-Female
D12101	6-Way	2750-3750	2,000	20,000	0.35	1.40:1	WR284, N-Female
D9582	16-Way	3100-3500	2,000	16,000	0.25	1.50:1	WR284, N-Female
D12102	6-Way	5100-6000	850	4,500	0.35	1.35:1	WR159, N-Female
D12484	6-Way	8200-8600	600	700	0.35	1.25:1	WR112, SMA-Female
D12485	6-Way	9000-11,000	500	700	0.40	1.35:1	WR90, SMA-Female

Specifications subject to change without notice.

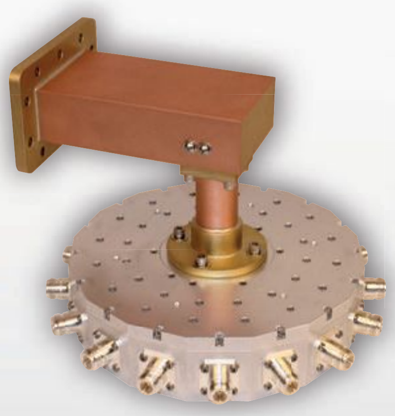




Werlatone, Inc. 17 Jon Barrett Road Patterson, NY 12563 845-278-2220 sales@werlatone.com www.werlatone.com